

12-15-2014

A Three-Dimensional-Engineered Matrix to Study the Microenvironment of Cancer Stem Cells

Samaneh Kamali Sarvestani
University of South Carolina - Columbia

Follow this and additional works at: <http://scholarcommons.sc.edu/etd>

 Part of the [Chemical Engineering Commons](#)

Recommended Citation

Sarvestani, S. K. (2014). *A Three-Dimensional-Engineered Matrix to Study the Microenvironment of Cancer Stem Cells*. (Doctoral dissertation). Retrieved from <http://scholarcommons.sc.edu/etd/3011>

This Open Access Dissertation is brought to you for free and open access by Scholar Commons. It has been accepted for inclusion in Theses and Dissertations by an authorized administrator of Scholar Commons. For more information, please contact SCHOLARC@mailbox.sc.edu.

**A THREE-DIMENSIONAL-ENGINEERED MATRIX TO STUDY
THE MICROENVIRONMENT OF CANCER STEM CELLS**

by

Samaneh Kamali Sarvestani

Bachelor of Science
University of Tehran, 2007

Master of Science
University of South Carolina, 2013

Submitted in Partial Fulfillment of the Requirements

For the Degree of Doctor of Philosophy in

Chemical Engineering

College of Engineering and Computing

University of South Carolina

2014

Accepted by:

Esmail Jabbari, Major Professor

Melissa A. Moss, Committee Member

Francis Gadala-Maria, Committee Member

Tarek Shazly, Committee Member

Lacy Ford, Vice Provost and Dean of Graduate Studies

© Copyright by Samaneh Kamali Sarvestani, 2014
All Rights Reserved.

DEDICATION

To my parents, for their endless love, support and encouragement

To my Advisor Dr. Esmail Jabbari and all my friends at USC

ACKNOWLEDGEMENTS

I would like to express the sincere appreciation to my advisor Dr. Esmail Jabbari for his guidance and support. Giving me the opportunity to perform this work is something that I will always appreciate.

I would like to thank my committee members, Dr. Moss, Dr. Gadala and Dr. Shazly for their support and presence in my defense session.

My gratitude also extends to my friends in our research group, Sina, Danial, Ozan, Tahereh, Ramin and Leily for their continuous help through this process.

I owe my deepest gratitude to my family and my best friend. Your motivation and support has always lighted my way. I am eternally grateful to you.

ABSTRACT

Maintenance of cancer stem cells (CSCs) is regulated by their microenvironment. As cancer cells are affected by many factors in their microenvironment, a major challenge is to isolate the effect of a specific factor on CSCs while keeping other factors unchanged. We developed a synthetic inert 3D Poly Ethylene Glycol Di-Acrylate (PEGDA) gel culture system as a unique tool to study the effect of microenvironmental factors on CSCs response. Synthetic hydrogels provide the flexibility to design three-dimensional (3D) matrices to isolate and study individual factors in the tumor microenvironment.

The first objective of this work was to investigate the effect of physical properties of microenvironment including modulus and geometry on maintenance of CSCs isolated of 4T1 (mouse breast cancer cell line), MCF7 and MDA-MB-231 (human Breast carcinoma cells) HCT116 (Colon), AGS (Gastric) and U-2 OS (Bone) human cancer cell lines in an inert microenvironment. We have shown that the gel elastic modulus had a strong effect on tumorsphere formation. CSCs formed in the inert PEGDA gel keep their stemness within certain ranges of gel stiffness. Briefly, mouse and human breast cancer cells encapsulated in the gel with approximate modulus of 5 kPa formed the largest and highest density of tumorspheres with highest expression of breast CSC markers. The highest number, diameter and CSC marker expression of HCT116 and AGS spheroids were observed in 25 kPa where it occurred at an optimum modulus of 50 kPa for U-2 OS cell line.

We have also shown that geometry and spatial properties of ECM can significantly affect the proliferation rate and size of tumorspheres formed by MDA-MB-231 cells in PEGDA micropatterned hydrogels. We introduced a 3D culture system as a model that controls the uniformity, size and proliferation of tumorspheres.

As this secondary objective, we investigated the effect of ECM composition on CSCs maintenance by using ECM-derived cell binding peptides active in malignancy. CD44 binding peptide (CD44bp), Integrin binding peptides (Ibps) and Heparin binding peptides (Hbps) were conjugated to the gel or dissolved in polymer solution to study their effect on the maintenance of CSCs.

We have shown that peptides derived from ECM proteins with different mechanisms of action can influence the microenvironment and cancer cells functions by either promotion or abolition of the spheroid forming ability in the inert 3D PEGDA hydrogel cell culture system. Conjugation of CD44bp and Ibps to the gel inhibited tumorsphere formation *in vitro* and *in vivo* where Hbps enhanced tumorsphere formation and CSCs marker expression compared to cells in the gel without peptide.

TABLE OF CONTENTS

DEDICATION.....	iii
ACKNOWLEDGEMENTS	iv
ABSTRACT	v
LIST OF FIGURES	viii
CHAPTER 1, INTRODUCTION	1
CHAPTER 2, MATERIALS AND METHODS	12
CHAPTER 3, RESULTS AND DISCUSSION	23
CHAPTER 4, CONCLUSION	85
REFERENCES	88

LIST OF FIGURES

Figure 3.1 Evolution of tumorsphere formation in different number densities	27
Figure 3.2 Effect of macromer concentration on elastic modulus of 4T1-cell-loaded PEGDA hydrogels with incubation time	28
Figure 3.3 Comparing <i>in vivo</i> tumor formation of 4T1 cells from adhesion plates (A) with 4T1 cells from tumorspheres on ultralow-attachment plates (B).....	29
Figure 3.4 Live and dead image of 4T1 cells 2 days after encapsulation in PEGDA hydrogels with moduli of (A) 2 kPa, (B) 5 kPa, (C) 25kPa, and (D) 50 kPa	31
Figure 3.5 Evolution of tumorsphere formation by 4T1 tumor cells encapsulated in PEGDA hydrogels, as a function of incubation time.....	32
Figure 3.6 Representative images of tumorsphere density for 4T1 cells encapsulated in PEGDA hydrogels with various elastic modulus after 8 days	34
Figure 3.7 Average tumorsphere size (A), tumorsphere size distribution (B), and cell count (C) for 4T1 tumor cells encapsulated in PEGDA hydrogels	35
Figure 3.8 BrdU staining of 4T1 tumorspheres formed in suspension culture on low-adhesion plates (A, C) and formed by encapsulation in PEGDA hydrogels (B, D).	38
Figure 3.9 Effect of gel elastic modulus on the relative mRNA expression levels of cancer stem cell markers of 4T1 cells in PEGDA hydrogels.....	39
Figure 3.10 Expression pattern of CD44 marker of 4T1 tumorspheres formed in suspension culture on low-adhesion plates and formed by encapsulation in PEGDA hydrogel	40
Figure 3.11 Evolution of tumorsphere formation by different tumor cell lines.....	41
Figure 3.12 Effect of gel elastic modulus on the relative mRNA expression levels	43
Figure 3.13 Effect of patterns size on tumorsphere formation	44
Figure 3.14 Effect of patterns size on tumorsphere formation and the relative mRNA expression levels	45

Figure 3.15 Sphere formation and the effect of cell type encapsulated in PEGDA gel on the expression of CSC markers.	58
Figure 3.16 Viability of the cells encapsulated in PEGDA gel.	59
Figure 3.17 CSC population in the cells encapsulated in PEGDA gel.	60
Figure 3.18 Effect of CD44bp on tumorsphere formation and CSC marker expression..	61
Figure 3.19 Effect of CD44bp conjugated to the gel on tumor formation <i>in vivo</i>	64
Figure 3.20 Comparison of tumorsphere formation in PEGDA gels conjugated with CD44bp, Ibp, or FHbp	65
Figure 3.21 CSC population in cells encapsulated in PEGDA gel conjugated with CD44bp, Ibp, or FHbp.	66
Figure 3.22 Expression of the markers related to CSC maintenance in cells grown in the gel conjugated with CD44bp, Ibp, or FHbp.....	67
Figure 3.23 Effect of CD44 binding peptide on tumorsphere formation by human tumor cell lines.....	71
Figure 3.24 Effect of heparin and integrin binding peptides on tumorsphere formation by human breast tumor cell lines	75

CHAPTER 1
INTRODUCTION

1.1 BACKGROUND

Cancer is one of the main causes of death worldwide[1]. It develops with uncontrollable cell growth in a process, which may take several years. This process can originate from any damage or mutation in genes.

Tumors are heterogeneous in their nature. It means that cells population in different levels of differentiation and invasiveness coexists together. The resistance of high grade tumors with none or poorly differentiated cancer cells to conventional cancer therapies such as chemotherapy is the major challenge in cancer treatment. Cells in the high grade tumors look abnormal, spread quickly and have high potential to relapse. Cancer stem cells (CSCs) theory relates the aggression of high grade tumors to the high fraction of CSCs with the ability of self-renewal and differentiation to all cell types in a tumor i.e., the triple negative breast cancer, one of the most aggressive types of breast cancer, contains a high fraction of CSCs [2-4].

Cancer stem cells model relates this heterogeneity to the existence of Cancer Stem Cells (CSCs) with the ability to give rise to all cell types in a tumor tissue and regenerating it. Therefore, it is necessary to know the properties and mechanisms of action in CSCs to find new ways in cancer treatment and prevention.

1.2 CANCER STEM CELLS MODEL

The body's continuous cell turnover and tissue repair system is related to stem cells, a small population of undifferentiated cells with unique potential of

- 1) Differentiation: the ability to give rise to different short-lived mature cell types of a tissue with the specialized functions.

- 2) Self-renewal: the ability to proliferate and make copies of themselves for long periods of time
- 3) Homeostatic control: the ability to make a balance between differentiation and self-renewal based on micro environmental stimuli and cues.

Stem cells categorizes in different groups based on their potential of differentiation. It ranges from totipotent stem cells having the ability of differentiation to any cell type in an organism to unipotent stem cells with the ability to differentiate to one cell type. Adult Stem Cells have mostly defined as multipotent cells. They are able to develop all cell types of a specific organ. Stem cells can stay dormant and inactive for a long period. They start their activity and division under certain physiological conditions. The fate of daughter cells through cell division is strongly dependent on the microenvironmental signals and cues. Daughter cells can keep their stemness properties and remain unspecialized or can differentiate to specific cells with defined functions[5].

There is a specific microenvironment for stem cells of different tissues. This microenvironment called stem cells niche consisting of neighboring cells and their extracellular matrices helps stem cells to optimize their function and keep their unique potential of self-renewal and differentiation. Various factors such as signals from proteins and cytokines in extracellular matrix or physical interaction to surrounding stromal cells cooperate to keep stem cells niche highly organized and inhibit the differentiation of stem cells. Consequently, detachment of stem cells of their niche can cause stem cell to lose their extraordinary potential. Outside their niche, they need sufficient intrinsic factors to keep their stemness properties and avoid differentiation. Cancer can result from multiple step process of genetic mutation in a single target cell over a long period and stem cells,

as the long-lived cells in many tissues can be good target for this transforming mutation. Like normal tissues, tumors are composed of heterogeneous populations of cells in different levels of differentiation.

Cancer cells in a tumor can be divided to different groups according to the expression of specific surface markers. Being injected to appropriate host such as immune-deficient mouse, tumorigenic capacity of each subset will be compared. Based on CSC model, only a minority of cancer cells with specific surface markers (CSC subset) is able to form tumors, whereas the majority of differentiated cells should not. Irrespective of the origin of CSCs, they provide a hierarchical system with the unique potential to self-renew and maintain tumor heterogeneity by giving rise to all different cell types of tumor. This heterogeneity comes from the cancer stem cells ability of dividing asymmetrically and giving rise to daughter cells which keep stemness properties of parental stem cells as well as progenitor cells that lacks self-renewal property and have a tendency to differentiate to other non-tumorigenic cancer cells forming the bulk of the tumor.

CSCs model has been verified in different tumor systems including breast and brain solid tumors. The results showed that, in human breast cancers, only a small subset of tumor cells, defined as [CD44⁺ CD24^{-/low}] comprising 11%–35% of total cancer cells has the tumorigenic potential to regenerate the whole tumor. In brain tumors, the stem cells properties has been successfully applied to the specific subset of CD133⁺ cells which usually include 5%–30% of total tumor cells. As expected this subset of CD133⁺ cells was able to form the whole tumor tissue after injection [5]. It is not easy to isolate the cancer stem cells in tumors. Recent progress in this way has introduced some new methods for this isolation that are similar with the strategies used to identify and enrich

normal stem cells. Implanting cells in immunodeficient mice at different cell doses can assess the level of tumorigenicity of these isolated CSCs. Tumor initiating cells are supposed to be able to develop tumors in low densities.

This hypothesis that cancer recurrence is related to the existence of cancer stem cells (CSCs) with the ability of differentiation into multiple cell types and resistance to conventional therapies comparing bulk tumor cells caused much effort to explore better ways of treatment based on this subpopulation of tumor tissues. Although conventional therapies such as chemotherapy or radiotherapy can kill differentiated, cancer cells but they are not able to eradicate CSCs population. CSCs are slow in cell division and this helps their resistance to chemotherapeutic drugs, which are more effective on rapidly replicating differentiated cancer cells. They are also provided with some transmembrane proteins such as ATP-binding cassette (ABC) transporters family known as drug resistance proteins with the ability of pumping out the chemotherapeutic drugs and DNA repairing agents. CSCs survive conventional therapies and cause relapse of tumor.

In regard of CSCs theory, tumor eradication will need specific agents to target CSCs selectively without killing normal stem cells of the body. These agents and other similar ways like enforcing CSCs to be differentiated to progenitor cells with more restricted properties will ultimately result in CSCs elimination and tumor regression as well as metastasis prevention. Some studies have focused on the possibility of identifying specific markers that distinguish CSCs from the bulk of the tumor and normal stem cells as well as specific agents that are able to discriminate between these markers and other ones. One of these agents are inhibitory peptides which are short proteins used in clinical research to examine their effects on CSCs. This method is highly selective, less toxic in

comparison with novel developed toxic drugs and more efficient among different methods of cancer therapy. Although peptides in comparison with proteins are more specific, stable and bio-available in their nature, identifying effective peptide sequence that can specifically target CSCs or induce their differentiation is still a main issue.

Among Bioactive peptides, only a few are therapeutically useful and show moderate efficacy in cancer treatment. Using these peptides with conventional drugs reduce their toxicity level and make them more selective for killing CSCs.

Direct interaction and inhibitory effect of some peptides on protein markers has drawn more attention to knowing and isolating specific markers of CSCs in cancer research including CD133, CD90, CD44, CD24, ABCG2, SCA1 and ALDH. Although these markers are not exclusively expressed in cancer stem cells, but can be useful for isolation the enriched subset of CSCs as a base for further studies including self-renewal assays.

CD44, a cell-surface glycoprotein has been recognized as one of the main markers to identify CSCs in several tumor tissues i.e., CD44 positive CSC-like cells showed enhanced ability for metastasis in different tumor cells [6-8]. For instance, this protein has been widely expressed in breast cancer tumors that is used to enrich cells population with stem-like characteristics [9, 10]. This marker binds to various ECM ligands mainly HA and collagen to regulate many signaling pathways related to tumor invasion, metastasis and growth [11, 12]. Extensive studies used the anti-CD44 antibodies as a therapeutic agent to target CD44 [13-15]. Therefore, identifying specific agents to target CD44 is potentially a promising method for tumor suppression, especially in CD44 overexpressed tumors. Recently it has been reported that the laminin alpha5 synthetic peptide A5G27 (RLVSYNGIIFFLK, residues 2,892-2,904), a CD44 binding peptide

inhibits tumor cell migration, invasion, and angiogenesis of B16-F10 melanoma cells in a dominant-negative manner and inhibits Cancer stem cells microenvironment [16].

CSCs with the properties of normal stem cells use similar signaling pathways to maintain their stemness. However, they may respond to the environmental cue differently. Under normal conditions, stem cells keep the balance between proliferation and differentiation but CSCs, due to mutations in the cell, are self-sufficient and involve unregulated cell proliferation [17, 18]. It has been proposed that the stem cell niche is converted from proliferation inhibitory to signals favoring cell proliferation in the case of CSCs. For instance, the tumor stroma is characterized by extracellular matrix (ECM) remodeling and stiffening. The limited knowledge of the relation between ECM stiffening and tumor progression has brought many questions into this field of study [19].

Two major factors make it difficult to study tumor microenvironment *in vivo*. First, animal models may not adequately reproduce the features of human cancers *in vivo*. The process of cancer development may take many years and immune-compromised animals frequently used to study molecular pathways or drug response, in most cases cannot provide a complete model for human tumor because of their short life span. Second, it is difficult to study the effect of a specific factor in the microenvironment while keeping all other factors unchanged. Therefore, there is a need to develop *in vitro* models to study the molecular basis of tumorigenesis and progression.

Most *in vitro* studies use standard two-dimensional (2D) cell culture. However, cells grown on 2D tissue culture lack proper cell–cell and cell–matrix interactions and behave differently from those grown in 3D environment. Removing cells from their natural tissues and culturing them in conventional culture systems such as 2D culture plates

changes all aspects of cell behavior from morphology to gene expression and differentiation pattern [20, 21]. For example, it has been reported that culturing human breast carcinoma cells on flat 2D culture plates changed their proliferation and differentiation pattern and reduced their malignancy compared with those under *in vivo* conditions [22]. Thus, developing 3D culture systems in which cells sustain their tissue specific phenotype is critical. This helps cancer researchers to understand the mechanisms by which CSCs maintain and progress. Most 3D models promote cell–cell interaction, adhesion, migration, and *in vivo*–like morphogenesis.

Among existing *in vitro* culture methods, growing tumorspheres in suspension on ultra-low-attachment plates is a commonly used traditional method to enrich CSCs *in vitro* but cannot mimic the tissue specific chemical and mechanical properties of ECM for cells.

Various types of materials have been used to generate a 3D matrix. naturally-derived 3D matrices used for immobilization of CSCs *in vitro* reduced difficulties of following progression of these cells *in vivo* but still do not allow studying the effect of environmental factors individually, due to their many ligand-receptor interactions. Type 1 collagen and Matrigel are the most widely used matrices [23] because they are biocompatible and support adhesion and growth of many cell types [24, 25]. Alginate and agarose gels are also used as a matrix to study the behavior of breast cancer cells under a 3D condition [26, 27]. Several studies have used natural hydrogels to study the effect of microenvironmental factors on cancer cells fate [28-31]. However, it is difficult to isolate and study cell response to individual factors in the microenvironment with naturally derived matrices that have many interactions with cell surface receptors [32]. Compared to natural hydrogels, the synthetic hydrogels with defined structure can be a good choice

to study the independent effect of ECM factors in vitro. These matrices allow precise control of different factors such as conjugated bioactive peptides on CSCs behavior and differentiation followed by studying targeted cancer therapy using antibodies or bioactive peptides to bind to specific markers on the surface of tumor stem cells. . Among them, polyethylene glycol (PEG) hydrogel has been extensively used as an engineered matrix for cell encapsulation to elucidate the effect of factors in the microenvironment on cell fate [33-36].

Recent advances in cancer research have highlighted the importance of CSCs interaction with the microenvironment at cellular and molecular levels [37]. The maintenance of CSCs is highly dependent on their interactions with ECM and surrounding cells i.e., proper intercellular interaction plays a critical role in cancer pathogenesis [38]. Epithelial cells interact with surrounding cells through different mechanisms of adherens, gap and tight junctions. Making changes in the pattern of interactions between adjacent cells may affect the phenotype and functionality of cancer cells [39]. Growing evidence show that major signaling pathways involved in maintenance of both normal and cancer stem cells including Notch, Wnt and Hedgehog depend on the level of interactions with their adjacent cells [40].

Several studies suggest that the role of ECM in self-renewal and differentiation of stem cells is not limited to the matrix mediated chemical cues but the role of physical signaling in cancer progression and stem cells functionality is indisputable [41-45]. ECM stiffness will increase tension and change cells properties in regard of growth, survival, migration and morphogenesis. Reducing this tension, malignant behavior of cancer cells will be repressed. Geometrical condition of ECM can also affect the way cells reach nutrients

and growth factors which plays critical roles in cancer initiation, progression, and metastasis [20]. Cells sense and respond to geometry of the microenvironment in various levels. For example they respond the morphology of ECM and arrangement of neighboring cells in microscale [46, 47].

In vivo, the stiffness of cells microenvironment is highly variable ranging from softer (breast, gastric) to hard (bone, teeth) tissues. Cells have the ability to sense and respond to matrix stiffness by synthesizing the appropriate extracellular matrix (ECM) composition as the mechanical properties and composition of hard and soft tissues differ significantly. In 3D culture systems, elastic modulus of the matrix can direct differentiation of encapsulated stem cells and shift the balance of cell proliferation and apoptosis [48-50]. Likewise, the proliferation, differentiation, migration, and apoptosis of cancerous cells in the tumor tissue are regulated by matrix stiffness [38, 51, 52].

Therefore, cells need to respond appropriately to the environmental cues for survival [53] and it is important to provide the appropriate range of stiffness in the local microenvironment for cells to survive [54, 55].

Recent advances in studying the mechanical properties of ECM allow researchers to investigate the higher aspects of ECM biomechanics and their key role in stem cells fate. For example, microfabrication techniques have been recently used to control the size of spheroids in substrates through the physical confinement of the micropatterned wells [56-58]. Several studies have focused the effect of microenvironmental factors on the maintenance of normal stem cells [59-61]. However, the individual role of mechanical and chemical properties of ECM on CSCs in an inert matrix has not been investigated. In this study, primarily we investigated the effect of cancer cells density on tumorsphere

formation using MDA-MB-231 encapsulated in the 5kPa PEGDA hydrogel. We show that tumorsphere formation is highly dependent on the number density of encapsulated cells and happens in a certain range of density. This study continued with the effect of matrix elastic modulus on the formation, growth, and maintenance of CSCs using 4T1, MCF7, MDA-MB-231 breast cancer cell lines with different level of malignancies, HCT116, AGS and U-2 OS cancer cell lines encapsulated in a range of moduli of PEG hydrogels, in the absence of attached ligands that interact with cell surface receptors. MCF10a, a normal human breast epithelial cell line was used as control to be compared with the cancer cell lines by their sphere formation ability. We showed that the formation and maintenance of tumorspheroids in these cancer cell lines are modulated by the elastic modulus of the PEG matrix.

For the purpose of comparison, we used the layer-by-layer micropatterning technique to employ pre-defined zones of cell encapsulation in PEGDA hydrogels and control the size of formed spheroids. We compared the CSCs properties of formed tumorspheroids in micropatterns with the control group of non-patterned hydrogels and indicate that the spatial limitation of micropatterns may control the size of formed spheroids and maintain the CSCs properties.

Following the study of mechanical properties, the inert PEGDA hydrogel, in certain range of moduli, was used as a 3D cell culture model to investigate the role of cell binding peptides in the maintenance of CSCs. More specifically, we investigated the effect of A5G27 peptide on CD44 overexpressed breast, colon and bone CSCs. We also studied the effect of additional ECM-derived cell binding peptides that are active in malignancy on the maintenance of CSCs.

We chose two peptides of fibronectin, the major components of ECM mediating tumorigenicity, a well-known integrin binding RGD peptide (I1) and FC/HV a fibronectin-derived heparin-binding peptide (H1). It has been shown in several studies that laminin-111, one of 15 isoforms of laminin, plays a major role in tumor cells adhesion, migration, growth and metastasis [62, 63]. We chose YIGSR (I3), a well-studied laminin-derived active peptide located on the β 1 chain, and IKVAV (I2) another peptide sequence on α chain of laminin-111 to study their effect on CSCs maintenance. Col IV is the other structural protein that plays an important role in tumor progression [64, 65]. In this study, we investigated the effect of two different heparin binding peptides derived from Collagen IV, Hep I (H2) and Hep III (H3) on the tumorspheroid formation and CSCs maintenance.

1.3 HYPOTHESIS

1.3.1 PEG based hydrogels with a wide range of mechanical properties and water content as an inert engineered 3D matrix can provides a novel tool to control and investigate the effect of microenvironmental factors on maintenance of CSCs *in vitro*.

1.3.2 Culturing cancer cells in confined areas of PEGDAmicropatterns may provide a useful 3D *in vitro* culture system to mimic the spatial limitations of CSCs microenvironment and controlsthe proliferation and size of tumorspheres.

1.3.3 CD44, Integrin and heparin binding peptides conjugated to the gel can affect the maintenance of CSCs encapsulated in PEGDA hydrogel culture system.

CHAPTER 2
MATERIALS AND METHODS

2.1 MACROMER SYNTHESIS AND CHARACTERIZATION

The PEG macromer was functionalized with acrylate groups to produce PEGDA by the reaction of acryloyl chloride with hydroxyl end-groups of PEG. TEA was used as the reaction catalyst. Prior to the reaction, PEG was dried by azeotropic distillation from toluene to remove residual moisture. The polymer was dissolved in dried DCM in a reaction flask and the flask was immersed in an ice bath to cool the solution. In a typical reaction, 5.6 ml acryloyl chloride and 9.7 ml TEA, each dissolved in DCM, were added drop-wise to the reaction with stirring. The reaction was allowed to proceed for 12 h under nitrogen flow. After completion of the reaction, the solvent was removed by rotary evaporation and the residue was dissolved in anhydrous ethyl acetate to precipitate the by-product triethylamine hydrochloride salt. Next, ethyl acetate was removed by vacuum distillation; the macromer was re-dissolved in DCM and precipitated twice in cold ethyl ether. Then, the macromer was dissolved in Dimethyl sulfoxide (DMSO) and dialyzed against distilled deionized (DI) water to remove the by-products. The PEGDA product was freeze-dried and stored at -20°C. A hydrolytically degradable version of the PEGDA gel (dPEGDA) was synthesized with a similar procedure as described previously[36]. The chemical structure of the functionalized macromer was characterized by a Varian Mercury-300 1H-NMR (Varian, Palo Alto, CA) at ambient conditions with a resolution of 0.17 Hz. The sample was dissolved in deuterated chloroform at a concentration of 5 mg/ml and 1% v/v TMS was used as the internal standard.

2.2 HYDROGEL SYNTHESIS AND MEASUREMENT OF GEL MODULUS

The PEGDA macromers were cross-linked in aqueous solution by ultraviolet (UV)-initiated radical polymerization with 4-(2-hydroxyethoxy)phenyl-(2-hydroxy-2-propyl)

ketone (Irgacure 2959; CIBA, Tarrytown, NY) photoinitiator. 10 milligrams of initiator were dissolved in 1mL PBS by vortexing and heating to 50°C. To prepare 2, 5, 25, 50, and 70 kPa moduli of PEGDA hydrogel precursor solutions, 5, 10, 15, 20, and 25 wt% of PEGDA macromer were dissolved in the initiator solution, respectively. The hydrogel precursor solutions were degassed and transferred to a polytetrafluoroethylene (PTFE) mold (5 cm × 3 cm × 750 μm), covered with a transparent glass plate, fastened with clips, and UV irradiated with a BLAK-RAY 100W mercury, long-wavelength (365 nm) UV lamp (Model B100-AP; UVP, Upland, CA) for 10 min. Disk-shaped samples were cut from the gel using an 8-mm cork borer and swollen in PBS for 24 h at 37°C. To measure the elastic modulus of gels, samples were loaded on the Peltier plate of the rheometer (TA Instruments, New Castle, DE) and subjected to a uniaxial compressive force at a displacement rate of 7.5 mm/s. The slope of the linear fit to the stress–strain curve for 5%–10% strain was taken as the elastic modulus (E) of the gels.

2.3 CSC CULTURE AND CHARACTERIZATION

4T1, MDA-MB-231, MCF7, HCT116 and AGS tumor cell lines were cultured in RPMI-1640 medium supplemented with 10% FBS. U-2 OS cells were grown in DMEM medium with 10% FBS where MCF10a were cultured in DMEM-F12 supplemented with 0.5 mg/ml Hydrocortisone, 10 μg/ml insulin, 100 ng/ml Cholera toxin, 20 ng/ml EGF and, 5% horse serum. Cells were trypsinized after reaching 70% confluency. PEGDA macromer was dissolved in PBS and sterilized by a 0.2 μm filter. Next, 5×10^5 /ml cells were added to the macromer solution with final PEGDA concentrations ranging 2–70kPa and mixed gently with a pre-sterilized glass rod. The cell-suspended hydrogel precursor solution was cross-linked with UV for approximately 10 minutes. After crosslinking, the

gel was cut into disks and incubated in stem cell culture medium under 5% CO₂. The stem cell medium consisted of DMEM-F12 supplemented with 0.4% BSA, 5 mg/mL insulin, 40 ng/mL bFGF, 20 ng/mL EGF, 5% horse serum, 100U/mL penicillin, and 100 mg/mL streptomycin [66]. For growing tumorspheres in suspension, trypsinized 4T1 cells were cultured on ultra-low-attachment tissue culture plates with stem cell culture medium under 5% CO₂ at 37°C as described previously [66-68]. The gold standard for characterization of CSC tumorspheres for stemness is by the ability to form tumor *in vivo*[69, 70]. To test for tumor formation, a stable 4T1 cell line that expressed luciferase (4T1-Luc) was established as described. Luciferase expression vector pGL4.50 [Luc2/CMV/Hygro] (Promega, Madison, WI) was transfected into 4T1 cells by Lipofectamine 2000 (Invitrogen), according to the manufacturer's instructions, to generate a cell line expressing luciferase as a reporter [71]. After 24 h, cells were trypsinized and cultured in RPMI-1640 medium with 400 mg/mL of hygromycin for 3 weeks to generate 4T1-Luc cells. 4T1-Luc cells were cultured on adhesion plates with regular RPMI-1640 culture medium or on ultra-low-attachment plates with stem cell culture medium as described previously. After one week, cells were trypsinized and counted. Different number of cells (5000 and 50,000 cells from adhesion plates or 500, 1000, and 5000 tumorsphere cells from ultra-low attachment plates) was injected subcutaneously in syngeneic Balb/c mice (6 mice/group). One week after inoculation, 100 mL of D-Luciferin (30mg/mL; Caliper, Hopkinton, MA) was injected subcutaneously and mice were imaged 10 min after Luciferin injection by Caliper's IVIS Spectrum imaging system (Caliper Life Sciences, Hopkinton, MA).

2.4 CELL IMAGING AND DETERMINATION OF CELL NUMBER

To determine cell viability, gels were stained with cAM/EthD live/dead dyes 2 days after encapsulation to image live and dead cells, respectively. Stained samples were imaged with an inverted fluorescent microscope (Nikon Eclipse Ti-e; Nikon, Melville, NY). Cell viability was quantified by dividing the image into smaller squares and counting the number of live and dead cells. At each time point, the gel samples were removed from the culture media and stained for imaging. Samples were rinsed twice with PBS and fixed with 4% paraformaldehyde for 3h. After fixation, cells were permeabilized using PBS containing 0.1% Triton X-100 for 5min. After rinsing, cells were incubated with Alexa 488 phalloidin (1:200 dilution) and DAPI (1:5000 dilution) to stain actin filaments of the cell cytoskeleton and cell nuclei, respectively.

Stained samples were imaged with a Nikon Eclipse Ti-e inverted fluorescent microscope. For visualization of cell uniformity, a confocal fluorescent microscope (Zeiss LSM-510META Axiovert; Carl Zeiss, Germany) was used to obtain 2D images (90- μm -thick layers) of the stained gels in the direction of thickness, as described [72]. For determination of cell number the gel samples were homogenized, cells were lysed, and aliquots were used to measure the dsDNA content using a Quant-it PicoGreen assay as described [73]. Briefly, an aliquot (100 μL) of the working solution was added to 100 μL of the cell lysate and incubated for 4 min at ambient conditions. The fluorescence of the solution was measured with a plate reader (Synergy HT; Bio-Tek, Winooski, VT) at emission and excitation wavelengths of 485 and 528nm, respectively. Measured fluorescent intensities were correlated to cell numbers using a calibration curve constructed with cells of known concentration ranging from zero to 10^6 cells/mL.

2.5 BRDU RETENTION ASSAY AND IMMUNOFLUORESCENT IMAGING

BrdU label retention was used to identify mammary CSCs as described [74, 75]. Nonconfluent 4T1 cells were incubated with 10 mM of BrdU for 10 days to label the DNA by incorporating BrdU into replicating DNA in place of thymidine. Next, the BrdU-labeled cells were encapsulated in the gel and incubated in stem cell culture medium to form tumorspheres as described previously. At each time point, the retention of BrdU in the encapsulated cells was imaged by immunofluorescent staining with anti-BrdU antibodies as described [75]. At each time point, tumorspheres encapsulated in the gel samples were processed and stained for immunofluorescent imaging of BrdU-labeled cells or CD44 marker as described [76]. Gel samples were fixed and permeabilized for 3 h at 4°C in PBS containing 4% paraformaldehyde and 1% Triton X-100, followed by rinsing with PBS (3×10 min). Tumor spheroids were then dehydrated in an ascending series of methanol at 4°C in PBS (25%, 50%, 75%, and 95% for 30 min each and 100% for 5 h) and rehydrated in the same descending series and washed in PBS (3×10 min). Next, samples were blocked with PBS containing 0.1% Triton X-100 (PBST) and 3% BSA overnight at 4°C and washed with PBS (2 × 15 min). Then, samples were incubated with primary antibodies (anti-CD44 antibody or anti-BrdU antibody) diluted in PBST on a gently rocking rotator at 4°C overnight followed by rinsing with PBST (4 × 30 min). Samples were then incubated with Alexa Fluor-conjugated secondary antibodies for 2 h and rinsed with PBST (4 × 10 min). The cell nuclei were counterstained with DAPI (1:5000 dilution in PBS) and imaged with a Nikon Eclipse Ti-e inverted fluorescent microscope.

2.6 RNA ANALYSIS

Total cellular RNA of the gel samples was isolated using TRIzol (Invitrogen) as described [73]. About 250 ng of the extracted purified RNA was reverse transcribed to cDNA by SuperScript II Reverse Transcriptase (Invitrogen) with the random primers. The obtained cDNA was subjected to realtime quantitative polymerase chain reaction (RT-qPCR) amplification with appropriate gene-specific primers. RT-qPCR was performed to analyze the differential expression of CSC marker genes with SYBR green RealMasterMix (Eppendorf, Hamburg, Germany) using Bio-Rad iCycler PCR system (Bio-Rad, Hercules, CA). The expression level of GAPDH gene was used as an internal control. The primers for RT-PCR were designed by Primer 3 software (<http://frodo.wi.mit.edu>). The forward and reverse primer sequences, listed in Table 2.1. The relative gene expression levels were quantified by the 2^{-DDCT} method as described [77, 78]. The relative gene expression was expressed as fold difference compared with that at time zero.

2.7 MICROPATTERN FABRICATION

Briefly, 40 μ L of the gel precursor solution (without cells and peptides) was transferred onto a glass base between two tape spacers (separated by 2 cm) and covered with a glass slide. Upon hydrogel crosslinking under UV irradiation for 8 minutes, the cover was removed and the gel was washed with PBS five times to remove the unreacted macromers. The second layer was fabricated by thickening the spacer with placing another tape layer, transferring 40 μ L of the gel precursor solution on top of the first layer, crosslinking of solution for 8 minutes and washing the gel five times. The masks

were designed using Autocad software and printed on a transparent paper. MDA-MB-231 cells were suspended in gel precursor solution and transferred on the gel layer.

Table 2.1 The forward and reverse primer sequences

PCR Primer	Forward Sequence	Reverse Sequence
mGAPDH	CATGGCCTTCCGTGTTTCCTA'	CCTGCT TCACCA CCT TCTTGA'
hGAPDH	GAGTCAACGGATTTG GTCGT	TTGATTTTGGAGGGATCTCG
mCD44	GAATGTAACCTGCCGCTACG'	GGAGGT GTT GGA CGT GAC'
mABCG2	AGCAGCAAGGAAAGATCCAA'	GGAATACCGAGGCTGATGAA'
mSCA1	TGGACACTTCTCACACTA-	CAGAGCAAGAGGGTCTGCAGGAG
mCD24	CTTCTGGCACTGCTCCTACC	GAG AGAGAG CCAGGAGACCA'
hCD44	GGCTTTCAATAGCACCTTGC	ACACCCCTGTGTTGTTTGCT
hABCG2	CACCTTATTGGCCTCAGGAA	CCTGCTTGGAAGGCTCTATG'
hCD133	GCATTGGCATCTTCTATGGTT'	CGCCTTGTCCTTGGTAGTGT
h Oct4	CGCCGTATGAGTTCTGTG'	GGTGATCCTCTTCTGCTTC'
hTGFb	CCGGAGGTGATTTCCATCTA'	CTCCATTGCTGAGACGTCAA'
hEGFR	CAGCGCTACCTTGTCATTCA	TGCACTCAGAGAGCTCAGGA'

The spacers were thickened and the mask was placed on top of the spacers and was pressed flat by a glass slide. After 5 minutes UV crosslinking of the sample, the mask was removed; the gel was washed three times and was cured for 3 minutes under UV. The patterned gel was then washed three times with PBS, removed from the glass base and transferred to the media.

2.8 PEPTIDE SYNTHESIS AND CHARACTERIZATION

CD44 binding peptide (CD44bp), integrin-binding peptides (Ibps), and heparin-binding peptide (Hbps) as well as their mutants, selected according to previous reports [79-81], were synthesized peptides manually on Rink Amide resin in the solid phase using a

previously described procedure [82]. The sequences of these peptides and their mutants are listed in Table 2.2.

Table 2.2 Peptides sequence and the origin

Peptide Name	Sequence	Protein of Origin
FC/HV	WQPPRARI-Ac	Fibronectin
HepI	TAGSCLRKFSTMY-Ac	Collagen IV
HepIII	GEFYFDLRLKGDKY-Ac	Collagen IV
I1	GRGDS-Ac	Fibronectin
I2	IKVAV-Ac	Laminin
I3	YIGSR-Ac	Laminin

Briefly, the Fmoc-protected amino acid (6 eq.), DIC (6.6 eq.), and HOBt (12 eq.) were added to 100 mg resin and swelled in DMF (3 mL). Next, 0.2 mL of 0.05 M DMAP was added to the mixture and the coupling reaction was allowed to proceed for 4-6 h at 30°C with orbital shaking. The resin was tested for the presence of unreacted amines using the Kaiser reagent [82]. If the test was positive, the coupling reaction was repeated. Otherwise, the resin was treated with 20% piperidine in DMF (2×15 min) and the next Fmoc-protected amino acid was coupled using the same procedure. After coupling the last amino acid, the peptides were functionalized with an acrylamide group directly on the peptidyl resin by coupling acrylic acid to the N-terminal amine group under conditions used for the amino acid coupling reaction [82]. The acrylamide-terminated peptide was cleaved from the resin by treating with 95% TFA/ 2.5% TIPS/ 2.5% water and precipitated in cold ether. The acrylamide-terminated (Ac) peptides were further purified by preparative HPLC on a 250 x 10 mm, 10 µm Xterra Prep RP18 column (Waters, Milford, MA) with a flow rate of 2 mL/min using a gradient 5–95% MeCN in 0.1% aqueous TFA at detection wavelength of 214 nm. The HPLC fraction was

lyophilized and the product was characterized with a Finnigan 4500 Electro Spray Ionization (ESI) spectrometer (Thermo Electron, Waltham, MA).

2.9 FLOW CYTOMETRY ANALYSIS

Cells encapsulated in the gel were fixed with 4% paraformaldehyde for 30 min followed by washing with PBS. Next, the gel was incubated in oxidative degradation solution (0.1M CoCl in 20% hydrogen peroxide) [83]. After the gel was degraded, cells were washed three times with cold PBS containing 5% BSA. MCF7 cells were incubated with phycoerythrin (PE) mouse anti-human CD24 and fluorescein isothiocyanate (FITC) mouse anti-human CD44 (BD Biosciences, Franklin Lakes, NJ), and 4T1 cells were incubated with PE-anti-mouse CD24 and FITC-anti-mouse CD44 (eBioscience, San Diego, CA) in 100 μ l PBS with 5% BSA for 45 min on ice in dark. Cells were then washed with cold PBS with 5% BSA three times and analyzed by a flow cytometer (FC500, Beckman Coulter, Brea, CA). Flow cytometry was done multiple times on each sample to ascertain reproducibility of the results.

2.10 WESTERN BLOT

The cell encapsulated gel was washed with PBS and homogenized in RIPA buffer (1% NP40, 1% SDS, 150mM NaCl, 20mM Tris-Cl pH7.4, 1mM EDTA protease inhibitors) to extract the proteins. The homogenized sample was centrifuged for 5 min to isolate total proteins. Next, proteins were separated by standard SDS-PAGE using Mini-gel system (Bio-Rad) and transferred to a nitrocellulose membrane by the semi-dry transfer apparatus (Bio-Rad). Membranes were incubated in the blocking buffer (5% fat-free dry milk in TBST buffer) at ambient conditions for 1 h followed by incubation with primary

antibodies (1:200-1:2000) overnight at 4°C. After washing, the membrane was incubated with HRP-conjugated secondary antibodies for 1 h at ambient conditions. After extensive washing with TBST, the membrane was incubated with ECL detection reagents and exposed to an X-ray film. The intensity of the band was quantified with the Image-J software (National Institutes of Health, Bethesda, MD).

2.11 STATISTICAL ANALYSIS

Data are expressed as mean +/- standard deviation. All experiments were done in triplicate. Significant differences between groups were evaluated using a two-way analysis of variance (ANOVA) with replication test followed by a two tailed Student's t-test. A value of $p < 0.05$ was considered statistically significant.

CHAPTER 3
RESULTS AND DISCUSSION

3.1 EFFECT OF CELLS NUMBER DENSITIES ON TUMORSPHERES FORMATION IN HYDROGEL

MDA-MB-231 tumor cells with initial number densities of 0.3, 0.6, 1, 1.5 and, 2 (10^6 /ml) were encapsulated in 5kPa PEGDA hydrogels and cultured in stem cell medium for 9 days. Fluorescent images in Figure 3.1 show the extent of cell aggregation and spheroid formation after 9 days (column 2) for MDA-MB-231 encapsulated cells with initial number densities (column 1) of 0.3 (Fig 3.1, row 1), 0.6 (Fig 3.1, row 2), 1 (Fig 3.1, row 3), 1.5 (Fig 3.1, row 4) and 2 (Fig 3.1, row 5) (10^6 /ml). Spheroid formation was observed in two initial number densities of 0.6 and 1 (10^6 /ml). While cells with low initial density of 0.3 (10^6 /ml) did not change significantly in morphology, densities of 1.5 and, 2 (10^6 /ml) showed significant increase in the number and shape of cells aggregates during 9 days.

The number density of viable cells is shown in Figure 3.1B. Although, the cell count did not increase in the group with 0.3 (10^6 /ml) of cells, it increased with time for the other groups after 9 days. This change was bimodal that the cell count initially increased about 4 and 5 times in the groups with densities of 0.6 and 1 (10^6 /ml) respectively and then decreased to 3 times for cells with initial densities of 1.5 and 2 (10^6 /ml) suggesting that the highest potential for growth was observed in the groups with the ability of tumorspheroids formation.

The expression of breast CSC markers for tumorspheres and cell aggregates grown in PEGDA gels with different cell number densities is shown in Figure 3.1 C–E. Cells with 0.6 and 1 (10^6 /ml) initial number density had the highest expression of all markers suggesting that sphere formation was correlated with the expression of CSC markers. The

CD44 expression initially increased and reached a maximum at the cell number density of 1×10^6 /ml) then decreased sharply for higher densities at both timepoints of 6 and 9 days. The highest expression of ABCG2 and EGFR markers were observed in the group with 0.6×10^6 /ml) density which formed larger sizes of tumorspheroids compared to the group with 1×10^6 /ml) density. Aggregates in the groups with high cell number densities showed very low fold expression of these two markers at both timepoints. Therefore, the biphasic behavior was also observed for these two markers that the fold expression of markers had a decreasing trend for the cell densities higher than 0.6×10^6 /ml). The CSC expression in the group with low cells density of 0.3×10^6 /ml) did not increase significantly in 9 days of incubation and remained in a very low level.

Increasing the cell number density will directly affects the quantity and level of cell-cell interaction and may affect the fate of encapsulated cancer cells. Although normal and cancer stem cells regulate similar signaling pathways to keep their stemness, their degree of dependency to the environmental cues including neighboring cells is totally different. Under normal conditions, the microenvironment provides transient signals for both proliferation and differentiation of stem cells and plays a critical role to maintain their stemness. On the other hand, CSCs due to the mutations, are self-sufficient with respect to proliferation [37, 38]. CSCs do not need to be in tight junctions with their surrounding cells to grow and form tumorspheroids *in vitro*. Encapsulation of epithelial cancer cells harvested from 2D culture plates in form of aggregates eliminates the chance of spheroid formation. This may be explained by the fact that cells in form of aggregates with apical and basal surfaces remain polarized after being cultured in PEG hydrogels. However, culturing cells individually at an appropriate number density leads regular cancer cells to

lose their polarity and ECM adhesion tendency resulting in development of CSCs-like properties accompanied with sphere formation. This loss of polarity inhibits the growth of polar non-CSCs. Consistent with this notion, Epithelial to Mesenchymal Transition (EMT), one of the main biological events involved in tumor spheroids formation needs cells to lose their polarity. [39-41]. Besides, the direct cell-cell contact between cells act as a barrier to the diffusion of small signaling molecules vital for induction of CSC-like properties through the intercellular space [16].

Signaling pathway involved in CSCs progression, may not need the tight junction of cells to be regulated but still need close communication of cells together i.e., culturing cells at a very low number density of 0.3×10^6 /ml, prevents cells to receive the signals of adjacent cells.

High expression of CD44 as the most important marker for breast CSCs identification correlates to formed tumorspheroids with higher population of CSCs compared to groups with single cells or aggregates. The larger diameters of spheroids in groups with 0.6×10^6 /ml cells showed higher expression of EGFR and ABCG2 markers which may be related the higher level of cell-cell interaction in larger spheroids.

3.2 EFFECT OF MATRIX MODULUS AND TOPOGRAPHY ON STEM CELLS AND TUMORSPHERE FORMATION

3.2.1 HYDROGEL MODULUS

Disk-shaped hydrogels with 8mm diameter and 750mm thickness were fabricated for determination of elastic modulus and cell encapsulation. The effect of macromer concentration and incubation time on the elastic modulus of PEGDA hydrogel is shown

in Figure 3.2. Macromer concentration in the precursor solution affected the elastic modulus of the hydrogel. The elastic modulus increased from 2 to 70 kPa as the

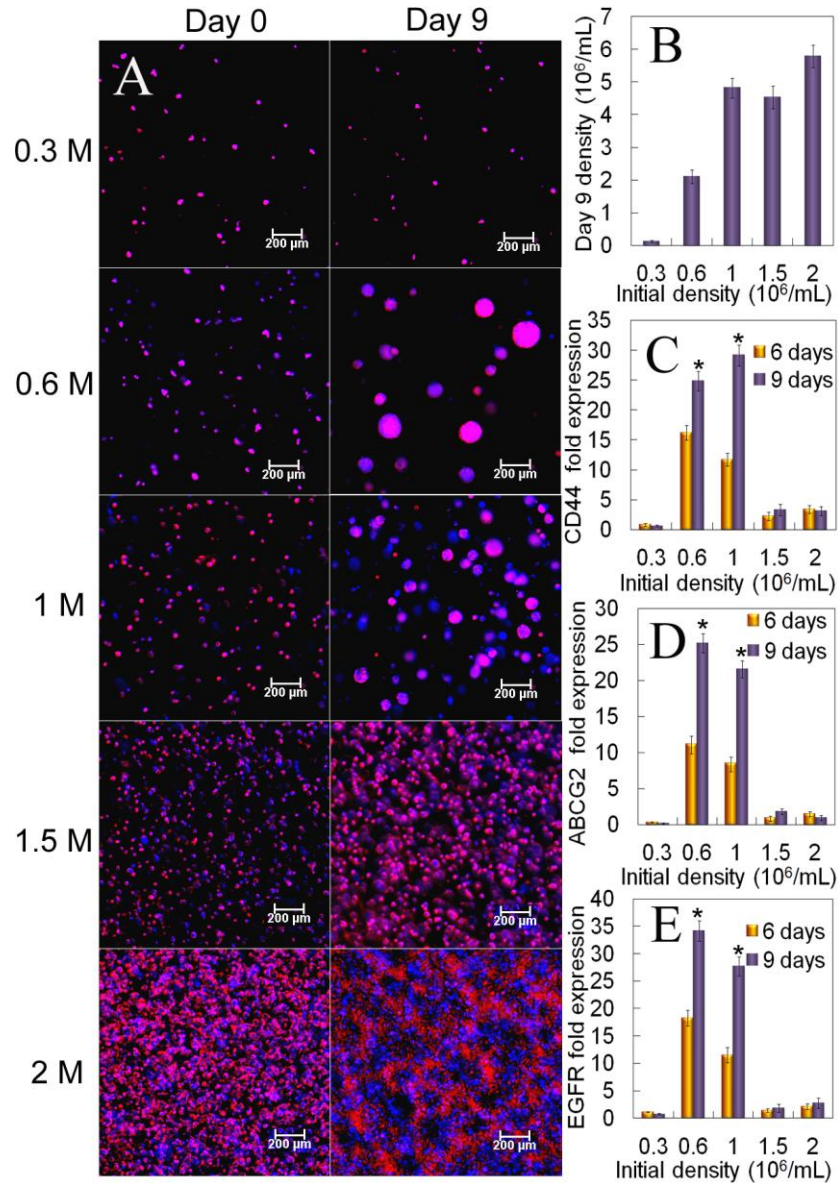


Figure 3.1 Evolution of tumorsphere formation in different number densities Cells Encapsulated in PEGDA hydrogels with number densities of 0.3, 0.6, 1, 1.5, 2 (10⁶/ml) (Rows 1 to 5) as a function of incubation time. Columns 1 and 2 correspond to incubation times of 0 and 9 days, respectively. At each time point, encapsulated cells were stained with Phalloidin for cytoskeleton (red) and DAPI for nucleus (blue), and imaged with an inverted fluorescent microscope (A) Cells density (B) CD44 fold expression (C), ABCG2 fold expression (D), and EGFR fold expression (E)

macromer concentration was increased from 5% to 10%, 15%, 20%, and 25%, respectively.

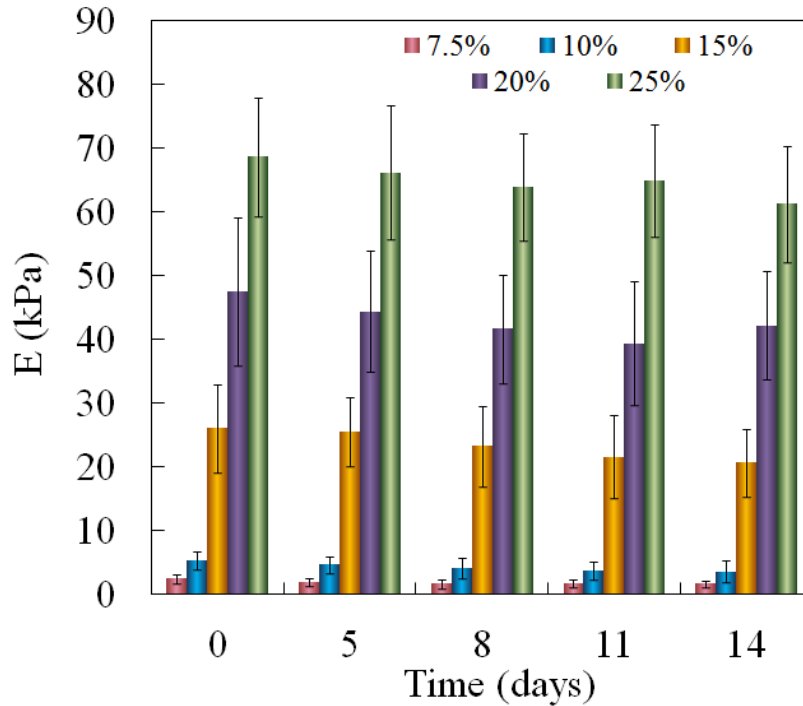


Figure 3.2 Effect of macromer concentration on elastic modulus of PEGDA gels with time

3.2.2 TUMORSHERE CHARACTERIZATION

Tumorsphere formation on ultra-low-attachment plates is a commonly used method to enrich CSCs *in vitro*, while the gold standard for characterization of CSC tumorspheres is by the ability to form tumor *in vivo* [69, 70]. 4T1-Luc cells were cultured on regular adhesion plates or ultra-low-attachment plates. After one week, cells in monolayers (adhesion plates) and in spheres (ultra-low-attachment plates) were collected and subcutaneously inoculated in syngeneic Balb/c mice.

Tumor formation in mice was determined by imaging the expression of luciferase one week after inoculation. Figure 3.3 compares tumor formation by cells on adhesion plates

(Fig 3.3 A) and cells from tumorspheres on ultra-low-attachment plates (Fig 3.2 B). The left and right images in Figure 3.3 A are for 5000 and 50,000 4T1-Luc cells on adhesion plates. The left, center, and right images in Figure 3.3 B are for 500, 1000, and 5000 4T1-Luc cells

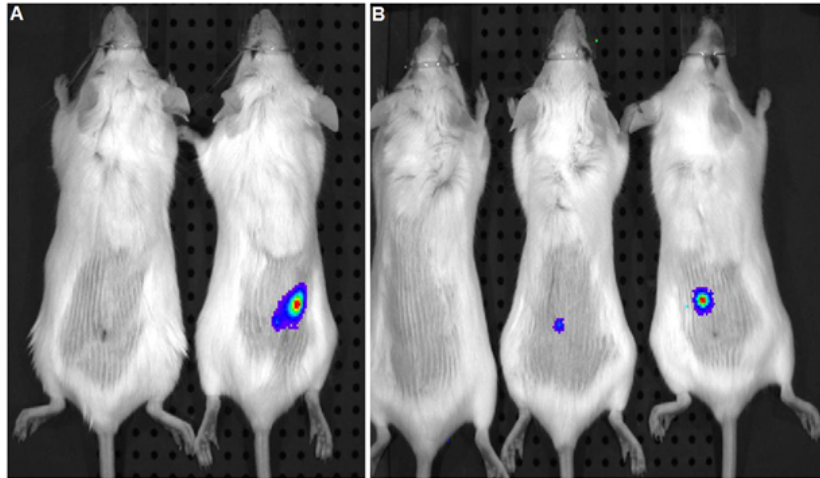


Figure 3.3 Comparing *in vivo* tumor formation of 4T1 cells from adhesion plates (A) with 4T1 cells from tumorspheres on ultralow-attachment plates (B). The left and right images in (A) show tumor formation by inoculation of 5000 and 50,000 4T1-Luc cells, respectively. The left, center, and right images in (B) show tumor formation by inoculation of 500, 1000, and 5000 4T1-Luc cells from tumorspheres. 4T1-Luc cells were inoculated subcutaneously in Balb/c mice. After one week, the expression of luciferase in tumors was imaged. The light blue, dark blue and red color images correspond to low, medium, and high luciferase intensity, proportional to the size of the tumor formed.

from tumorspheres on ultra-low-attachment plates. According to the images in Figure 3.3, 1000 tumorsphere cells were sufficient to form a tumor *in vivo* while it required 50,000 regular tumor cells to form a tumor. These results demonstrate that tumorspheres formed by 4T1 cells *in vitro* had enriched CSC subpopulation.

3.2.3 TUMORSPHERE FORMATION IN HYDROGEL

In modulus study, we have focused on encapsulation of 4T1 mouse breast cancer cell line and human carcinoma cells including MCF7, MDA-MB-23 (Breast), HCT116 (Colon), AGS (Gastric) and U-2 OS (Bone) cancer cell lines. Cell lines were cultured in stem cells

medium up to 14 days at different PEGDA hydrogels moduli ranging from 2 to 70 kPa. MCF10a, a normal human breast epithelial cell line was encapsulated in 5 kPa modulus gel and used as control to be compared with the cancer cell lines by their sphere formation ability. Tumor spheroids are a 3D representative of the CSCs population and a level of malignancy of cancer cells, *in vitro*[84].4T1 tumor cells were encapsulated in PEGDA hydrogels with elastic moduli ranging from 2 to 70 kPa and cultured in stem cell medium for 2 weeks. Images of live and dead cells 2 days after encapsulation in PEGDA gels with moduli of 2, 5, 25, and 50 kPa are shown in Figure 3.4 A through 3D, respectively. Based on image analysis, the percent viable cells for 2, 5, 25, 50, and 70kPa gels were 94 ± 4 , 91 ± 3 , 92 ± 3 , 90 ± 4 , and 89 ± 4 , respectively. These results show that the gel modulus did not have a significant effect on viability of 4T1 cells after encapsulation. To determine cell uniformity and viability, a confocal microscope was used to image cells in the direction of thickness and the results are shown in Figure 3.5 E1±E8. Images in Figure 3.4 E show uniform cell seeding and cell viability within the gel in the thickness direction.

Fluorescent images in Figure 3.5 show the extent of cell aggregation and spheroid formation with incubation time for 4T1 gels with modulus of 2 kPa (Fig 3.4, column 1), 5 kPa (Fig 3.4, column 2), 50 kPa (Fig 3.4, column 3). Rows 1, 2 and 3 in Figure 3.5 correspond to incubation times of 5, 8, 11, and 14 days, respectively. Spheroid formation was observed in soft gels with moduli of 2 and 5 kPa as early as day 5 (columns 1, 2 in Fig 3.4) while cells in the more stiff gels with modulus of 50 kPa and higher remained as single cells or small cell aggregates ($< 25 \mu\text{m}$). At any time point, size of the tumorspheres in the 5 kPa gel was higher than that of 2 kPa gel.

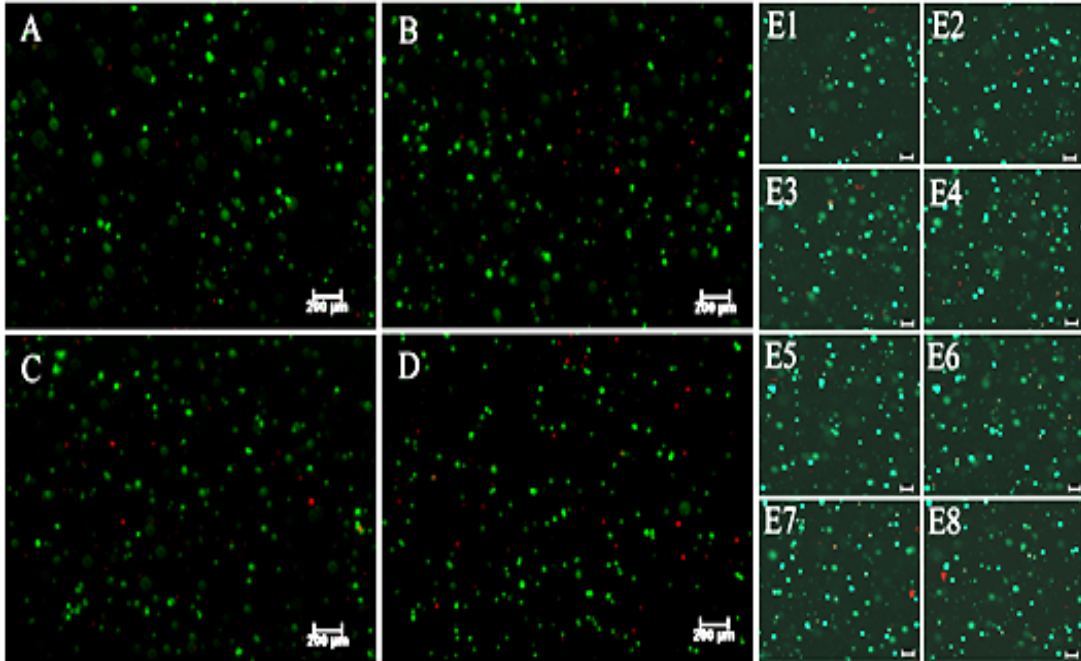


Figure 3.4 Live (green) and dead (red) image of 4T1 cells 2 days after encapsulation in PEGDA hydrogels with moduli of (A) 2 kPa, (B) 5 kPa, (C) 25 kPa, and (D) 50 kPa. The scale bar in images (A–D) is 200 μ m. Based on image analysis, the percent viable cells for 2, 5, 25, 50, and 70 kPa gels was 94 ± 4 , 91 ± 3 , 92 ± 3 , 90 ± 4 , and 89 ± 4 , respectively. Images (E1–E8) on the right show the uniformity of cell seeding and cell viability in successive 90 μ m layers in the direction of thickness for 5.3 kPa gel obtained with a confocal fluorescent microscope. The scale bar in images (E1–E8) is 200 μ m.

Lower magnification images showing the number density of 4T1 (Fig 3.5, column 1) and MCF7 (Fig 3.5, column 2) tumorspheres in PEGDA gels with elastic moduli of 2 kPa (Fig 3.5, row 1), 5 kPa (Fig 3.5, row 2), 25 kPa (Fig 3.5, row 3), and 50 kPa (Fig 3.5, row 4) after 8 days of incubation are shown in Figure 3.6, respectively. According to Figure 3.6, the tumorsphere size and number density initially increased with increasing matrix modulus from 2 to 5 kPa and then decreased when modulus was increased to 25 and 50 kPa. Tumorspheres with diameter $>100\mu$ m were observed only in the gels with modulus of 2 and 5 kPa but the fraction of large tumorspheres ($> 100 \mu$ m) was significantly higher in the 5 kPa gel.

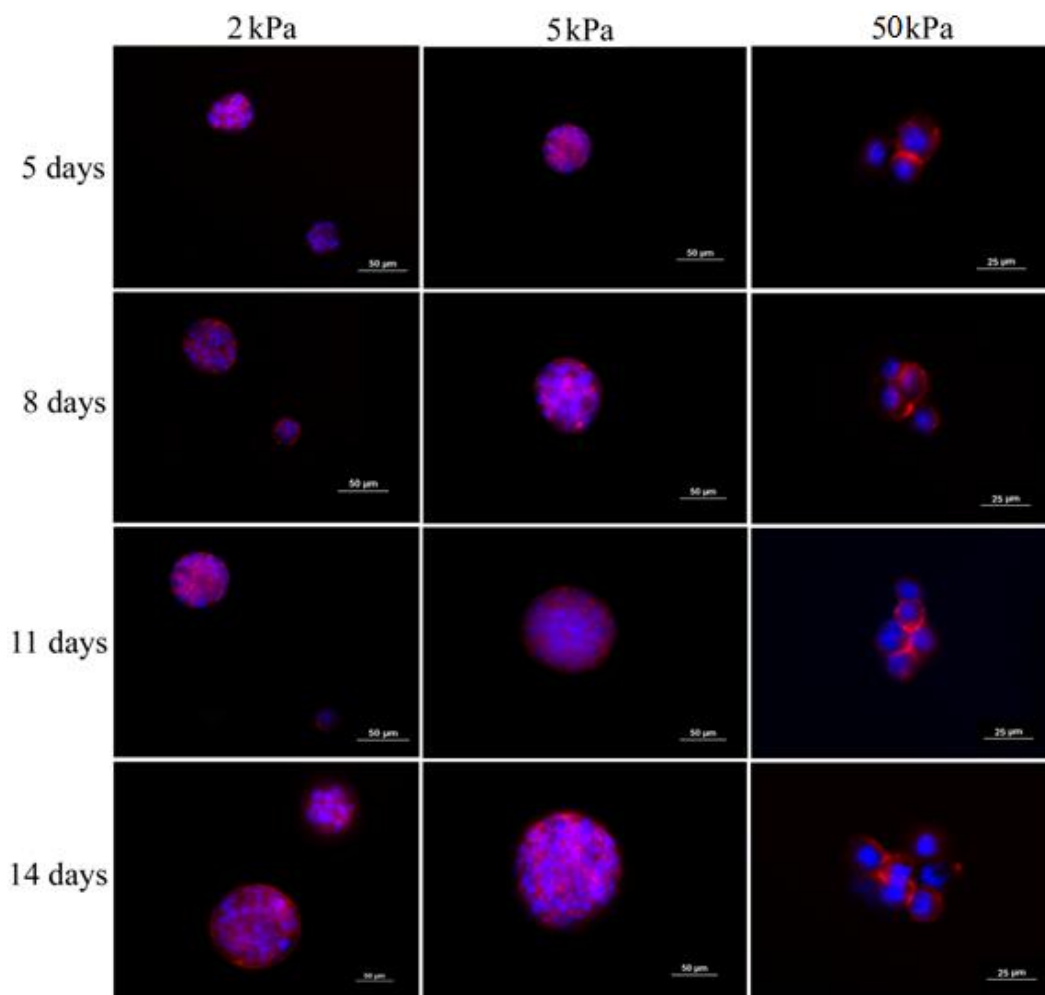


Figure 3.5 Evolution of tumorsphere formation by 4T1 tumor cells encapsulated in PEGDA hydrogels with elastic modulus of 2 kPa (left column), 5 kPa (center left column), and 50 kPa (right column) as a function of incubation time. Rows 1, 2, 3, and 4 correspond to incubation times of 5, 8, 11, and 14 days, respectively. At each time point, encapsulated cells were stained with Phalloidin for cytoskeleton (red) and DAPI for nucleus (blue), and imaged with an inverted fluorescent microscope.

It should be noted that the size of MCF7 spheroids in the gels was less than that of 4T1.

The evolution of tumorsphere for human cell lines is presented in Figure 3.11.

Fluorescent images in Figure 3.11 A show the optimum modulus for spheroid formation of each cell line as a function of time. The optimum moduli in columns 1 to 6 correspond to 5, 5, 5, 25, 50 and, 25 kPa, respectively. At these moduli the single-cells fraction of cancer cells started to form tumor spheroids after 6 days of encapsulation. Deviations

from optimum stiffness led to reduction of the size and number of the formed tumorspheres in each cell line (Fig 3.11 C, D). For example MCF7 and MDA-MB-231 cell lines formed the largest and most number of spheroids in their optimum modulus of 5 kPa at each time point which is similar to the moduli of breast tumor tissues reported in the literature [85]. Tumorspheres formed in the softer gels (with modulus of 2 kPa) were smaller in size and

number and cells in the stiffer gels (25 kPa and higher) did not form spheres and remained as single cells or small colonies ($< 25 \mu\text{m}$). The highest number and diameter of spheroids in HCT116 and AGS cancer cell lines was observed in 25 kPa. In the case of U-2 OS cell line the spheroid formation maximized at 50 kPa. As illustrated in Figure 3.11 D, for HCT116 and AGS cell lines increasing the matrix modulus up to 25 kPa increased the number of formed spheres 6 and 4 times, respectively. However, further increase of matrix modulus reduced the number and the size of spheres. Similarly, the highest number and size of formed spheroids for U-2 OS cell line observed at an optimum modulus of 50 kPa.

The effect of hydrogel modulus on average tumorsphere diameter and size distribution with incubation time is shown in Figure 3.7 A and B for 4T1 cells, respectively. The average 4T1 tumorsphere diameter increased from 10 μm at day zero to 80, 140, 30, 15, and 10 μm after 14 days as the gel modulus increased from 2 kPa to 5, 25, 50 and 70 kPa respectively. For 4T1 cells in the softest gel (2 kPa modulus), 25% of the cell aggregates at day 8 had $< 20 \mu\text{m}$ size (single-cell fraction) while there was no single-cell subpopulation in the gel with 5 kPa modulus. Further, for the gel with 5 kPa modulus, 23% and 8% of 4T1 tumorspheres had size in the range of 80–120 and 120–200 μm ,

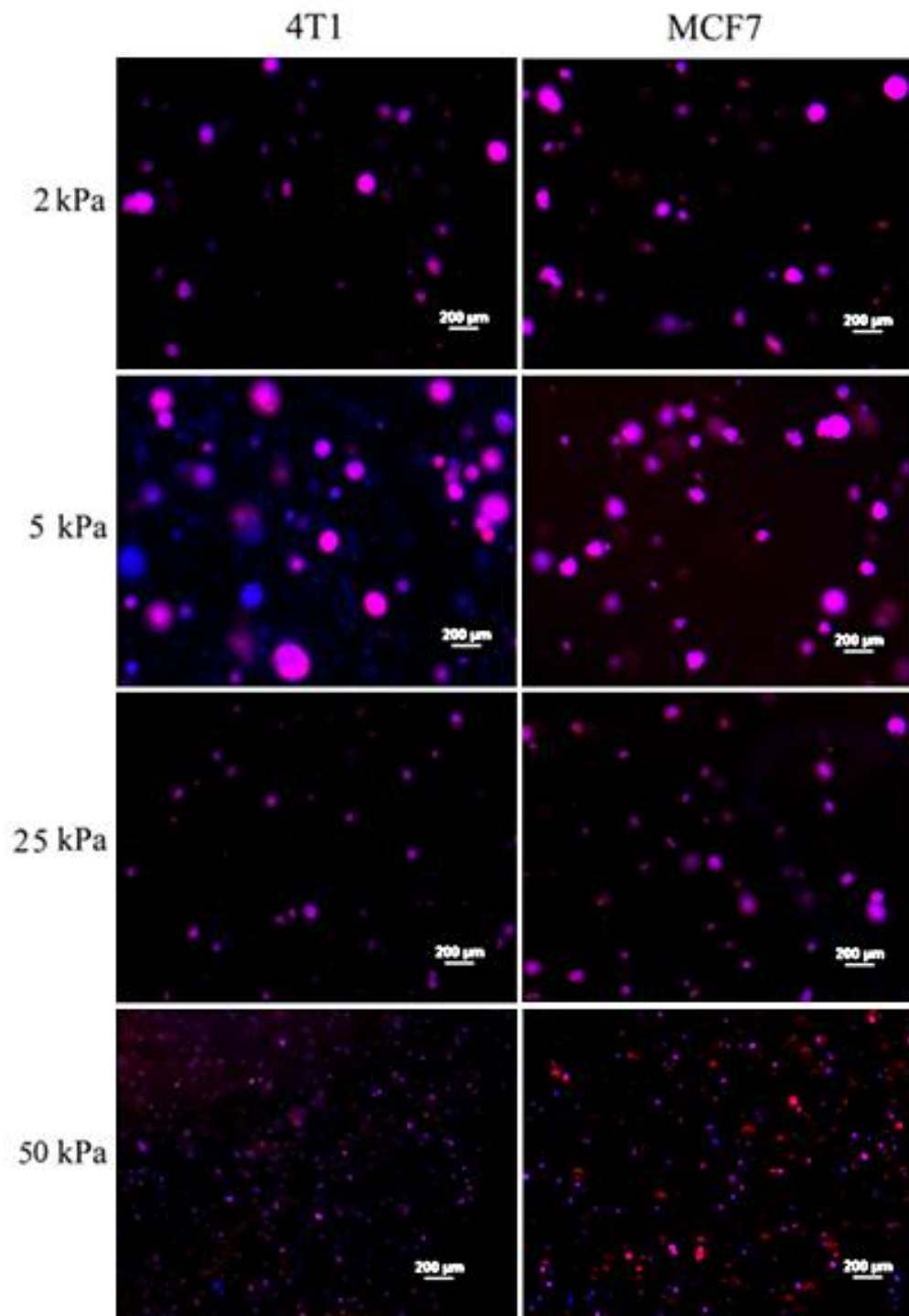


Figure 3.6 Representative images of tumorsphere density for 4T1 (left column) and MCF7 (right column) cells encapsulated in PEGDA hydrogels with elastic modulus of (A) 2 kPa (first row), 5 kPa (second row), 25 kPa (third row), and 50 kPa (fourth row) after 8 days of incubation. At each time point, encapsulated cells were stained with Phalloidin for cytoskeleton (red) and DAPI for nucleus (blue), and imaged with an inverted fluorescent microscope.

3.2.4 TUMORSHERE SIZE AND NUMBER DENSITY

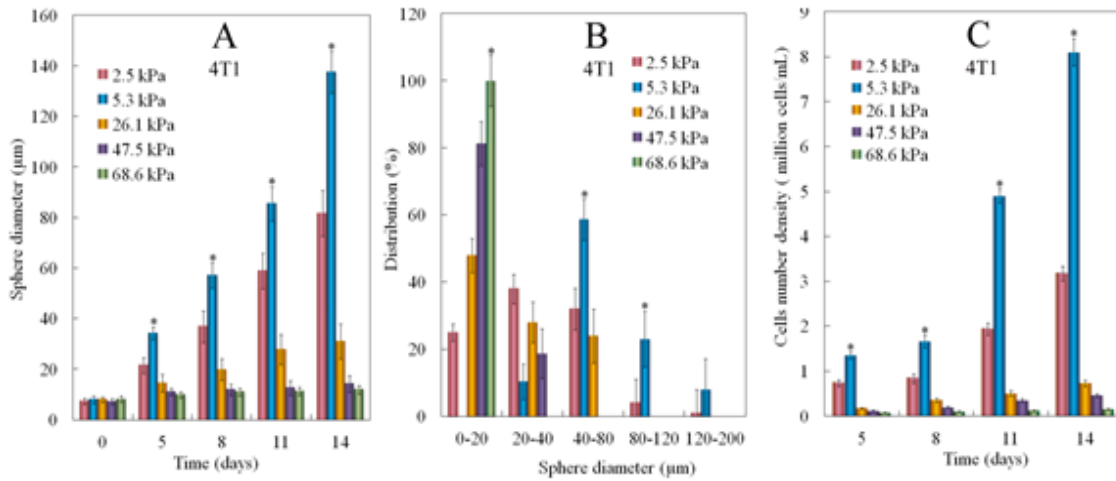


Figure 3.7 Average tumorsphere size (A), tumorsphere size distribution (B), and cell count (C) for 4T1 tumor cells encapsulated in PEGDA hydrogels with different elastic moduli and incubated for up to 14 days. The symbol asterisk indicates statistically significant difference between the test group and all other groups at the same time point

respectively. The fraction of tumorspheres with 0–20µm diameter (single-cell fraction) increased with increasing gel modulus for 4T1 cells and all of the cells in the highest modulus gel (70 kPa) remained as single cells.

The number density of viable 4T1 cells in PEGDA gels with different moduli is shown in Figure 3.7 C. The cell count increased with time for all groups but the gels with moduli of 2 and 5kPa had the highest cell count at all-time points. At each time point, the change in cell count with gel modulus was bimodal; that is, the cell count initially increased for moduli of 2 and 5 kPa and then decreased for gels with moduli > 25 kPa. At day 14, the 5 kPa gel had 3-fold higher 4T1 cells than the 2 kPa gel; the 5 kPa gel had 10-fold higher 4T1 than those gels with > 25 kPa modulus. In general, the gel modulus has similar effects on 4T1 cells. These results demonstrated that the gel with modulus of 5 kPa had the highest potential for tumorsphere formation in the absence of ligand–receptor interactions.

The human cell number density at different moduli is shown in Figure 3.11 B. Although the cell count in all groups increased after 9 days, the highest increase was observed in the optimum modulus of each cell line. This caused a bimodal behavior in cell number density of all cell lines i.e. the cell count increased up to the optimum modulus and decreased with further modulus increase. This is notable in MDA, MCF7 and HCT116 cell lines.

The malignancy level of cancer cell lines can affect the density and size of tumorspheres. For example, it has been shown that nonmalignant MCF10a epithelial cells are relatively insensitive to the matrix stiffness within a wide range of stiffness while cancer cell lines are sufficiently sensitive [86]. The size distribution of spheroids after 9 days shown in Figure 3.11 E confirms this finding. MCF10a cells were almost non-sensitive to matrix stiffness in the range of 2-70 kPa and 100% of cells had an average diameter less than 20 μm . On the other hand, MDA-MB-231 a triple negative breast cancer cell line, showed the highest potential in cells aggregation and spheroids growth. No single-cell subpopulation (less than 20 μm) of MDA-MB-231 cells was observed in the optimum modulus of 5 kPa. Near 75% of the cells population were in the range of 60 to 80 μm for this cell line whereas in MCF7 with a modest level of malignancy, only 20% of the cells were in this range and about 60% of them were in the range of 40-60 μm .

In the optimized modulus of 25 kPa for HCT116 more than 70% of the spheroids were in the range of 40 to 60 μm and about 5% of them were in range 60 to 80 μm . The single-cell fraction increased with increasing the optimum gel modulus. About 50% of spheroids formed in AGS cell line were in the range of 20-40 μm . For U-2 OS about 60% of the spheroids had diameters in this range. For both cases the rest of the spheroids had

diameters less than 22 μm (Fig 3.11 E).

One of the unique properties of CSCs is asymmetrical division and retention of DNA labeling [70]. Based on this feature, BrdU retention is a commonly used method to characterize CSCs. 4T1 cells were labeled with BrdU before encapsulation in the PEGDA gel with 5 kPa modulus and the intensity of BrdU staining was compared with those cells cultured on ultra-low-attachment plates. Figure 3.8 compares BrdU staining of 4T1 cells in suspension culture on ultra-low attachment plates (Fig 3.8 A, C) with those encapsulated in PEGDA hydrogels (Fig 3.7 B, D). Images A and B in Figure 3.8 are after 8 days of culture while images C and D are after 14 days. After 8 and 14 days, cells encapsulated in the gel displayed higher level of BrdU retention than those in suspension cultures, suggesting that the encapsulated tumorspheres had higher fraction of CSCs. The expression of breast CSC markers for tumorspheres grown in PEGDA gels with different moduli is shown in Figure 3.9. Figure 3.9A–D shows the expression of CD44, CD24, ABCG2, and SCA1 for 4T1 cells. ABCG2 of ABC transporter proteins is responsible for CSC drug resistance and SCA1 (stem cell antigen-1) is a cell surface protein known to be associated with breast CSCs [87-89]. CD44 and ABCG2 are well-studied markers in both mouse and human breast CSCs [90, 91]. Although CD24 - is also a marker often used as a breast CSC marker, recent studies indicate that both CD44 + /CD24 - and CD44 + /CD24 + cells display CSC phenotypes in breast cancer cells [92]. 4T1 cells in the gel with elastic modulus of 5 kPa had the highest CD44 expression and lowest CD24 expression for all time points. CD44 expression of 4T1 cells initially increased and reached a maximum at day 8 for 2 and 5 kPa gels and at day 11 for 25 kPa gels. CD44 expression then decreased with incubation time. 4T1 cells encapsulated in the gels with

3.2.5 Tumorsphere marker expression

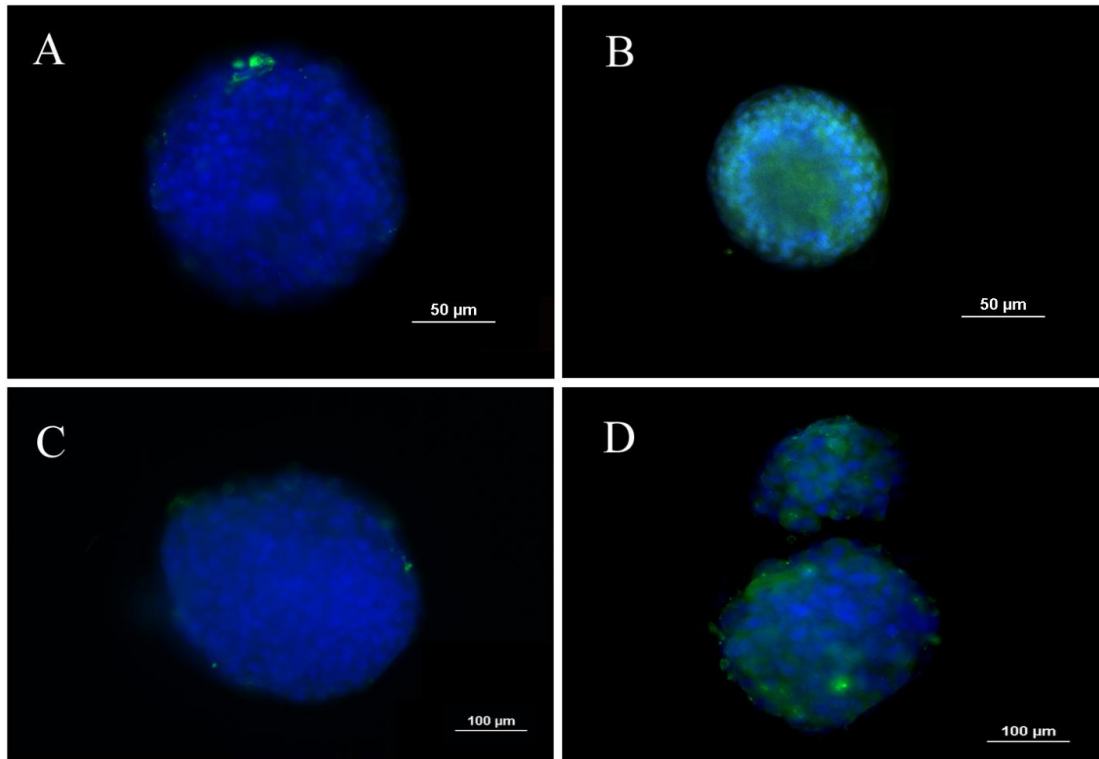


Figure 3.8 BrdU staining of 4T1 tumorspheres formed in suspension culture on low-adhesion plates (A, C) and formed by encapsulation in PEGDA hydrogels (B, D). Images (A) and (B) are after 8 days of incubation while images (C) and (D) are after 14 days. The presence of BrdU in the cells was confirmed by immunofluorescent staining (green). The cell nuclei were stained with DAPI (blue).

moduli of 50 and 70 kPa did not show an increase in CD44 expression in 14 days. At day 8, CD44 and ABCG2 expression of 4T1 cells increased by 2.2 and 1.8 fold with increase in gel modulus from 2 to 5 kPa, respectively. Figure 3.12 illustrates the effect of modulus on the expression of two of these CSC markers for human cancer cell lines in time. CD44 has been extensively used in CSC identification and characterization for different human cell lines [93-96]. Figure 3.12 demonstrates the expression of CD44 and ABCG2 –an ABC transporter protein that is responsible for breast CSCs drug resistance– in MCF7 cell line [87, 88].

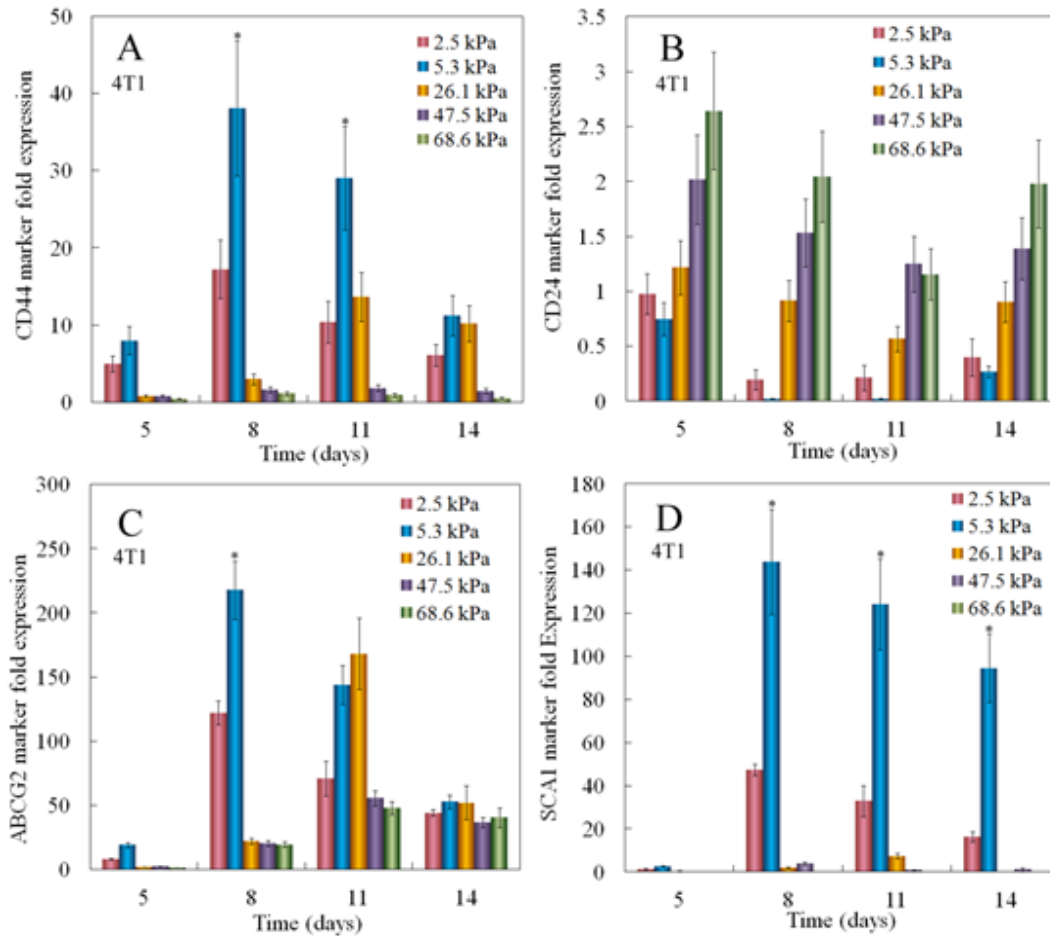


Figure 3.9 Effect of gel elastic modulus on the relative mRNA expression levels of CD44 (A), CD24 (B), ABCG2 (C), and SCA1 (D) markers of 4T1 cells encapsulated in PEGDA hydrogels with incubation time. The mRNA expression levels of the markers for 4T1 cells before encapsulation were used as reference (set equal to one).

MCF7 cells encapsulated in the gel with elastic modulus of 5 kPa expressed the highest level of CD44 and ABCG2 proteins at both time points of 6 and 9 days. The expression for these markers maximized in 5 kPa gels and then decreased sharply at stiffer gels. This biphasic behavior was also observed in MDA-MB-231 breast cancer cell line. Cells had the highest expression of CD44 and EGFR –a cell surface protein associated with CSCs population– at 5 kPa and significantly lower expression in other moduli.

The expression of CD44 and TGF β –a main protein in colon CSCs progression– are

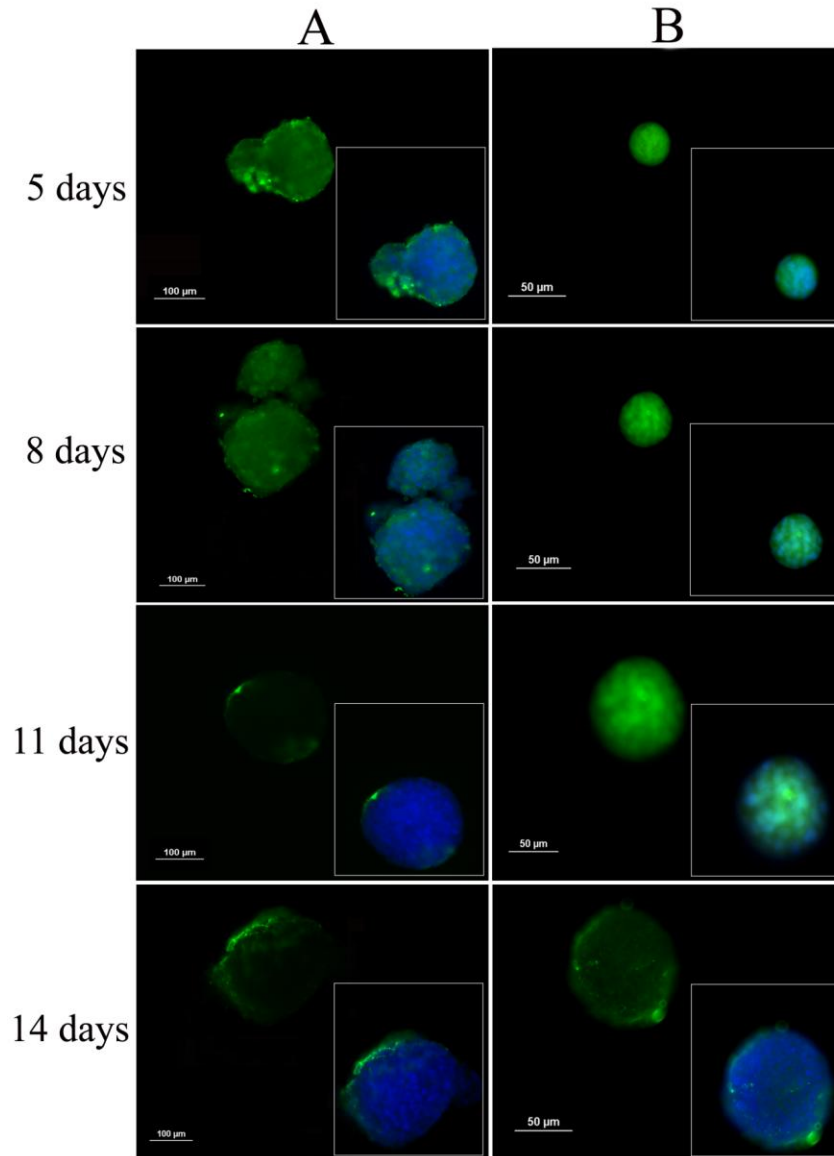


Figure 3.10 Expression pattern of CD44 marker of 4T1 tumorspheres formed in suspension culture on low-adhesion plates (column A) and formed by encapsulation in PEGDA hydrogel with 5 kPa elastic modulus (column B). Images in rows 1, 2, 3, and 4 are after 5, 8, 11, and 14 days of incubation, respectively. The cell nuclei were stained with DAPI (blue).

shown in Figure 3.12. The fold expressions of these markers in the optimum modulus of 25 kPa were more than 3 times higher than the other moduli and the sharp decline from optimum to other moduli is considerable.

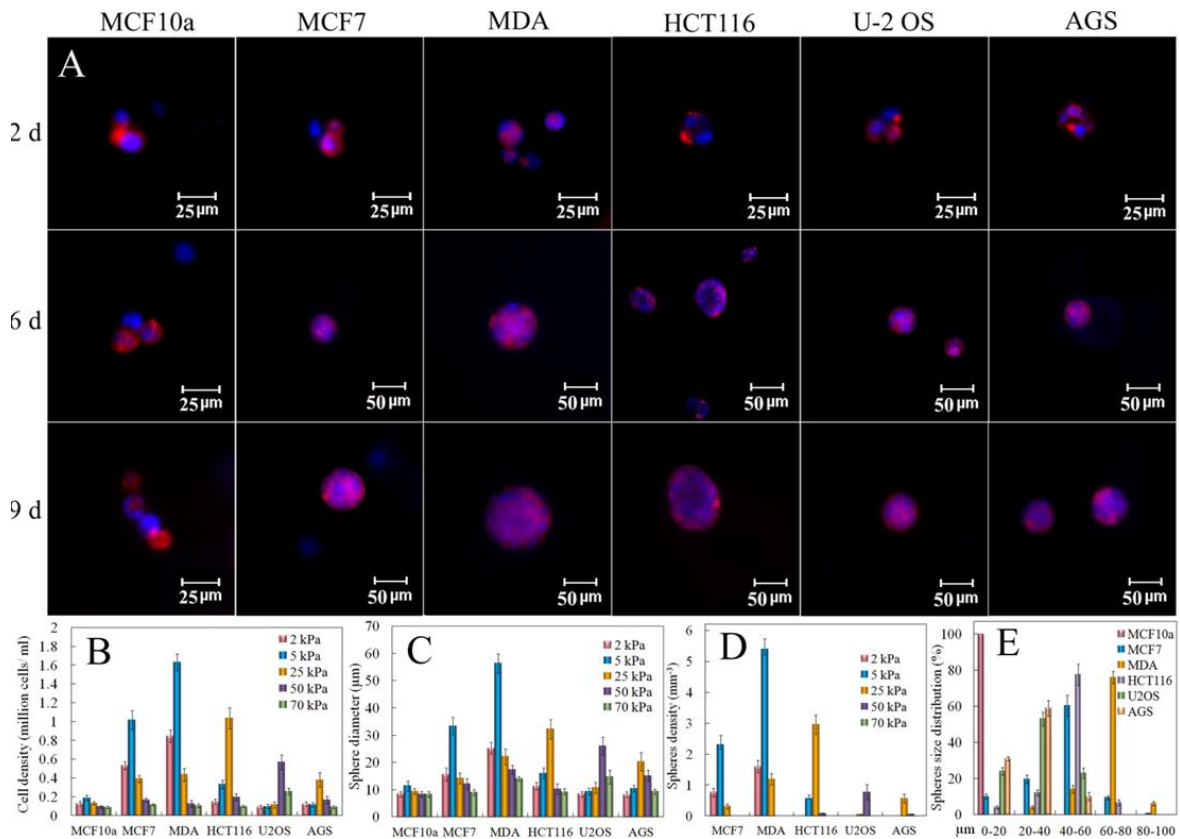


Figure 3.11 Evolution of tumorsphere formation by different tumor cell lines Cells Encapsulated in PEGDA hydrogels with elastic moduli of 5,5,5,25,50, 25 kPa respectively (left to right column) as a function of incubation time. Rows 1, 2, and 3 correspond to incubation times of 2, 6 and 9 days, respectively. At each time point, encapsulated cells were stained with Phalloidin for cytoskeleton (red) and DAPI for nucleus (blue), and imaged with an inverted fluorescent microscope (A). Cells density (B) Average tumorsphere size (C), tumorspheres no. density (D), and tumorspheres size distribution (E) for different tumor cell lines encapsulated in PEGDA hydrogels with different elastic moduli and incubated for 9 days.

A similar behavior was observed for the CD44 and Oct4 markers of AGS cell line. The expression of CD44 and Oct4 markers increased by 3 and 7 times, respectively, with increase in gel modulus from 5 to optimum modulus of 25 kPa and decreased again by 1.8 and 2.3 fold with increase in gel modulus from 25 to 50 kPa (Fig 3.12). The significantly higher fold expression of CD44 and CD133 markers for U-2 OS cell line in 50 kPa indicates that the expression of CSC markers in the optimum modulus correlates with spheroid formation and lack of this ability in cells of other modulus strongly affects the expression of these important CSCs markers (Fig 3.12). Although the size and density

of the spheroids are in correlation with CSCs markers expression, a biphasic behavior was observed in all cell lines that CSCs markers expression rises when spheres start to form but diminishes after a few days of growth. To determine whether tumorspheres in the hydrogel had a higher level of stem cell population than those formed on ultra-low-attachment plates, CD44 immunostaining of the 4T1 cells encapsulated in PEGDA gels (5 kPa modulus) was compared with those cultured on ultra-low-attachment plates after 5, 8, and 11 days of culture, and the results are shown in Figure 3.10. Tumorspheres grown in the gel and on ultra-low-attachment plate both had high level of CD44 staining after 5 and 8 days of culture and the intensity of CD44 staining started to decrease after 8 days of culture for both groups. This was consistent with our CD44 mRNA data (see Fig 3.8). However, tumorspheres grown in the gel had a more intensive CD44 staining than those on ultra-low attachment plates for longer incubation times of 11 and 14 days, suggesting that the 3D microenvironment and gel stiffness modulated the maintenance of stemness in CSCs.

3.2.6 Micropattern fabrication

Topography of ECM is an important biomechanical factor that influences stem cells fate [55]. Recent advances in studying mechanical properties of ECM allow researchers to investigate the higher aspects of ECM biomechanics and their key role in stem cells fate. In this work, layer by layer micropatterning technique was used to employ pre-defined zones of cell encapsulation in PEG hydrogels and study the effect of spatial limitations on the CSCs behavior. MDA-MB-231 cells were encapsulated in the micropatterned hydrogels with optimized modulus of 5 kPa and cultured in stem cells medium up to 14 days, as shown in Figure 3.14. The presented fluorescent images highlight the level of spheroid

days. Images of cell tracker stained cells in patterns with 75, 100, 150, and 250 μm diameters after 2 days of encapsulation are shown in Figure 3.13.

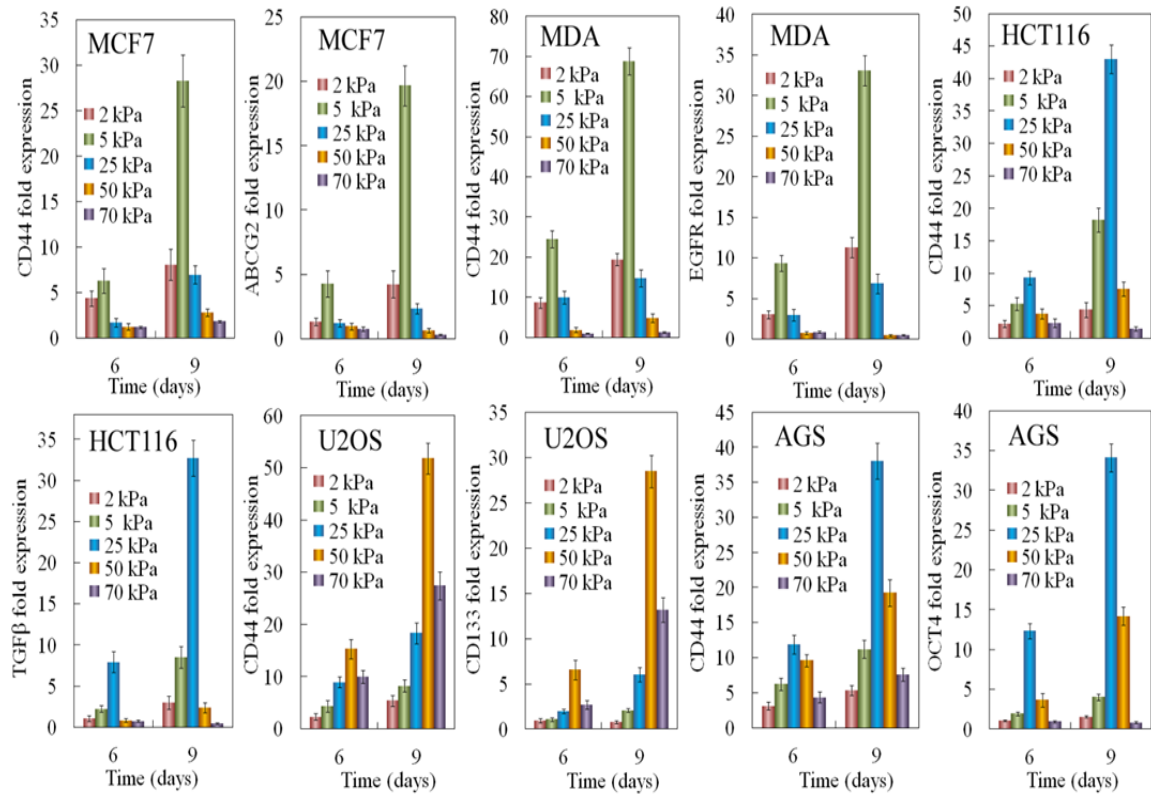


Figure 3.12 Effect of gel elastic modulus on the relative mRNA expression levels mRNA expression of CSCs markers for MCF7, MDA-MB-231, HCT116, U-2 OS and AGS cell lines encapsulated in PEGDA hydrogels with incubation time. The mRNA expression levels of the markers before encapsulation in the gel were used as reference in all cell lines.

formation with incubation time for MDA-MB-231 cells in different sizes of micropatterns with diameters of 75 μm (Fig 3.13, row 1), 100 μm (Fig 3.13, row 2), 150 μm (Fig 3.13, row 3), and 250 μm (Fig 3.13, row 4). Columns 1-3 in correspond to incubation time periods of 2, 9, and 14 days, respectively. Although after 14 days of encapsulation, the spheroids formed at all different sizes of micropatterns, a significant change in the size of the formed spheres was observed (column 3 in Fig 3.14).

The evolution of cell number density and spheres size for MDA-MB-231 cells in

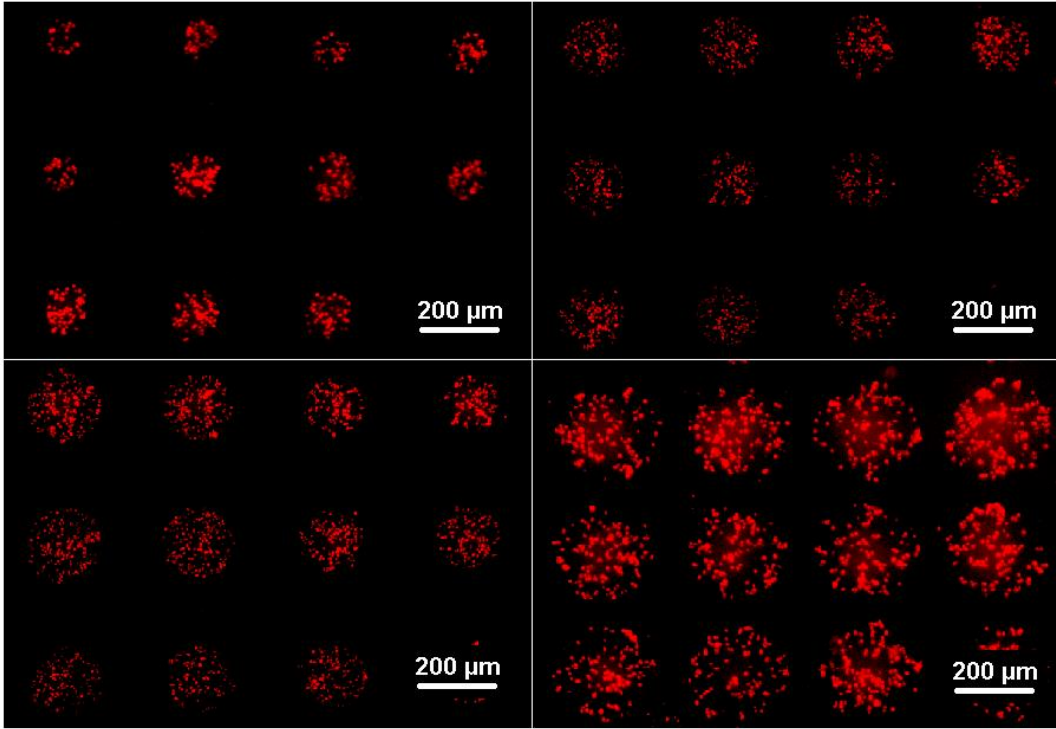


Figure 3.13 Effect of patterns size on tumorsphere formation MDA-MB-231 cells encapsulated in PEGDA patterned hydrogel with 5 kPa of elastic modulus and 75,100,150 and 250 micrometer of patterns diameter. Encapsulated cells were stained with cell tracker.

micropatterns at a time period of 2 weeks are presented in Figure (13 M, N). While the number of cells in 75 or 100 micropatterns remained at a low level, the cell number density of control (non-patterned hydrogel) or 250 μm patterns increased significantly after 2 weeks (Fig 3.14 M) suggesting that the size limitation affects the rate of proliferation in tumor cells. Similarly, the diameters of uniformly sized tumorspheres in 75 and 100 μm patterns were consistently smaller than tumorspheres formed in control or 250 μm patterns with various sizes of tumorspheres. After 14 days of encapsulation in the gel, the average diameters of spheres formed in non-patterned gel and 250 μm patterns were approximately 20 and 40 μm greater than those formed in 75 or 100 μm , respectively (Fig 3.14 N).

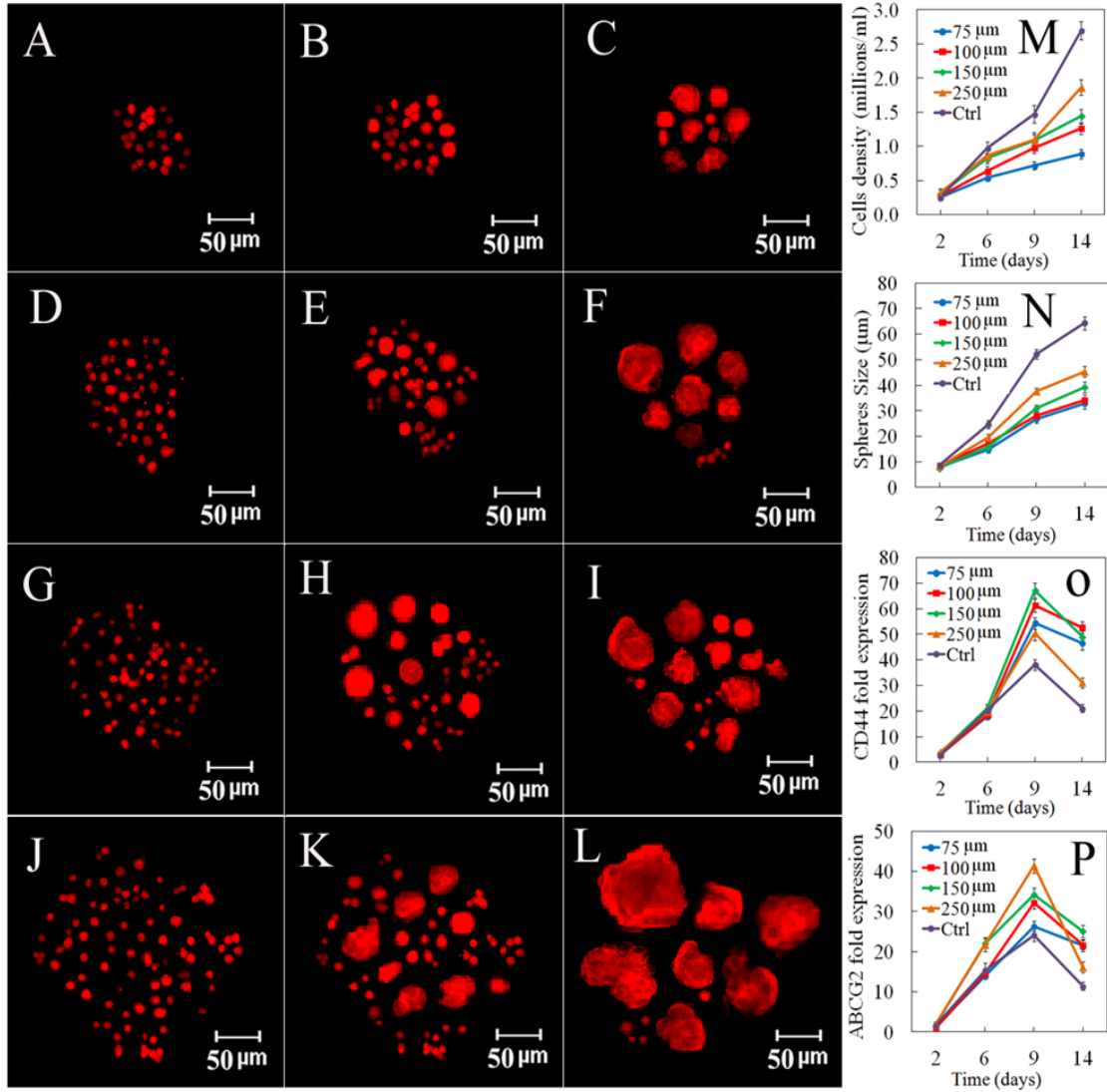


Figure 3.14 Effect of patterns size on tumorsphere formation and the relative mRNA expression levels. MDA-MB-231 cells encapsulated in PEGDA patterned hydrogel with 5 kPa of elastic modulus. Pattern with 75 μ diameter after 2 days (A). Pattern with 75 μ diameter after 9 days (B). Pattern with 75 μ diameter after 14 days (C). Pattern with 100 μ diameter after 2 days (D). Pattern with 100 μ diameter after 9 days (E). Pattern with 100 μ diameter after 14 days (F). Pattern with 150 μ diameter after 2 days (G). Pattern with 150 μ diameter after 9 days (H). Pattern with 150 μ diameter after 14 days (I). Pattern with 250 μ diameter after 2 days (J). Pattern with 250 μ diameter after 9 days (K). Pattern with 250 μ diameter after 14 days (L). Cells density (M) Average tumorsphere size (N) mRNA expression levels of different markers (O, P).

The expressions of breast CSC markers (CD44 and ABCG2) for cells encapsulated in different sizes of micropatterns are shown in Figure 3.13 O, P. After 9 days of culturing, CD44 fold expression increased nearly 60 times of the initial level in micropatterns of

150 μm and smaller then decreased slightly after 14 days. However, 40 and 30-fold expression of this marker for 250 μm and non-patterned hydrogel showed a sharp decrease from 9 to 14 days Fig 3.14 O. Similarly, in case of 250 μm and control group the expression of ABCG2 marker increased significantly in the first 9 days followed by a sudden decrease Fig 3.14 P suggesting that spheroids with consistent diameters may expand the population of CSCs in the same culture and maintain stemness properties for a longer time compared to traditional methods of culturing tumor spheroids.

Recent advances in cancer research have highlighted the importance of CSCs interaction with the ECM at cellular and molecular level. The ECM stiffness regulates proliferation and differentiation of many cell types [97-99]. Earlier studies demonstrated that increasing ECM stiffness deregulates cellular functions and causes cancer development. On the other hand, decreasing the rigidity and normalizing the tensional homeostasis can return them to normal conditions. For example, the stiffness of cancerous breast tissue is 20 times higher than that of normal tissue with approximate rigidity of 0.2 kPa [100]. Deviations in the mechanical properties of the normal tissues not only affects the shape and morphology of the cells, but also cause phenotypic and functional changes, e.g. while proliferation and morphogenesis of normal mammary epithelial cells tune with soft ECM cells interacting with progressively stiffening cancerous tissue become more contractile in morphology and over-responsive to environmental cues [57,58]. The malignancy level of cancer cell lines can affect the density and size of tumorspheres. For example, it has been shown that nonmalignant MCF10a epithelial cells are relatively insensitive to the matrix stiffness within a wide range of stiffness while cancer cell lines are sufficiently sensitive [60]. The size distribution of spheroids after 9 days shown in Figure 3.11 E

confirms this finding. MCF10a cells were almost non-sensitive to matrix stiffness in the range of 2-70 kPa and 100% of cells had an average diameter less than 20 μm . On the other hand, MDA-MB-231 a triple negative breast cancer cell line, showed the highest potential in cells aggregation and spheroids growth. No single-cell subpopulation (less than 20 μm) of MDA-MB-231 cells was observed in the optimum modulus of 5 kPa. Near 75% of the cells population were in the range of 60 to 80 μm for this cell line whereas in MCF7 with a modest level of malignancy, only 20% of the cells were in this range and about 60% of them were in the range of 40-60 μm . These results suggest that the response of cancer cells to matrix stiffness is not only dependent on the cancer but also on malignancy of the cancer. Further, it has been reported that nontumorigenic breast epithelial cells loose cell polarity and increase proliferation when cultured in matrices with 4.5 kPa stiffness [37]. In addition, normal murine mammary gland or well-differentiated mammary epithelial cells cultured in high-density collagen matrices display an invasive phenotype [101]. Cells respond to the mechanical properties of their ECM in different hydrostatic, tensional or compressional levels [44]. The dynamic balance between the intercellular and external forces results in the formation of interfacial stresses between the microenvironment and the cytoskeleton. These forces enable cells to sense cell-cell or cell-matrix resistance leading to the regulation of certain physicochemical pathways [101, 102]. Tumorogenesis mechanisms originate from the accumulation of membrane proteins, conformational changes, cytoskeletal contraction, and re-distribution of subcellular components. Direct sensing of cytoskeletal tensions originated mainly from actin stress fibers may be another possible contributor to re-distribution of subcellular components and activation of tumorigenic mechano-transductive pathways. Certain

proteins and ion channels present on cell membranes also initiate cell sensing of ECM mechanics leading to ion fluxes and additional biochemical effects [25]. The cell response to stiffness in the inert PEG matrix may be through the ECM secreted by the encapsulated tumor cells. For example, human mesenchymal stem cell (hMSCs) encapsulated in PEG hydrogels, in the absence of adhesive ligands, secret their own ECM through which differentiation is directed by mechanotransduction[103].According to rubber elasticity theory, the gel elastic modulus is proportional to the density of elastically active chains or crosslink density[104]. The network crosslink density increased with increasing acrylate concentration in PEGD precursor solution, leading to the increase in matrix modulus. The range of elastic moduli selected in this study was based on the reported stiffness of breast tumor tissue [85, 100].Increasing evidence suggests that CSCs are responsible for tumor initiation and metastasis as well as drug resistance [105].Maintenance of CSCs *in vivo* is highly dependent on the tumor microenvironment.

Stem cell microenvironments *in vivo* are polarized structures with individual stem cells exposed to different niche components [106, 107]. We have shown in this study that the formation of spheroids by tumor cells encapsulated in an inert matrix is biphasic with respect to matrix modulus in the 2–70 kPa range. The initial increase in tumor sphere size and cell number density with elastic modulus may be attributed to a deviation from normal tissue stiffness leading to matrix reorganization and change in the number and lifetime of integrin-mediated interactions and related pathways[59]. It has been reported that the sphere size of breast cancer cells encapsulated in collagen gels increased with elastic modulus from 0.17 to 1.20 kPa [37].In another study, it was shown that the

proliferation and sphere size of hepatocellular carcinoma cells encapsulated in PEG–collagen gels increased with decreasing elastic modulus from 4 kPa (corresponding to the modulus of healthy liver) to 0.7 kPa.⁷⁰ A decrease in sphere size and cell number for gel moduli > 5.3 kPa can be attributed to a decrease in mesh size and increase in retractive force of the gel network, leading to a negative contribution on the cell proliferation and sphere formation [108]. Variety of size and density in formed tumor spheres of each cell line may also be attributed to the fact that the stiffness of PEG hydrogel network increases with decrease in the mesh size. By increasing macromer concentration in the range of 2 to 70 kPa, the mesh size decreased sharply from 90 to 25 nm. The reduction in mesh size may hinder the diffusion of nutrients or oxygen and restrict the motility and proliferation ability of the cells [109-111] e.g., the size and density of the tumor spheres formed by U-2 OS cell line at 50 kPa were smaller compared with MCF7 breast tumor spheres formed at 5 kPa. Therefore, the bimodal effect of gel modulus on tumor sphere formation may be due to the changes in the network mesh size, as well as the gel modulus, that can affect cell–matrix interactions and nutrient diffusion. The formation of tumor spheres is associated with breast CSC markers, suggesting that sphere formation in the gel matrix is not caused by simple cell aggregation but by CSCs. It has been shown that matrix stiffness can alter the expression of CSC markers in hepatocellular carcinoma cells encapsulated in a collagen matrix [51]. Unlike collagen and other biological gels, varying PEGDA macromer concentration only changes the gel stiffness, not the ligand density in the matrix. Our results suggest that the stiffness of the tumor tissue alone is sufficient to affect the fate of tumor cells. A biphasic behavior of CSC marker expression with time may be attributed to the fraction of CSCs in the gel. The CSC fraction initially

increased with loss of normal tumor cells in the inert low-adhesive PEGDA gel. Then, the fraction started to decrease as the rate of differentiation of CSCs to normal cancer cells was higher than the rate of transformation of differentiated cells to CSCs[112]. The highest expression of CSCs markers at day 8 and 9 with largest tumorsphere size for cancer cells encapsulated in the gel with optimum modulus indicates the existence of highest fraction of stem-like subpopulation at this matrix modulus. The fraction of CSCs in a tumor also depends on the microenvironment[105]. The concentration of oxygen and nutrients in the center of large tumorspheres may be lower than that for small spheres, leading to the formation of a hypoxic condition in the central part of the spheres in the gel, which in turn can increase the expression of CSC markers[105, 111]. Naturally derived gels, such as alginate and agarose gels, have also been used to study the behavior of breast cancer cells under a 3D condition. For example, highly invasive rat mammary carcinoma MTLn3-Mena cells form tumorspheres when encapsulated into alginate hydrogels, and the formation of tumorsphere can be inhibited by coculture with embryonic stem cells [26]. In another study, encapsulation of neoplastic cells in a growth-restricting hydrogel composed of agarose matrix leads to the selection of a stem cell subpopulation and the formation of tumorspheres[27]. However, our work demonstrates for the first time that CSCs can be maintained in the inert microenvironment of synthetic PEG hydrogels and the elastic modulus of the gel affects the growth of tumorspheres. The growth and maintenance of CSCs in other synthetic gels, such as polyhydroxyethyl methacrylate, polyvinylpyrrolidone, and polyvinyl alcohol, is of interest and will be investigated in future works. Our results also show that cancer cells form higher number of tumorspheres when encapsulated in the PEG hydrogel

compared with suspension cultures on low-adhesion plates. There are two possible explanations for this observation. One explanation is that the 3D hydrogel culture system more closely mimics the *in vivo* tissue environment than the suspension cultures with respect to the survival of CSCs. Evidence supporting this notion is that cancer cells have fewer number of CSCs in 2D cultures than the *in vivo*[27]. The elastic retroactive force of the gel network can promote viability and proliferation of CSCs by enhancing specific proteins activation [113, 114]. The other explanation is that the retroactive force of the gel can induce the transformation of differentiated bulk cancer cells into CSCs. The transformation between CSCs and differentiated cancer cell is not unidirectional. Recent studies indicate that inducing epithelial-to-mesenchymal transition (EMT) is sufficient to transform a differentiated cancer cell into a CSC [115, 116]. In the process of EMT, tumor cells undergo cytoskeletal reorganization with subsequent changes in cell adhesion. At the molecular level, the key features of EMT include the altered expression of cell membrane proteins, such as E-cadherin and b-catenin, and cell polarity. It is known that mechanical properties as well as biochemical composition in the tumor microenvironment play profound roles in EMT [117, 118]. It is possible that the hydrogel stiffness shifts the balance of EMT by regulating the conformation of cell membrane receptors and cell polarity. One example of such mechanism is epidermal growth factor receptor (EGFR) signaling that has been associated with breast CSC maintenance [119]. Compression of the cell membrane by the gel refractive force can shrink the interstitial space and increase the local ligand and receptor concentrations, thus increasing the autocrine EGFR signaling [120]. Several signal transduction pathways, such as Notch, Wnt, and Hedgehog, have been identified to be critical for CSC maintenance[121]. It is

unclear how these pathways are regulated by the matrix modulus as these pathways are normally activated by ligand binding to cell surface receptors, which was absent in PEGDA gels. A possible explanation is receptor clustering induced by compression of the cell by the elastic retractive force of the gel network. Future work should focus on the effect of gel modulus, in the absence of ligand–receptor interaction, on the expression and activity of the components of these pathways and how stiffness modulated tumorsphere formation is altered when these pathways are blocked. It should be mentioned that the effect of matrix modulus on viability, growth, and differentiation of normal stem cells has been investigated. For example, the fate of MSCs encapsulated in alginate or agarose gels conjugated with cell-binding RGD peptides is regulated by the elastic modulus of the matrix. The encapsulated MSCs differentiated to the osteogenic lineage in the gel with an intermediate modulus (11–30 kPa) while they differentiated into the adipogenic lineage in the gel with a low modulus (2.5–5 kPa).²⁶ Similarly, MSCs encapsulated in PEG–silica gels with an intermediate elastic modulus (10–30 kPa) display edosteogenic phenotype [86]. It appears that matrix modulus affects the differentiation of normal stem cells while it affects maintenance and growth of tumorspheres in the case of CSCs. In this work, the effect of matrix modulus on tumorsphere formation and maintenance of CSCs was investigated in an inert matrix without the interference of other factors.

In vivo, the geometrical constraints of the niche controls geometry, morphology and functionality of the stem cells [55][94, 97]. However removing the cells from their native tissue and culturing them *in vitro* culture systems will hinder the microenvironmental interactions and their relevant functionalities. Thus, culturing cancer cells in confined

areas of micropatterns may provide a useful model to mimic the spatial limitations of ECM and neighboring cells [55].

PEGDA micropatterned hydrogel defines an *in vitro* culture system that controls the proliferation and size of tumorspheres. The size of tumorspheres is a critical factor in maintenance of CSCs properties. The spheres with large diameters act as a barrier for soluble oxygen and nutrients and may lead to stem cells differentiation. Spheroids with consistent size and homogeneous population of cells may be used as a reliable model in different studies such as investigating the diffusion gradients of soluble factors across the spheroids [55, 122].

PEGDA hydrogels may be introduced as an inert 3D microenvironment for studying the individual effects of different parameters (including the modulus) on the survival and maintenance of 4T1 murine breast CSCs. The current study showed that the effect of elastic modulus is not limited to 4T1 cancer cells but extends to different human cancer cell lines. In particular human breast, colon, gastric and bone cancer cell lines were also able to sense and respond to change in elastic modulus through the change in the rate of tumorigenicity. The optimized modulus for regulating tumorigenic capacity of cancer cells was markedly different for different cell lines and it was found that at certain modulus the proliferation capacity of cancer cells can be completely diminished.

Compared to conventional *in vitro* methods of culturing tumor spheroids in low-adhesion plates, the PEGDA engineered matrix increased the tumorigenicity (density and number of tumorspheres) and maintained CSCs properties for longer time periods. This could be reasonably attributed to the suitable structure and mechanical properties of the matrix.

Consequently the encapsulated cells mimic the actual tissue mechanobiology and

increase the possibility of EMT or similar biological events.

Our understanding of CSC maintenance mechanisms remains limited due to numerous uncertainties in the transduction pathways of CSCs [3]. This synthetic micro-engineered matrix can be used as a tool to improve the cellular interaction level and optimize temporal condition of microenvironment maintaining stem cells properties *in vitro* and studying the regulatory effect of specific proteins in biological pathways on CSC maintenance without interference of other factors.

3.3 EFFECT OF CELL-BINDING PEPTIDES IN CSCS MAINTANANCE

3.3.1 CD44 BINDING PEPTIDE CONJUGATED TO PEGDA INERT MATRIX ON MAINTENANCE OF 4T1 BREAST CANCER STEM CELLS AND TUMORSHERE FORMATION

We have shown shat tumorsphere formation in the PEGDA gel depended strongly on the gel modulus [123]. Both 4T1 mouse and MCF7 human breast carcinoma cells formed spheres in the gel with 5 kPa modulus, and the sphere formation was correlated with the expression of CSC markers [123]. To determine whether non-cancerous cells could form spheres in the PEGDA gel, MCF10a normal human breast epithelial cells were encapsulated in the gel with 5 kPa modulus and sphere formation was compared with those of 4T1 and MCF7 breast cancer cells. Fluorescent images a-c in Figure 3.15 show that 4T1 and MCF7 cancer cells encapsulated in the gel formed spheres but not the normal MCF10a cells, suggesting that the spheres originated from the CSC sub-population of 4T1 and MCF7 cancer cells. The cell number density, sphere size, and size distribution for 4T1, MCF7 and MCF10a cells encapsulated in the gel after 6 and 9 days incubation in stem cell culture medium are shown in Figures 1d-1f. The cell density of

4T1 and MCF7 cells significantly increased for both time points, while that of MCF10a remained at a low level (Figure 3.15 d), suggesting that the PEGDA gel promoted the proliferation of tumor cells, but not the normal cells. The density of 4T1 tumorspheres was slightly higher than that of MCF7 after 6 or 9 days of incubation. 4T1 cells also formed larger spheres than MCF7 as shown in Figure 3.15 e. After 9 days of culturing in the gel, nearly 40% of the 4T1 spheres were larger than 80 μm while most of the MCF7 spheres were between 40 and 80 μm (Figure 3.15 f). MCF10a remained as single cells in the gel with size smaller than 20 μm . The expressions of breast CSC markers CD44, CD24, and ABCG2 for the encapsulated cells are shown in Figures 1g-1i. After 6 days of incubation, CD44 expression level in 4T1 and MCF7 cells increased by 10 folds of the initial level (Figure 3.15 g). CD44 expression was further increased in 4T1 cells 9 days after encapsulation. However, as reported previously, the expression of CD44 in 4T1 and MCF7 cells started to decrease after 11 days of incubation irrespective of the extent of cell viability and the increase in tumorsphere size [123]. The expression of CD24 was significantly reduced in 4T1 cells but increased slightly in MCF7 (Figure 3.15 h). Although CD44⁺/CD24⁻ cells are considered breast CSCs, the expression of CD24 as a CSC marker in MCF7 is not conclusive. Previous studies have indicated that CD44⁺/CD24⁻ and CD44⁺/CD24⁺ cells both display CSC phenotypes in MCF7 cells [92]. The discrepancy may be due to different primers used for real time PCR quantification, and antibodies used for cell sorting as well as the methods used for analysis. The expression of ABCG2, a subunit of ABC transporter that is responsible for the drug resistance of CSCs was also increased in 4T1 and MCF7 cells (Figure 3.15 i). On the other hand, the expression of these markers in MCF10a cells did not change.

Figure 3.16 a-c shows representative images of live (green) and dead (red) 4T1 cells encapsulated in PEGDA gels with 5 kPa modulus after 2 (a), 6 (b) and 12 (c) days, respectively. The insets are the corresponding figures in the 70 kPa gel. For 5 kPa gel, cell viability after 2, 6, and 12 days increased from $91\pm3\%$ to $94\pm4\%$ and $97\pm2\%$, respectively. For the high modulus 70 kPa gel, no tumorsphere formed and cell viability decreased from $89\pm4\%$ at day 2 to $84\pm3\%$ and $78\pm2\%$ at days 6 and 12, respectively. Based on these results, the effect of peptide conjugation on tumorsphere formation was investigated with 4T1 cells in the PEGDA gel with 5kPa modulus and incubation time of 9 days.

The CD44+/CD24- marker expression is widely used for identification of breast CSCs. Flow cytometry analysis of MCF7 cells isolated from the gel is shown in Figure 3.17. The percentage of CD44+/CD24- cells before encapsulation in the gel was 2% (Figure 3.17 a) but it increased to 53% (Figure 3.17 b) and 76% (Figure 3.17 c) after 3 and 8 days incubation in the gel, respectively. However, the percent CD44+/CD24- cells decreased to 27% after 11 days incubation in the gel (Figure 3.17 d). These results are consistent with our previous results in which the CD44 mRNA expression of 4T1 and MCF7 cells initially increased with time, then began to decrease after 14 days of incubation in the gel [123]. The flow cytometry results demonstrate that the percentage of CSCs in the population of cells encapsulated in the gel increased dramatically after 8 days with incubation time and tumorsphere formation. Since the percentage of live cells in the gel increased with incubation times (see Figure 3.16), the decrease in the percentage of CSCs at day 11 (Figure 3.17 d) was presumably due to the differentiation of CSCs.

It has been shown that CD44bp inhibits breast tumorsphere formation and maintenance of

CSCs *in vitro*[79]. The focus of this work was to test the effect of cell binding peptides including CD44bp that interacts with the CD44 receptor up-regulated on CSCs, conjugated to the PEGDA hydrogel on tumorsphere formation in 4T1 tumor cells. Groups included the PEGDA gel without peptide conjugation (control, labeled as Ctrl in Figure 3.18), the gel with CD44bp or scrambled CD44bp (s-CD44bp) dissolved in the gel and in the culture medium to maintain constant peptide concentration (labeled as Dis), and the gel with CD44bp or s-CD44bp conjugated to the gel (covalent attachment, labeled as Conj). Fluorescent images a-d in Figure 3.17 show the tumorspheres formed in conj CD44bp, conj s-CD44bp, dis CD44bp, and dis s-CD44bp, respectively.

Tumorsphere formation was abolished when 4T1 cells were encapsulated in the CD44bp conjugated gel, indicating the importance of CD44 signaling in the maintenance of CSCs. The effect of CD44bp was consistent with previous reports [79]. However, CD44bp dissolved in the gel (images c and d) did not inhibit sphere formation. These results suggested that CD44bp did not function as a soluble chemokine to inhibit CSC proliferation but functioned within the insoluble part of the ECM. We also tested the effect of a scrambled CD44bp (s-CD44bp). Conjugated or dissolved s-CD44bp had no significant effect on tumorsphere formation, indicating that bioactivity was specific to CD44bp. Figures 4e and f show the effect of CD44bp on cell number density and sphere size of 4T1 cells encapsulated in the gel after 9 days of incubation. The 4T1 cell density in the gel reached $14 \times 10^6/\text{mL}$ after 9 days with $1.4 \times 10^5/\text{mL}$ initial cell seeding in the gel. The density of 4T1 cells in the gel with CD44bp (conjugated or dissolved and with or without mutation) were lower compared with the gel without any peptide. However, cells in the conj CD44bp gel had the strongest effect on cell density and completely abolished

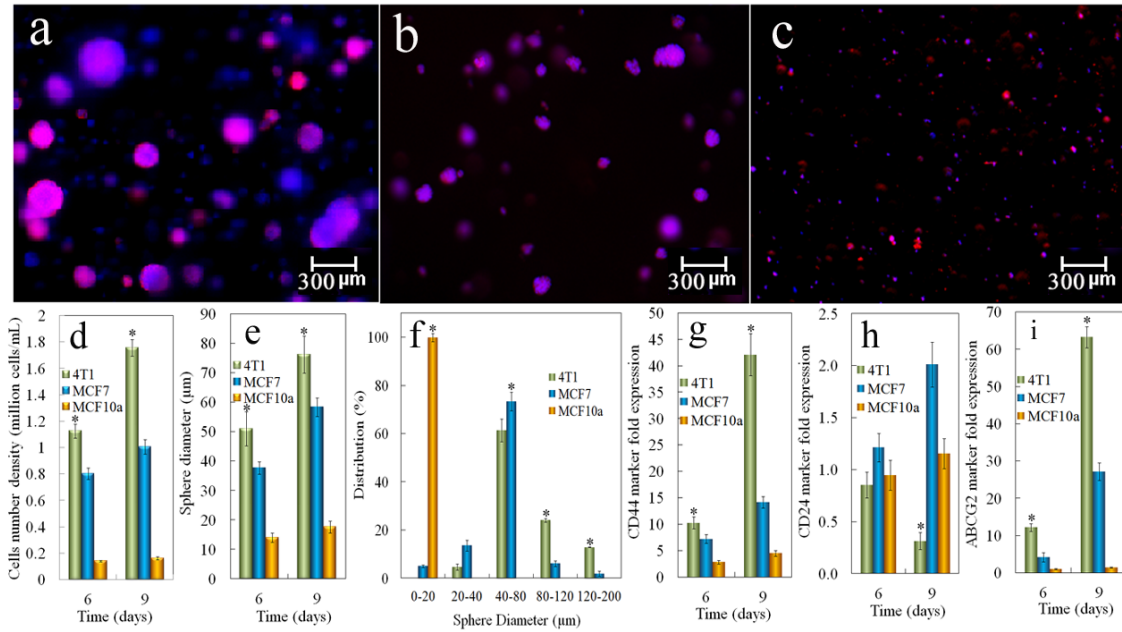


Figure 3.15 Sphere formation and the effect of cell type encapsulated in PEGDA gel on the expression of CSC markers. Representative fluorescent images of the tumorsphere size and distribution for 4T1 (a), MCF7 (b), and MCF10a (c) cells encapsulated in PEGDA gels (1.46105 cells/ml), and cultured in stem cell culture medium. Encapsulated cells were stained with phalloidin for cytoskeleton (red) and DAPI for nucleus (blue). Effect of cell type on cell number density (d) and tumorsphere diameter (e) for tumor cells encapsulated in PEGDA hydrogel and incubated in stem cell culture medium for 6 or 9 days. The sphere size distribution (f) was determined 9 days after encapsulation. Effect of cell type on CD44 (g), CD24 (h) and ABCG2 (i) mRNA marker expression for tumor cells encapsulated in PEGDA hydrogel and incubated in stem cell culture medium for 6 or 9 days. RNA levels of the cells were normalized to those at time zero. A star indicates a statistically significant difference ($p,0.05$) between the test group and the groups with different cell type in the same time point.

sphere formation (Figure 3.18 a). The expression of CSC markers, CD44, CD24, ABCG2 and SCA1 was also determined and the results are shown in Figures 4 g to j, respectively. 4T1 cells in the CD44bp gel that formed spheres (conj s-CD44bp, dis CD44bp and dis s-CD44BP) had high expressions of CD44, ABCG2 and SCA1 and low expression of CD24. On the other hand, cells in the conj CD44bp gel, which did not form tumorspheres, had decreased expressions of CD44, ABCG2 and SCA1, and increased expression of CD24. These results indicated that tumorsphere formation by 4T1 cells in the gel correlated with the CSC population.

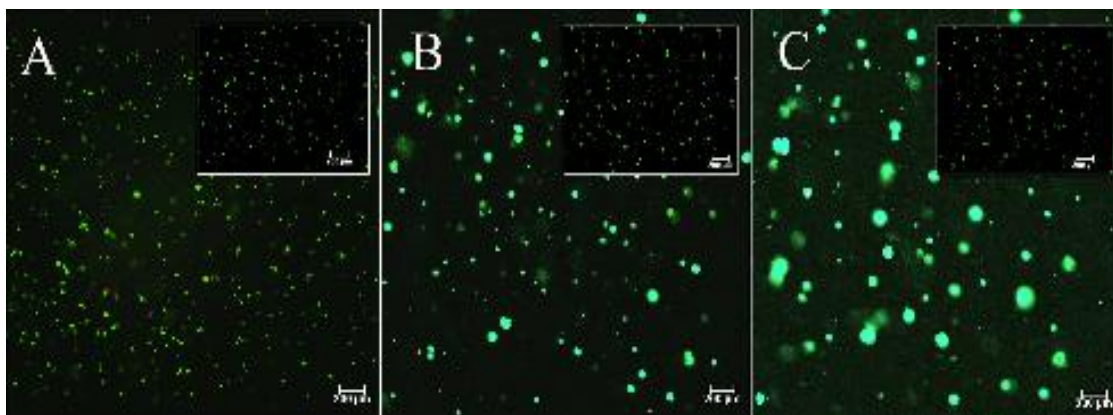


Figure 3.16. Viability of the cells encapsulated in PEGDA gel. Representative images of live (green) and dead (red) 4T1 cells encapsulated in PEGDA gels with 5 kPa modulus and cultured in stem cell culture medium for 2 (a), 6 (b) and 12 (c) days. Cells were stained with cAM/EthD for live (green) and dead (red) cell imaging. The insets in (a) to (c) are live/dead images of 4T1 cells in PEGDA gels with 70 kPa modulus after 2, 6, and 12 (day), respectively.

3.3.1.1 EFFECT OF CD44 BINDING PEPTIDE ON 4T1 TUMORFORMATION *IN VIVO*

It is well established that tumor growth *in vivo* requires a permissive environment that can support vascularization and matrix remodeling [124, 125]. Therefore, a degradable version of PEGDA gel (dPEGDA) was used to investigate the effect of CD44bp conjugated to the gel on tumor formation *in vivo* by the encapsulated 4T1 cells. Groups included 4T1 tumorspheres injected directly without the gel, gels without cell, gels without peptide conjugation but with 4T1 tumorspheres, and gels with 4T1 cells conjugated with CD44bp. The gels without cell did not form a visible tumor after 4 weeks (Figure 3.19). Tumors became measurable after 10 days with direct subcutaneous injection of 4T1 tumorspheres. 4T1 tumorspheres in the gel without CD44bp conjugation also formed a tumor after 13 days of inoculation. Even though the formation of tumor was delayed when cells were encapsulated in the gel, the growth rate (the slope of the tumor size curve) did not differ significantly between the group with 4T1 in PBS and 4T1

in the gel (Figure 3.19). The observed lag time in tumor formation for the encapsulated cancer cells is presumably related to the degradation time of the gel and connection of the tumor cells to the surrounding tissue [126]. However, 4T1 cells encapsulated in the conj CD44bp gel did not form a visible tumor after 4 weeks of inoculation, indicating that CD44bp conjugated to the gel inhibited tumor formation *in vivo*.

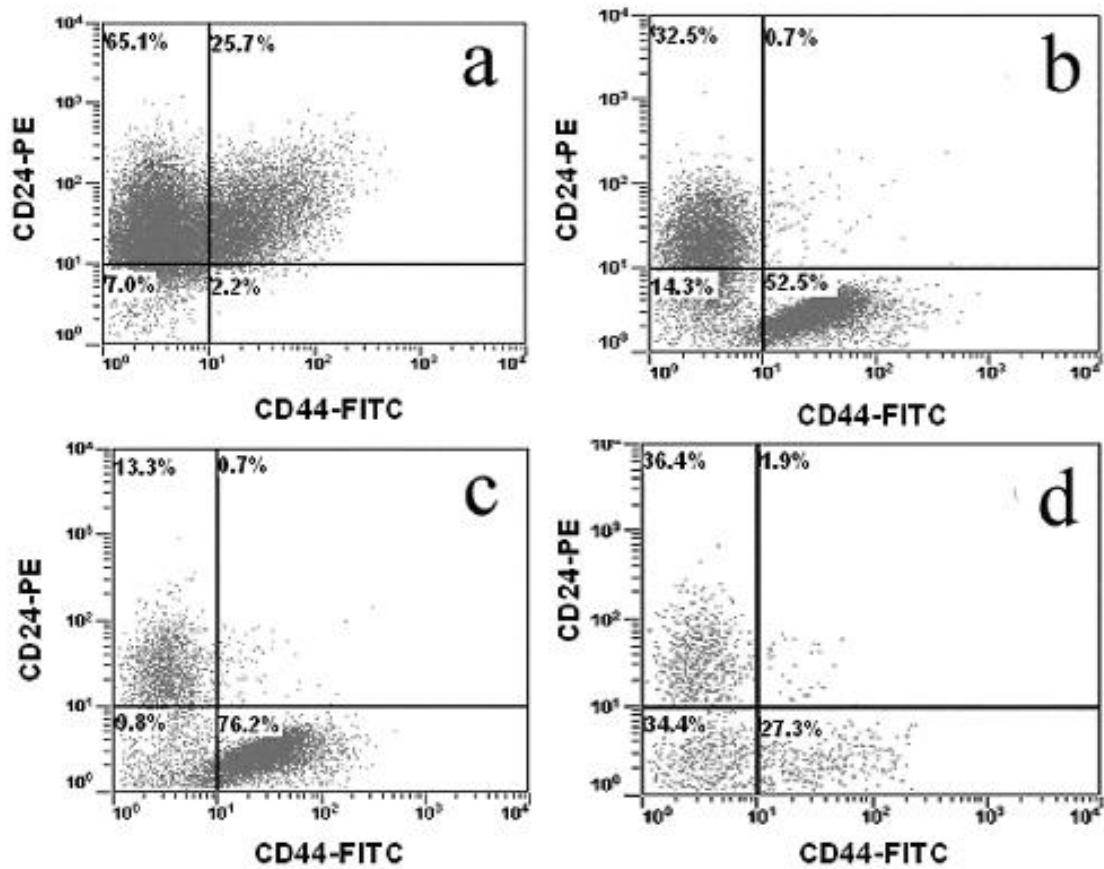


Figure 3.17 **CSC population in the cells encapsulated in PEGDA gel.** MCF7 cells were encapsulated in PEGDA gels with 5 kPa modulus and cultured in stem cell culture medium. Cells before encapsulation (a), 3 days (b), 8 days (c) and 11 days (d) after encapsulation were stained with CD44-FITC and CD24-PE antibodies. The population of CD24+, CD44+ and CD44+/CD24+ cells was determined by flow cytometry. Flow cytometry was repeated multiple times on each sample to ascertain reproducibility of the result

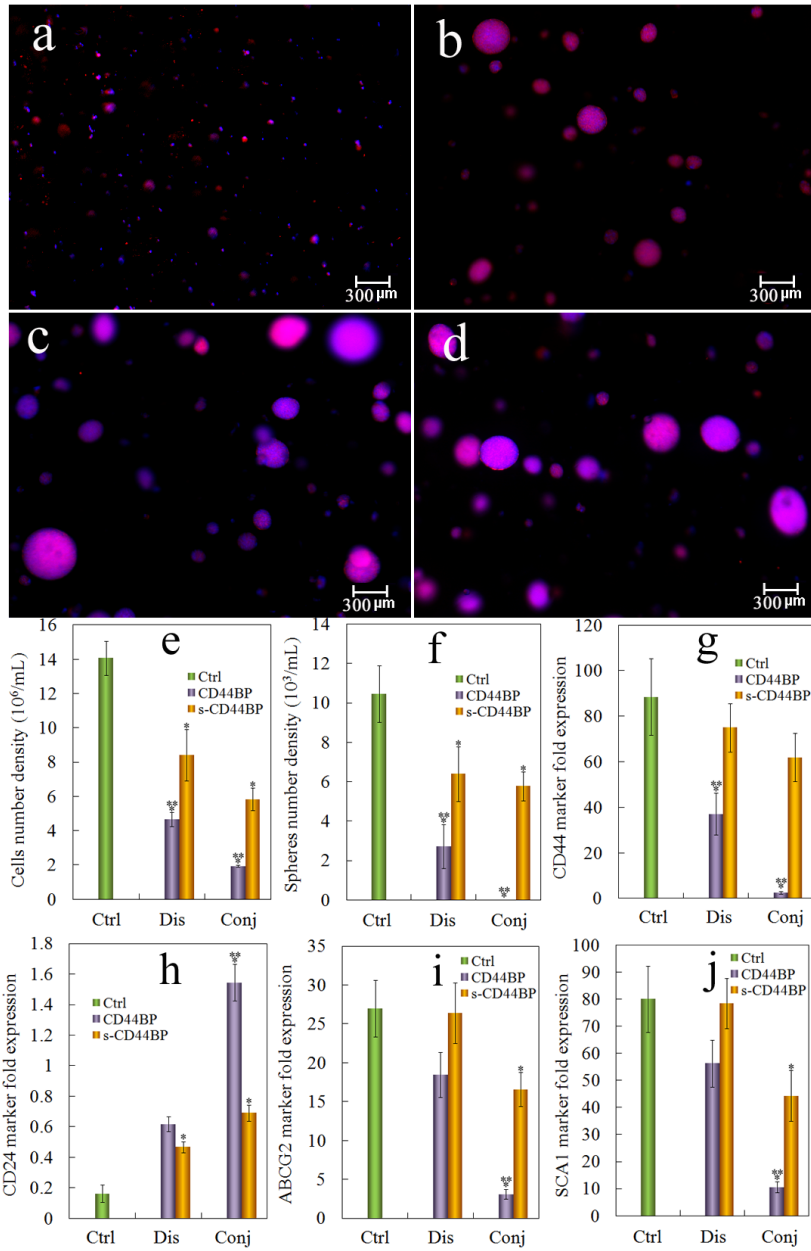


Figure 3.18 .Effect of CD44bp on tumorsphere formation and CSC marker expression.Representative fluorescent images of the tumorsphere size and distribution for 4T1 cells encapsulated in PEGDA gels (1.46105 cells/ml) conjugated with CD44bp (a, conj CD44bp), conjugated with a scrambled sequence of CD44bp (b, conj s-CD44bp), CD44bp dissolved in the gel (c, dis CD44bp), and s-CD44bp dissolved in the gel (d, dis s-CD44bp) and cultured in the stem cell culture medium for 9 days. Effect of CD44bp on cell number density (e) and tumorsphere number density (f) for 4T1 tumor cells encapsulated in PEGDA hydrogel and incubated in the stem cell culture medium for 9 days. Effect of CD44bp conjugation on CD44 (g), CD24 (h), ABCG2 (i) and SCA1 (j) mRNA marker expression for 4T1 tumor cells encapsulated in PEGDA gel and incubated in the stem cell culture medium for 9 days. RNA levels of the cells were normalized to those at time zero. A star indicates a statistically significant difference (p,0.05) between the test group and “Ctrl”.

3.3.2 COMPARING THE EFFECT OF CD44 BINDING PEPTIDE ON TUMORSPHERE FORMATION OF 4T1 CELLS WITH INTEGRIN AND HEPARIN BINDING PEPTIDES

The effect of CD44bp on tumorsphere formation in the gel prompted us to test other cell-binding peptides. Ibp, an integrin receptor binding peptide and FHbp, a heparin-binding domain of fibronectin that binds to cell surface heparin sulfate proteoglycans, were conjugated to the gel. Groups included 4T1 cell seeded gel without peptide conjugation, the cell-seeded gel with CD44bp conjugation, the cell-seeded gel with Ibp conjugation, and the cell-seeded gel with FHbp conjugation. For determination of marker expression, gels conjugated with a scrambled sequence of the peptides were also tested. Fluorescent images a-d in Figure 3.20 show sphere formation by 4T1 cells in the gels without peptide, with conj CD44bp, conj Ibp, and conj FHbp, respectively. The Ibp conjugation, similar to CD44bp, abolished 4T1 tumorsphere formation in the gel (Figure 3.20 c). However, tumorsphere formation increased when 4T1 cells were encapsulated in the FHbp conjugated gel (Figure 3.20 d). Further characterization of the cells in these gels (see Figures 6 e-g) showed that the cells in Ibp and CD44bp conjugated gels had reduced cell number, did not form sphere, and remained as single cells or small cell aggregates (<25 μm). On the other hand, the cells in FHbp conjugated gel had higher cell number and larger spheres compared with those in the gels without peptide conjugation.

To determine whether the size and number density of tumorspheres in the gel correlated with the CSC sub-population, CD44 and CD24 expression of the cells in the peptide-conjugated gels were measured. 4T1 cells in the gels without any peptide conjugation and with FHbp conjugation had elevated expression of CD44 marker while the cells in gels

conjugated with CD44bp or Ibp had decreased CD44 expression (see Figure 3.20 h). More importantly, the CD44 expression in the cells encapsulated in FHbp conjugated gel was significantly higher than that without peptide conjugation. The expression of CD24 in those gels had an opposite pattern to that of CD44 (see Figure 3.20 i). In breast cancer, the expression of epidermal growth factor receptor (EGFR) is also closely related to the maintenance of CSCs [119, 127]. The expression of EGFR marker by 4T1 cells encapsulated in the peptide-conjugated gels is shown in Figure 3.20 j. Similar to CD44 marker, the expression of EGFR was increased in the cells encapsulated in FHbp conjugated gel but decreased in CD44bp and Ibp conjugated gels. Furthermore, conjugation of a mutant sequence of the peptides to the gel had insignificant or limited effect on tumorsphere formation and the expression of CSC markers, compared to the wild type (see Figures 3.20 h-j).

The effect of cell binding peptides on CSC sub-population was further examined in 4T1 cells by flow cytometry. The percentage of CD44⁺/CD24⁻ cells in 4T1 cells cultured without gel encapsulation was about 6% (Figure 3.21 a). This percentage doubled to 12% for cells encapsulated in the PEGDA gel without peptide conjugation (Figure 3.21 b). When 4T1 cells were encapsulated in the gel conjugated with FHbp, the sub-population of CD44⁺/CD24⁻ cells was further increased to about 21% (Figure 3.21 c). Conversely, the fraction of CSC sub-population in the gel decreased to the original level (5.4% for Ibp and 6.5% for CD44 bp) when 4T1 cells were encapsulated in the gels conjugated with Ibp (Figure 3.21 d) or CD44bp (Figure 3.21 e) that inhibited sphere formation. These results suggested that tumorsphere formation by 4T1 cells in the gel was related to the CSC sub-population.

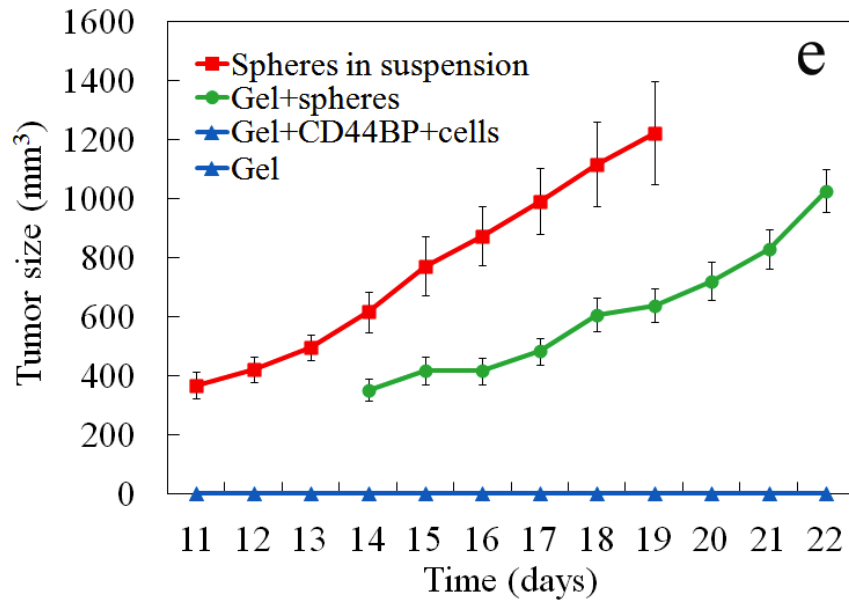


Figure 3.19 Effect of CD44bp conjugated to the gel on tumor formation *in vivo*. The gel without cell (negative control, light blue), 4T1 tumospheres in suspension (positive control, red), 4T1 cells encapsulated in the gel without CD44bp (green), and 4T1 cells encapsulated in the gel with CD44bp (light blue) were inoculated subcutaneously in syngeneic Balb/C mice. Tumor sizes were measured daily from post-inoculation day 11 (n = 6/group). Tumor growth was not observed in the negative control group (the gel without cell) and the group with 4T1 cells in the gel with CD44bp (the lines for these two groups are overlapped in the figure).

3.3.3 EFFECTS OF CELL BINDING PEPTIDES ON THE EXPRESSION OF OTHER CSC RELATED MARKERS

One of the pathways to transform differentiated cancer cells into CSCs is epithelial to mesenchymal transition (EMT) [115, 116]. The hallmark of EMT is the decreased expression of E-Cadherin and increased expression of N-Cadherin [128, 129]. The expressions of E-Cadherin and N-Cadherin 3 and 9 days after cells were encapsulated in the peptide-conjugated gels are shown in Figures 8 a and b, respectively. At the early time point (3 days), the expression of E-Cadherin was decreased while the expression of N-Cadherin was increased in the gel with FHbp, suggesting that EMT was a possible mechanism for the enhanced tumorsphere formation

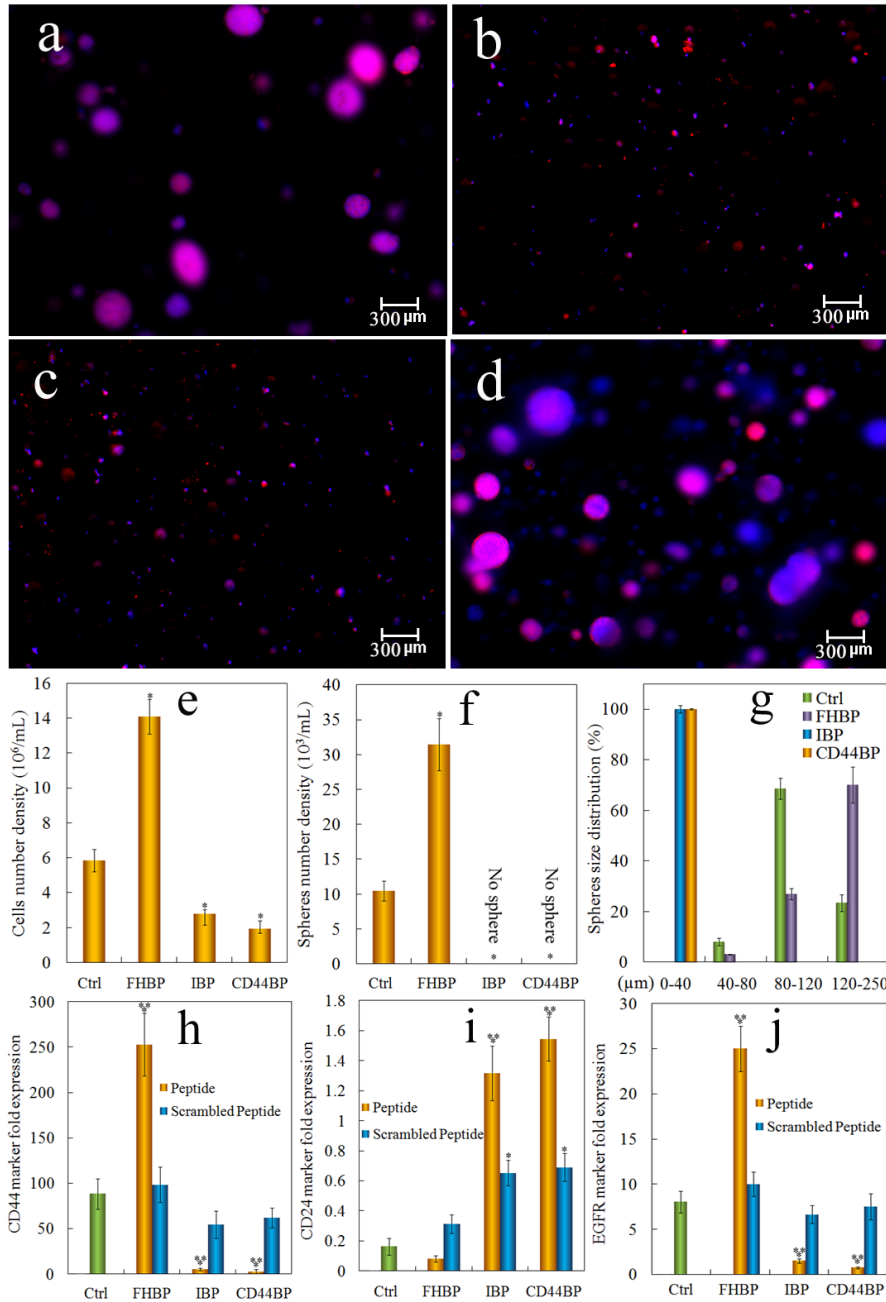


Figure 3.20 Comparison of tumorsphere formation in PEGDA gels conjugated with CD44bp, Ibp, or FHbp. Representative fluorescent images of the tumorsphere size and distribution for 4T1 cells encapsulated in PEGDA gels (1.46105 cells/ml) without peptide conjugation (a), conjugation with CD44bp (CD44bp, b), conjugation with RGD integrin-binding peptide (Ibp, c) and conjugation with fibronectin-derived binding peptide (FHbp, d) and cultured in the stem cell culture medium for 9 days. Effect of cell binding peptide on cell number density (e), tumorsphere number density (f) and sphere size distribution (g) for 4T1 tumor cells encapsulated in PEGDA gel and incubated in the stem cell culture medium for 9 days. Effect of cell binding peptide on CD44 (h), CD24 (i) and EGFR (j) mRNA marker expression for 4T1 tumor cells encapsulated in PEGDA hydrogel and incubated in the stem cell culture medium for 9 days. RNA levels of the cells were normalized to those at time zero.

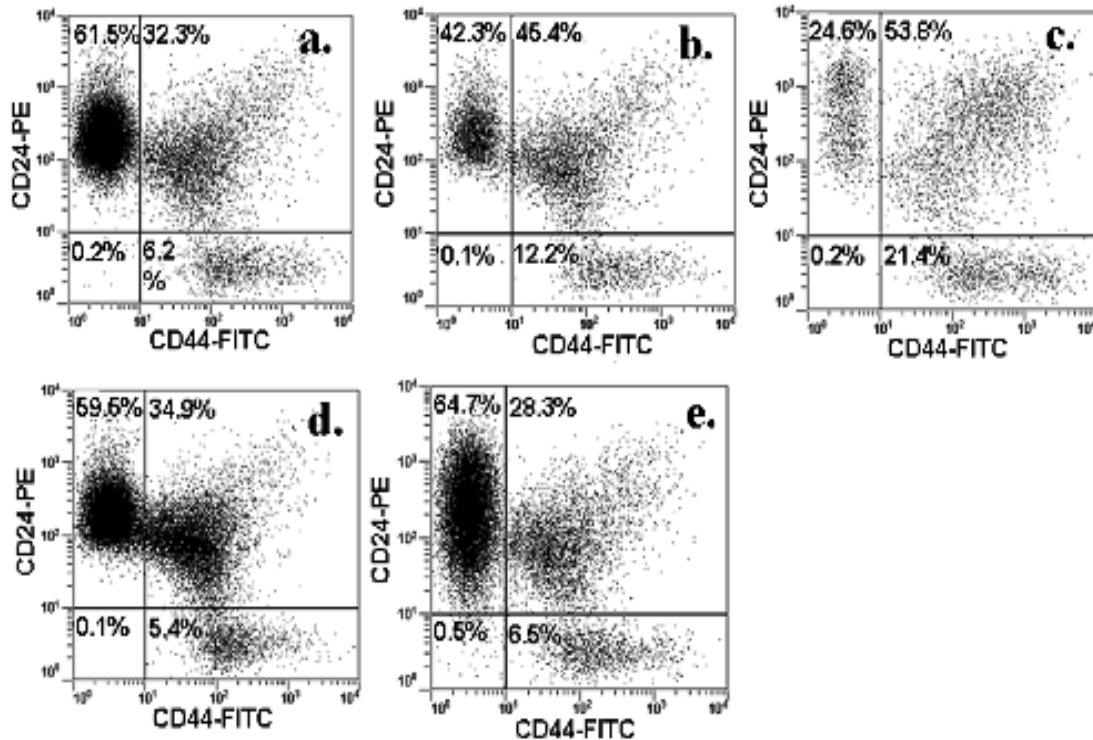


Figure 3.21 CSC population in cells encapsulated in PEGDA gel conjugated with CD44bp, Ibp, or FHbp. 4T1 cells were encapsulated in PEGDA gels with 5 kPa modulus and cultured in stem cell culture medium. Cells before encapsulation (a), 9 days after encapsulation in the gel without peptide (b), 9 days in the gel conjugated with FHbp (c), 9 days in the gel conjugated with Ibp (d), and 9 days in the gel conjugated with CD44bp were stained with CD44-FITC and CD24-PE antibodies. The population of CD24+, CD44+ and CD44+/CD24+ cells was determined by flow cytometry. Flow cytometry was repeated multiple times on each sample to ascertain reproducibility of the results.

in the gel. However, at the later time point (9 days), the expression of E-Cadherin in the cells grown in FHbp gel was much higher than that in other groups. This was probably due to sphere formation in the FHbp gel. E-Cadherin is a cell adhesion protein and its expression increases with increased cell-cell interaction [130]. Consistent with that, cells in the Ibp and CD44bp gels, which did not form spheres, had low expressions of E-Cadherin (see Figure 3.22 b).

The importance of integrins in cancer and CSC maintenance is well known [131]. Since RGD is an integrin binding peptide, we examined the expression of integrin α_v and β_3 ,

two integrin subunits required for RGD binding, and the expressions are shown in Figures 3.21 c, d, respectively.

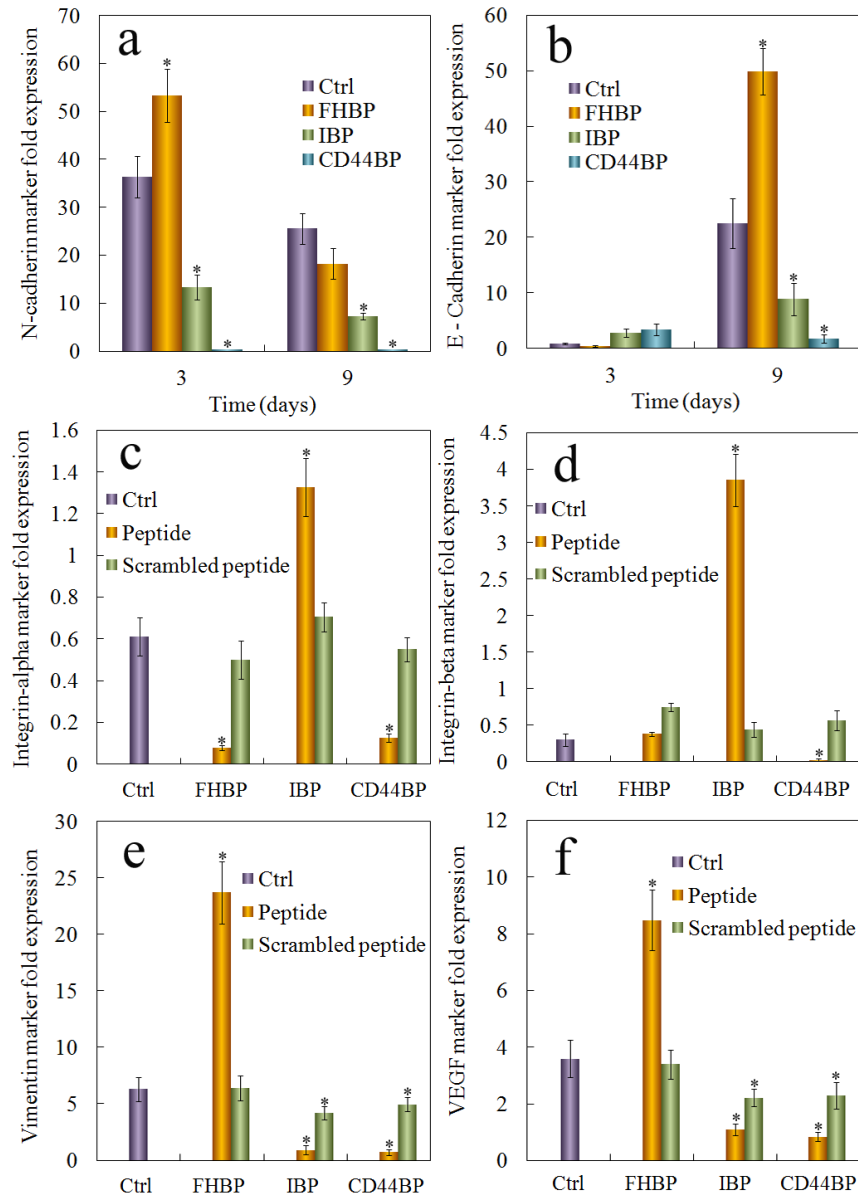


Figure 3.22 Expression of the markers related to CSC maintenance in cells grown in the gel conjugated with CD44bp, Ibp, or FHbp. Effect of cell binding peptide on N-Cadherin (a), E-Cadherin, (b), integrin α V (c), and integrin β 3 (D) mRNA marker expression for 4T1 tumor cells encapsulated in PEGDA hydrogel and incubated in the stem cell culture medium for 9 days. Effect of cell binding peptide on vimentin (e) and VEGF (f) protein expression. The protein expression was determined by western blot and quantified with imageJ. Actin was used as the internal control and the protein expressions were normalized to those at time zero. RNA levels of the cells were normalized to those at time zero.

The expression of integrin α_v and β_3 was reduced in cells grown in FHbp and CD44bp gels, even though the cells in FHbp gel formed spheres while those in CD44bp gel did not. Interestingly, the expression of integrin α_v and β_3 was significantly increased in the cells in Ibp gel. It is possible that blocking integrin signaling by RGD activates a feedback loop to induce integrin expression. These results suggest that the expression of integrin does not correlate directly with tumorsphere formation or CSC maintenance of 4T1 cells. Conjugation of a mutant sequence of the peptides to the gel had limited effect on the expression of CSC markers, indicating that the effect was specific to the wild type. The expression of vimentin [132] and VEGF, two other markers related to invasive breast cancer and CSC maintenance [133], was also determined at the protein level, as shown in Figure 3.22 e, f. The expression of vimentin and VEGF was high in cells that formed spheres, and their expression correlated with the sphere size and number (Figure 3.20 e, f).

3.3.4 EFFECT OF CD44 BINDING PEPTIDE CONJUGATED TO AN ENGINEERED INERT MATRIX ON MAINTENANCE OF HUMAN CANCER STEM CELLS

We have shown that conjugating CD44 binding peptide to the PEG engineered matrix abolished tumorspheres formation by the encapsulated 4T1 breast cancer cells in the optimum modulus of 5kPa whereas CD44bp dissolved in the gel did not have any specific inhibitory effect on spheroid formation [27]. These results suggested the functionality of CD44bp as an insoluble part of ECM not a soluble chemokine.

Here, we investigate the effect of CD44bp conjugated to the PEGDA hydrogel on the maintenance of breast, colon and, bone CSCs in their optimum reported moduli of 5, 25

and 50 kPa and compare this effect to scrambled sequence of the peptide as a control. Fluorescent images in Figure 3.21 show the evolution of tumorsphere for these cell lines in the presence of mutant CD44bp (Row 1) and CD44bp (Row 2). Columns 1, 2 and 3 correspond to tumorsphere distribution for MDA-MB-231, HCT116 and U-2 OS cells encapsulated in PEGDA gel with elastic modulus of 5, 25 and 50 kPa respectively after 9 days of encapsulation. Images B, D and F in Figure 3.21 show that conjugated CD44bp completely inhibited tumorsphere formation in MDA-MB-231, HCT116 and U-2 OS cell lines respectively. This highlights the importance of CD44 signaling in the maintenance of CSCs for these cell lines. Yeung et al. reported that CD44 can be used as a marker to enrich for CSCs from primary colorectal tumor tissue and clearly identify CSCs in colorectal cancer-derived cell lines [28]. It has also been shown in another study that CD44 protein plays an important role in colorectal tumor progression and metastasis in humans [29]. Several clinical studies suggested that CD44 expression correlates with bone metastasis by enhancing tumorigenicity and downregulation of this marker markedly suppressed tumorigenicity and bone metastases in nude mice [16, 30, 31].

However, mutant CD44bp conjugated to the gel (images A, C and E) was not able to stop sphere formation suggesting that bioactivity is specific to CD44bp. The effect of CD44bp on cell number density, spheres size and density of MDA-MB-231, HCT116 and U-2 OS cells in the gel are shown in Figures 7 G, H and I, respectively. After 9 days of incubation, The MDA cell count of viable cells in the control (ctrl) group of the gel without any peptide reached $1.4 \times 10^6/\text{ml}$ cells where the density of MDA cells in the gel with conjugated peptide (CD44bp) was about half of the initial number density of $0.6 \times 10^6/\text{ml}$ and did not show any growth potential.

Although cells number density in the group of mutant peptide (mCD44bp) was lower than control group without peptide but it was significantly higher than the number of cells in CD44bp group. Similar behavior was observed in the control and mutant peptide groups of colon and bone cancer cells after 9 days. A significant change in number density and sphere formation of both groups was observed while they showed approximately same level of low number density in the CD44bp group with no spheroid formation (fig 3.1G). The number density of cells in control group and mutant peptide of colon and bone cancer cell lines is lower than MDA cells which can be related to level of malignancy and potential in sphereformation for each cell line. As we showed in our previous study, MDA a highly malignant breast cancer cell line shows higher potential of spheroid formation compared to HCT116 and U-2 OS with lower levels of malignancy.

The effect of CD44bp on average tumorsphere size and density after 9 days of encapsulation is shown in Figure 3.21 H, I for three cell lines. The average tumorsphere diameter in control groups of MDA, HCT116 and U-2 OS cell lines increased from approximate 10 μm at day zero to the range of 50, 30 and 30 μm respectively in 9 days where average diameter for the group with CD44bp without any spheres remained in the size range of single cells and aggregates ($< 20 \mu\text{m}$). The number density of spheroids in control group and mutant peptide of MDA cell lines reached as high as 6 ($10^3/\text{ml}$) after 9 days while it was in the range of 1.5 ($10^3/\text{ml}$) and 2.5 ($10^3/\text{ml}$) for colon and bone cancer cell lines respectively. The number of spheroids in CD44bp group with single cells and no spheres reported zero.

The effect of CD44bp on the expression of CSCs markers for each cell line is reported in Figure 3.23 J, K and L. Figure 3.23 J shows the expression of CD44 and EGFR, the well-

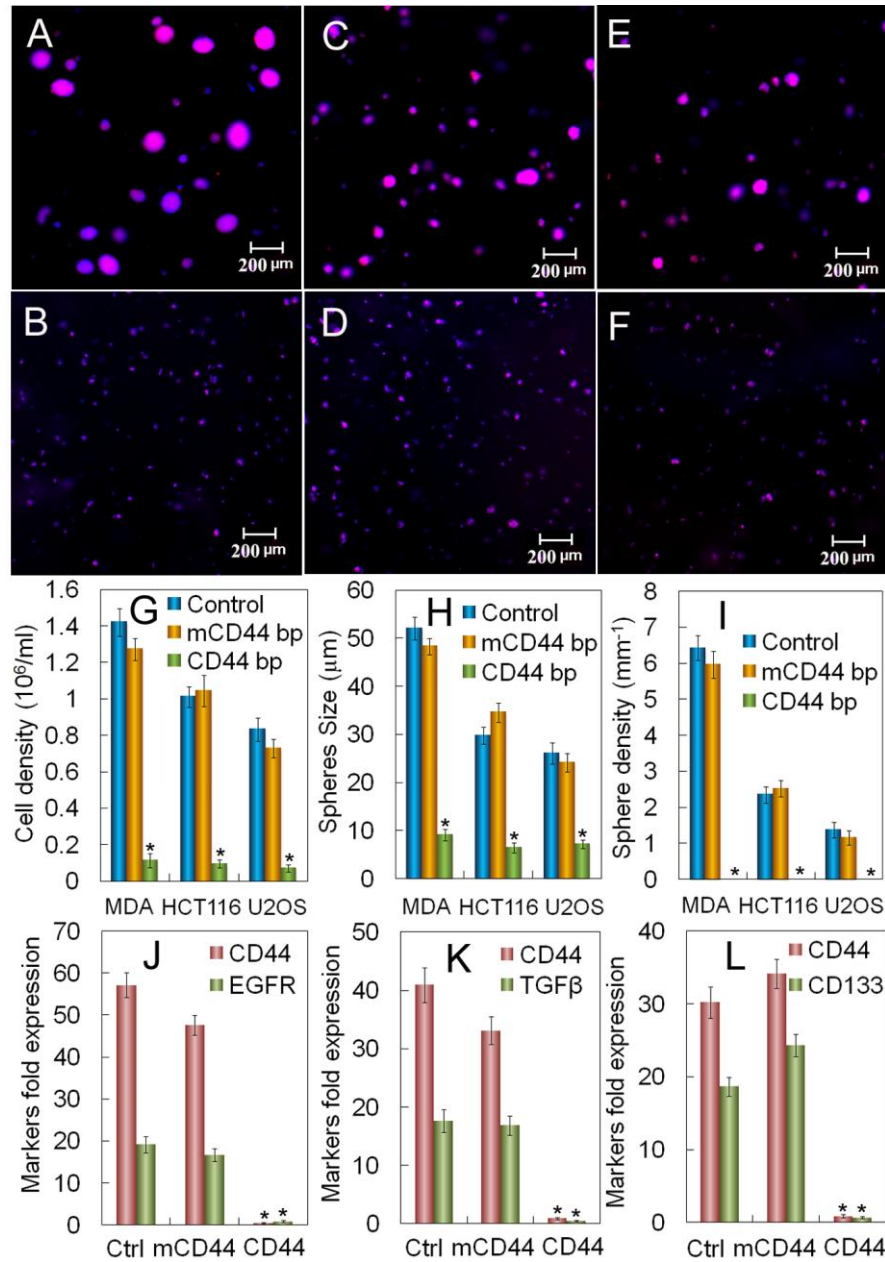


Figure 3.23 Effect of CD44 binding peptide on tumorsphere formation by human tumor cell lines

Columns 1,2 and 3 correspond to tumorsphere distribution for MDA-MB-231, HCT116 and U-2 OS cell lines encapsulated in PEGDA gel with elastic modulus of 5, 25, 50 kPa respectively. Row 1 and 2 correspond to the gels modified with mutant CD44 binding peptide as a control and CD44 binding peptide respectively after 9 days of incubation. Cells were stained with Phalloidin for cytoskeleton (red) and DAPI for nucleus (blue), and imaged with an inverted fluorescent microscope. (G) Cells density (H) Average tumorsphere size (I) Tumorspheres number density (J,K,L) mRNA expression levels of different markers for MDA-MB-231, HCT116 and U-2 OS cell lines encapsulated in PEGDA gel with elastic modulus of 5, 25, 50 kPa respectively. Groups were gels modified with CD44 binding peptide, gels modified with mutant CD44 binding peptide and gels without peptide as a control, for each cell line.

studied markers in human breast CSCs for MDA cells, after 9 days. Cells in the gel with no peptide and mutant peptide groups indicated about 60 and 50 fold increase in expression of CD44 marker respectively whereas the fold expression of this marker for cells with CD44bp was lower than one. Similarly, while the fold expression of EGFR for CD44bp did not change significantly, control and mutant peptide were highly expressed for this marker. Expression of CD44 and TGF β for colon CSCs has been shown in Figure 3.23 K. For control and mutant peptide groups cells reached more than 40, 35 times in CD44 fold expression respectively, and approximately 15 times of TGF β fold increase. Expression of CD44 was lower than one for peptide group. Similarly, CD44 and CD133 in bone cancer cells expressed more than 30 fold for control and mutant peptide groups and lower than one for CD44bp. These results demonstrate that CSCs markers expression by MDA, HCT116 and U-2 OS cells in the gel correlates with the ability of tumorsphere formation. The slight difference in results of mutant CD44bp compared to ctrl group can be explained by the non-specific binding of mutant peptide to the corresponding receptors with much lower affinity.

It has been reported in several studies that down-regulation of CD44 by different therapeutic agents leads to tumor suppression. For example, targeting CD44 with anti-CD44 monoclonal antibodies (H90, A3D8, HI44a) reversed differentiation blockage of leukemic cell lines, and in some cases, inhibit proliferation and stimulated apoptosis [32]. Mandal et al. showed in two different studies that down-regulation of CD44 marker in metastatic breast cancer cells correlated with inhibitory effects of simvastatin and fish oil on bone metastasis [33, 34]. In another study, a CD44 binding peptide, A6 peptide, inhibited melanoma cancer cell migration and metastasis *in vivo* [35].

In current study, using CD44bp inhibited breast, colon and bone tumorsphere formation in vitro.

These results are in agreement with previous studies on this peptide that Hibino et al. reported inhibition of tumor metastasis and growth as well as increased apoptosis in B16-F10 melanoma cells by A5G27 peptide [22]. Hibino et al. also explained the potential mechanism of A5G27 inhibitory effect on WiDr human colorectal carcinoma cells. They have shown that A5G27 inhibits metastasis and angiogenesis by blocking FGF2 binding to the heparan sulfate side chains of CD44. This adhesion blocked cells binding to fibroblast growth factor (FGF2) and inhibited regulation of FGF2 signaling including tyrosine phosphorylation [36].

3.3.5 COMPARING THE EFFECT OF CD44 BINDING PEPTIDE ON TUMORSHERE FORMATION BY HUMAN CANCER CELL LINES WITH INTEGRIN AND HEPARIN BINDING PEPTIDES

Integrin family of proteins is mainly responsible for ECM signaling and tumor progression in different types of cancer including breast cancer [37, 38]. These cell surface receptors with important role in cellular matrix interactions involves in cancer cell adhesion, growth, migration

and invasion [37, 39]. For example, ovarian cancer cell lines showed significantly high expression of multiple subunits of integrins mediating proliferation, adhesion, migration and invasion of cancer cells in response to ECM. Blocking antibodies against these integrin subunits inhibited tumor progression in these cell lines [39]. Birnie et al. reported the importance of integrins interaction with ECM in human prostate cancer stem cells maintenance [40].

One of the main subunits of integrin receptor is $\alpha V\beta 3$ and it has been associated with the pathogenesis of several types of cancer. Monferran et al. have shown that down-regulation of $\alpha V\beta 3$ integrin increased glioma cancer cells response to radiotherapy [27]. In another study, inhibition of $\alpha V\beta 3$ integrin blocked the CSC driven tumor formation in a prostate xenograft model [41]. Therefore, finding therapeutic agents to target integrins can be a promising method to reduce tumor progression *in vivo*.

Effect of heparin and integrin binding peptides on tumorsphere formation by breast cancer cells including MDA is shown in Figure 3.24. MCF10a, a normal human breast epithelial cells, MCF7, human breast cancer cell line with moderate malignancy, MDA (human) and 4T1 (mouse) highly malignant breast cancer cells were encapsulated in the gel with optimum modulus of 5 kPa and were used to study the effect of cell-binding peptides on breast cancer cells with different levels of malignancy.

Fluorescent images A–F in Figure 3.24 indicate tumorsphere distribution for MDA-MB-231, MCF7 and 4T1 cell lines encapsulated in PEGDA gel after 9 days of incubation in rows 1, 2 and 3 respectively. Column 1 and 2 correspond to the gels modified with FC/HV peptide and RGD peptide respectively. The RGD peptide, similar to CD44BP, abolished tumorsphere formation in MDA, MCF7 and 4T1 cells in the gel (Figure 3.24 B, D, F). It has been shown that RGD peptide as a well-known ligand of $\alpha V\beta$ integrin receptor hinders integrin-mediated signaling pathways in tumor progression [6]. Yu et al. reported in a recent study that RGD peptide can cause clustering of integrin receptors when cells are seeded on RGD peptide conjugated lipid membrane.

This clustering stimulates local actin polymerization and leads to cytoskeleton remodeling [42]. This integrin-blocking peptide prevents integrin from regular

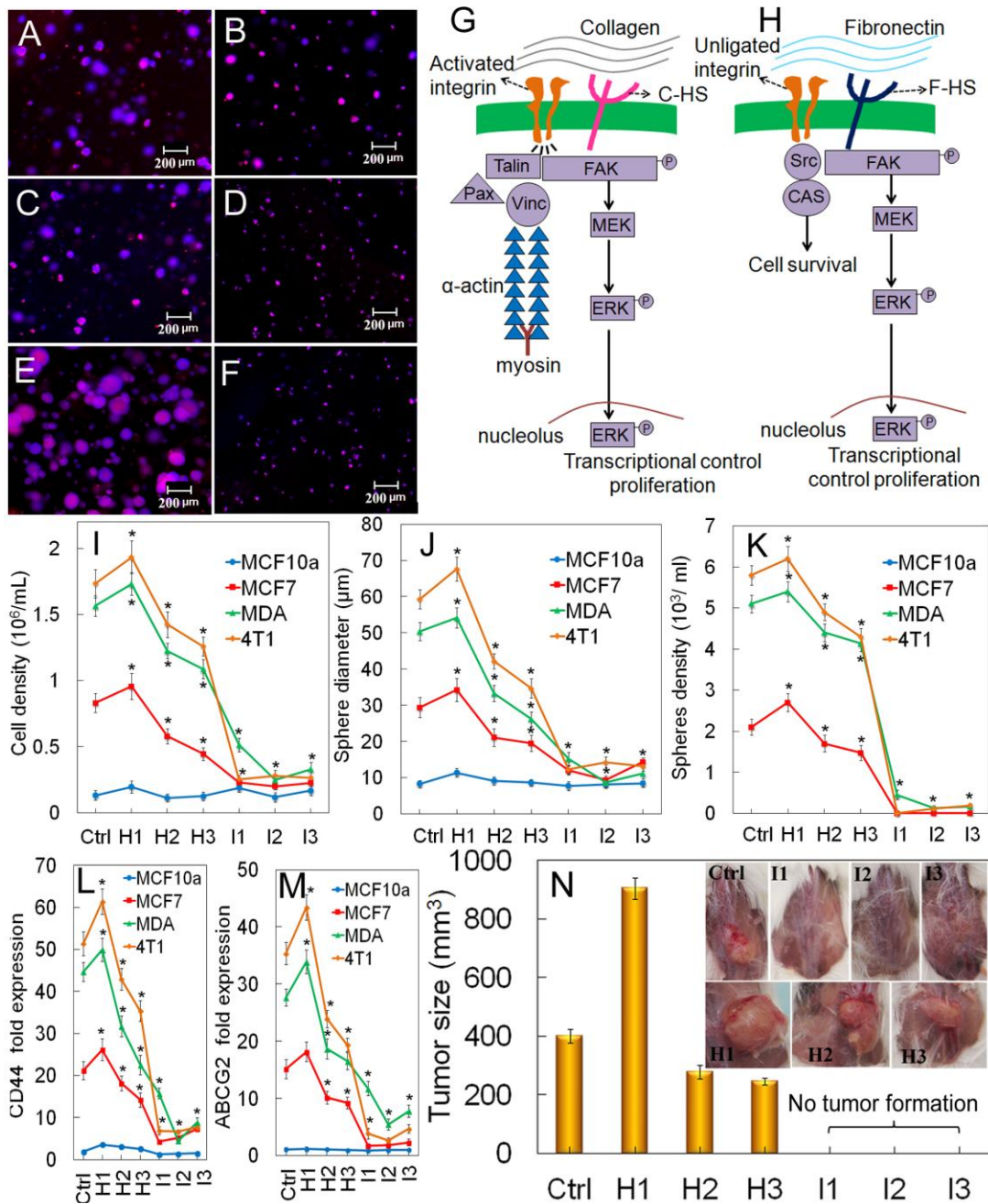


Figure 3.24 .Effect of heparin and integrin binding peptides on tumorsphere formation by human breast tumor cell lines

Rows 1,2 and 3 correspond to tumorsphere distribution for MDA-MB-231, MCF7 and 4T1 cell lines respectively, encapsulated in PEGDA gel with elastic modulus of 5 kPa after 9 days of incubation.. Column 1 and 2 correspond to the gels modified with FC/HV peptide and RGD peptide respectively. Cells were stained with Phalloidin for cytoskeleton (red) and DAPI for nucleus (blue), and imaged with an inverted fluorescent microscope. (I) cells density (J) average tumorsphere size, (K) tumorspheres number density and (L, M) mRNA expression levels of different markers for MDA-MB-231, MCF7 and 4T1 breast cancer cell lines respectively, encapsulated in PEGDA gel with elastic modulus of 5 kPa. (N) effect of Ibps and Hbps on tumor formation *in vivo*.

conformational shift necessary for transducing signals both inside and outside of the cells and does not let cells sense matrix rigidity. Due to our previous study tumorsphere formation in PEGDA hydrogel is rigidity dependent and this clustering prevents cells from spheroid formation.

The ability of sphere formation increased when cells were encapsulated in the FC/HV conjugated gel (Figure 3.24 A, C, E). The effect of all peptides on cell number density, average sphere diameter and sphere number density after 9 days is shown in Figure 3.24 I, J, K. While MCF10a cells did not change significantly for cell count, sphere diameter or density after 9 days, MCF7, MDA and 4T1 cells showed an increasing trend for all. The highest cell count was observed for the group with H1 peptide. The control, H2 and H3 groups were in next orders of growth potency respectively in all cell lines. This suggests the stimulating effect of these peptide on sphere formation and cells growth. The ability of these ECM-derived peptides to promote cell attachment and proliferation is reported in different studies [43-48]. It was shown that Heparin Sulfate Proteoglycans (HSPGs) present on the surface of tumor cells are important surface receptors for ECM components [44, 49]. The key role of HSPGs in biological activities including tumorigenesis has been shown in different studies [50-53]. It has been suggested that HSPGs in cooperation with integrins such as $\alpha V\beta 3$ integrin or independently create signals for cell spreading and activation of adhesion plaques [50, 54-57]. The interacting peptides with HSPGs activates the focal adhesion kinase (FAK), a mediator of cell-extracellular matrix signaling pathways that is over-expressed in tumor cells and has been shown to play a main role in promoting breast cancer invasion and metastasis [58, 59]. It has been reported that even in the absence of cell attachment, FAK is required as a

survival signal in breast tumor cells [60].

As shown in Figure 3.22 I, the number density of cells sharply decreased for Ibps that cell count remained in the same order of initial day of encapsulation. The effect of cell binding peptides on the average diameter of spheres in Figure 3.22 J confirms the highest potential in spheroids growth for H1 peptide where control, H2 and H3 peptides were in the next order respectively. Cells in the groups with Ibps did not form sphere and remained as single cells or small cell aggregates (<25 μm). Similarly, cells in H1 group showed the highest number densities of spheres about 6, 5 and 2 ($10^3/\text{ml}$) for 4T1, MDA and MCF7 cells respectively. While cells in the groups with conjugated Ibps did not form any spheres, the control, H2 and H3 showed secondary potential of spheroid formation for all cell lines except the MCF10a which did not show any sensitivity to the peptides.

To determine whether the size and number density of tumorspheres in the gel correlated with the CSC sub-population, the expression of CD44 and ABCG2 for the control and peptide-conjugated gels was measured. ABCG2, an ATP- Binding Cassette involves in efflux of chemotherapeutic agents and has been used to identify the presence of CSCs in breast tumours[61-63]. Cells in the gels with H1 conjugated peptide and control group had the highest fold expression of CD44 and ABCG2 markers for all cancer cell lines respectively. The elevated expression of CD44 marker was also observed in H2 and H3 groups. Cells in gels conjugated with Ibps showed a sharp decrease in CD44 and ABCG2 marker expression after 9 days of encapsulation compared to Hbps (Figure 3.24 L, M).

The effect of heparin and integrin binding peptides conjugated to the gel on tumor formation of encapsulated 4T1 cells has been investigated *in vivo* by implanting grown tumorspheroids encapsulated in a degradable version of PEGDA gel (dPEGDA) in mice.

After 4 weeks, the highest average volume of tumors was observed in group with H1 peptide with a size more than 800 mm³. Measurable tumors also observed in Control, H2 and H3 groups with approximate sizes of 400, 250 and 200 mm³ respectively. 4T1 cells encapsulated in the gel with conjugated Ibps did not form a visible tumor after 4 weeks of implantation, suggesting that these peptides in conjugated form are able to inhibit the tumor formation *in vivo*.

The inhibitory effect of I3 peptide on tumor growth, angiogenesis and metastasis has been shown in several studies. *In vivo*, this peptide inhibited lung and bone metastases by human melanoma cells in nude mice [64]. In another study, conjugation of I3 to polyethylene glycol has improved anti-metastatic activity due to a longer half-life in blood [65]. Two different studies reported that a repeating sequence of I3 peptide inhibited the metastatic formation in the lung of malignant tumor cells more effectively than I3 monomer [66] and the multi-meric I3 peptides showed enhanced activity in inhibiting tumor growth and metastasis compared to the monomer [67]. I3 also blocks angiogenesis i.e., in the presence of this peptide, tumors grew in the smaller size *in vivo* by reduced numbers of blood vessels [68]. The mechanism by which I3 peptide acts is not clear. Previous studies explained different possible mechanism for this antitumor behavior. For example, it has been reported that I3 peptide bound to the 32/67 kD cell surface receptor increased tyrosine phosphorylation [69]. In another study, Kim et al., reported that the presence of I3 polypeptide caused apoptosis in human fibrosarcoma cells while scrambled sequence did not induce apoptosis [70]. Finally, It has been shown that the inhibitory effect of I3 peptide on the growth and migration of human prostate

cancer cells *in vitro* associates with inhibited ATP synthesis and increased caspase-9 activity [71].

Unlike I3, I2 has been mainly known for increasing angiogenesis and metastasis *in vivo* [68]. It has been shown that intravenous injection of this peptide via the tail vein with B16F10 melanoma cells caused an increase in the number of colonies on the surface of the lungs [72]. It was reported that interactions of colon cancer cells with this peptide caused the formation of metastatic foci and promoted metastasis to liver [73]. The mechanism of action of this peptide is not defined but the ability of I1 in promoting tumor growth and metastasis could be its key role in promoting angiogenesis [37, 74]. The other potential mechanism is enhanced protease activity based on previous studies [68]. In this study we show that the stimulating effect of I1 peptide on encapsulated cancer cells is dose dependent [37, 74] and 2 wt% concentration of this peptide conjugated to the gel hinders spheroid formation. Higher than 1% of this peptide may cause the conformational changes in the $\alpha 3\beta 1$ and $\alpha 6\beta 1$ integrins which are important receptors in tumorigenesis and are suggested as receptors of IKVAV peptide [68]. This results in spheroid formation abolition. Besides, the possible mechanism involving protease enhancement and angiogenic activity of this peptide may change cells function and activate different signaling pathway, which lead to abolition of tumorspheres.

The concept of CSC niche is based on the evidence that both normal stem cells and CSCs utilize similar signaling pathways within a unique microenvironment to maintain stemness. Signaling pathways that have been identified within the stem cell niche include Notch, Hedgehog, PI3K, Wnt, STAT and TGF- β [134]. Processes such as inflammation, EMT, hypoxia and angiogenesis within the microenvironment regulate those pathways to

sustain the rare population of CSCs [115]. The cell microenvironment is composed of many cellular and non-cellular components such as cell binding proteins, growth factors, and nutrients. In addition, cells also respond to mechanical properties of the microenvironment such as stiffness and porosity of the ECM [135]. Therefore, cell fate is determined by the specific combination of signals presented in its microenvironment. Due to the complex biochemical composition of the niche, it is difficult to study the role of individual factors in cell behavior with *in vitro* models. We have developed an inert hydrogel as a 3D matrix that supports the proliferation and maintenance of breast CSCs in a certain range of elastic moduli without the interference of proteins, peptides, and other biomolecules in the ECM. In this study, we investigated the effect of conjugating cell-binding peptides to the inert gel with controlled stiffness on the maintenance of stemness of breast CSCs without the interference of other factors.

CD44 is the most widely used marker to identify breast CSCs. CD44 is a cell surface proteoglycan that functions in cell-cell and cell-matrix adhesion. It binds to many ECM ligands including hyaluronic acid (HA), osteopontin, fibronectin and collagen [136-139]. It also binds to matrix metalloproteinases (MMPs) and growth factors to promote tumor invasion and growth [11, 12]. Therefore, CD44 utilizes many signaling pathways to regulate cell behavior, and its activity depends on conformational changes and post-translational modifications after ligand binding. CD44bp is a peptide derived from the D-domain of laminin α_5 chain [79]. It binds to CD44 and inhibits lung colonization of tumor cells *in vivo* but does not inhibit tumor cell proliferation when added to the culture medium [79]. In this study, we found that CD44bp inhibits tumorsphere formation only

when conjugated (covalently attached) to the gel. Dissolving the peptide in the gel or in the medium did not have an effect on tumorsphere formation. This result suggests that CD44bp does not act as a soluble chemokine to block or activate CD44 signaling. We speculate that CD44bp induces a conformational change in CD44 receptor through a mechanism like receptor clustering. In previous studies, another CD44 binding peptide, A6, was found to enhance cell adhesion to HA and induce FAK and MEK phosphorylation in a CD44 dependent manner in breast and ovarian cancer cells [140]. A6 also inhibited cancer cell migration and metastasis *in vivo* [140]. It is unclear whether CD44bp binding also causes phosphorylation of these kinases in a CD44 dependent manner.

ECM signaling mainly occurs through the integrin family of proteins [141]. The main integrin receptor is $\alpha_v\beta_3$ and it has been implicated in the pathogenesis of several types of cancer. Down-regulation of $\alpha_v\beta_3$ integrin sensitized cancer cells to radiotherapy [142]. Inhibition of $\alpha_v\beta_3$ integrin blocked the CSC driven tumor formation in a prostate xenograft model [143]. Further studies suggest that blocking $\alpha_v\beta_3$ integrin leads to redistribution of β -catenin from the nucleus to the cytoplasm [80]. Nuclear localization of β -catenin is known to be one of the mechanisms for maintaining stemness. Therefore, $\alpha_v\beta_3$ integrin-mediated signaling is required for the maintenance of CSCs. RGD peptide, a well-known ligand of $\alpha_v\beta_3$ integrin receptor, blocks the integrin mediated cell adhesion. In this study, RGD peptide (Ibp) without conjugation to the hydrogel did not affect tumorsphere formation. Since the PEGDA hydrogel did not have cell-binding motifs, blocking cell adhesion sites by RGD might not have a significant effect. However, the matrix rigidity is sensed by the actin cytoskeleton through integrin receptors [144-146].

A recent study showed that membrane-bound RGD can induce the clustering of integrin receptors when cells are seeded on RGD peptide conjugated lipid membranes [147]. Furthermore, integrin receptor clustering stimulates local actin polymerization and leads to cytoskeleton remodeling [147]. We speculate that RGD peptide conjugated to the PEGDA hydrogel causes clustering of the integrin receptors, which in turn, alters cells' ability to sense matrix rigidity. Since tumorsphere formation in PEGDA hydrogel is rigidity dependent, it would be interesting to determine whether breast cancer cells can form spheres in the RGD conjugated PEGDA hydrogel under a different elastic modulus. The RGD integrin binding peptide is present in many ECM components, but there are other binding motifs in the ECM. For example, fibronectin has a RGD-independent heparin-binding domain in the C-terminus that binds to heparin sulfate proteoglycans on the surface of tumor cells [81, 148]. In this study, we found that unlike CD44 and RGD binding peptides, FHbp conjugated to the gel enhanced tumorsphere formation. It has been shown that FHbp promotes focal adhesion formation in culture cells [81] and it likely activates the focal adhesion kinase (FAK). Several lines of evidence have indicated the role of FAK in promoting breast cancer invasion and metastasis [149, 150] and FAK is required for the survival of breast cancer cells in the absence of cell attachment. The expression of FAK dominant negative mutant in breast cancer cells leads to deactivation and degradation of endogenous FAK and cell apoptosis without matrix attachment [151]. Therefore, FHbp, unlike CD44bp and Ibp that block the receptor signaling, may activate FAK and promote CSC survival. As a result, 4T1 cells encapsulated in the gel conjugated with FHbp formed larger and greater number of spheres.

Fibronectin is a mesenchymal marker and its expression is increased during the process of EMT. In the EMT process, certain epithelial cells lose cell-cell adhesion and invade the local tissue. It is thought that a similar transformation occurs during cancer metastasis [152]. Recent studies have shown that EMT induction is sufficient to turn differentiated cancer cells into CSCs [115, 116]. A recent study showed that mammary tumor cells displayed a more differentiated phenotype when cultured on collagen coated substrates, while they displayed an invasive phenotype and EMT-related gene expression pattern when cultured on fibronectin coated substrates [153]. Therefore, FHbp may induce EMT which in turn enhances tumorsphere formation. In the EMT process, the expression of E-Cadherin is down regulated but E-Cadherin may also be up-regulated with increasing cell-cell interaction. Consistent with this, the expression of E-Cadherin was initially reduced in our study in the cells encapsulated in FHbp gel but increased at a later time point. The expression pattern of some of the examined EMT markers also suggests that enhanced EMT may contribute to the increased tumorsphere formation in FHbp conjugated gels.

This study also included the mutant forms of the peptides. Although the mutants did not affect tumorsphere formation, they slightly affected the expression of some of the markers. It is possible that the mutants bind to the corresponding receptors but with much lower affinity or non-specifically. In summary, this study demonstrated that cell adhesion peptides could either increase or diminish CSC population in the inert 3D PEGDA hydrogel cell culture system, as the mechanisms for CSC maintenance among these peptides are different.

Using the 3D PEGDA matrix with a certain stiffness, we demonstrated that the cell

adhesion CD44 binding peptide (CD44bp), RGD integrin binding peptide (Ibp), and fibronectin-derived heparin binding peptide (FHbp) can be individually conjugated to the inert PEGDA gel and their effect on the maintenance of breast cancer stem cells can be investigated without the interference of other factors. The CD44bp and Ibp conjugated to the inert gel completely abolished tumorsphere formation by the encapsulated 4T1 breast cancer cells while FHbp enhanced tumorsphere formation compared to those without peptide. The inert 3D hydrogel cell culturesystem provides a novel tool to investigate the individual effect of factors in the microenvironment on maintenance of CSCs without the interference of other factors.

CHAPTER 4

CONCLUSION

We introduced PEGDA hydrogels as an inert 3D microenvironment for studying the individual effects of different parameters including ECM modulus on the survival and maintenance of 4T1 murine breast CSCs to human cancer cell lines.

In particular, human breast, colon, gastric and bone cancer cell lines were also able to sense and respond to change in elastic modulus through the change in the rate of tumorigenicity. The optimized modulus for regulating tumorigenic capacity of cancer cells was markedly different for different cell lines and it was found that at certain modulus the proliferation capacity of cancer cells can be completely diminished. Compared to conventional *in vitro* methods of culturing tumor spheroids in low-adhesion plates, the PEGDA engineered matrix increased the tumorigenicity (density and number of tumorspheres) and maintained CSCs properties for longer time periods. This could be reasonably attributed to the suitable structure and mechanical properties of the matrix. Consequently, the encapsulated cells mimic the actual tissue mechanobiology and increase the possibility of EMT or similar biological events.

Our understanding of CSC maintenance mechanisms remains limited due to numerous uncertainties in the transduction pathways of CSCs. Our developed synthetic micro-engineered matrix can be used as a tool to improve the cellular interaction level and optimize temporal condition of CSCs microenvironment. This maintains stem cells properties *in vitro* and makes it possible to study the regulatory effect of specific proteins in biological pathways on CSC maintenance without interference of other factors.

By Using the 5kPa PEGDA matrix, we demonstrated that the cell adhesion CD44 binding peptide (CD44bp), Integrin binding peptide (Ibps), and Heparin binding peptide (Hbps) can be individually conjugated to the inert PEGDA gel and their effect on the

maintenance of breast cancer stem cells can be investigated without the interference of other factors. The CD44bp and Ibps conjugated to the inert gel abolished tumorsphere formation by the encapsulated 4T1 breast cancer cells while Hbps enhanced tumorsphere formation compared to those without peptide. The inert 3D hydrogel cell culture system provides a novel tool to investigate the individual effect of factors in the microenvironment on maintenance of CSCs without the interference of other factors.

REFERENCES

1. Castaño, Z., K. Tracy, and S.S. McAllister, *The tumor macroenvironment and systemic regulation of breast cancer progression*. International Journal of Developmental Biology, 2011. **55**(7): p. 889.
2. Giatromanolaki, A., et al., *The CD44+/CD24- phenotype relates to 'triple-negative' state and unfavorable prognosis in breast cancer patients*. Medical oncology, 2011. **28**(3): p. 745-752.
3. Rennstam, K., et al., *Numb protein expression correlates with a basal-like phenotype and cancer stem cell markers in primary breast cancer*. Breast cancer research and treatment, 2010. **122**(2): p. 315-324.
4. Pece, S., et al., *Biological and molecular heterogeneity of breast cancers correlates with their cancer stem cell content*. Cell, 2010. **140**(1): p. 62-73.
5. Dalerba, P., R.W. Cho, and M.F. Clarke, *Cancer stem cells: models and concepts*. Annu. Rev. Med., 2007. **58**: p. 267-284.
6. Sheridan, C., et al., *CD44+/CD24-breast cancer cells exhibit enhanced invasive properties: an early step necessary for metastasis*. Breast Cancer Res, 2006. **8**(5): p. R59.
7. Croker, A.K., et al., *High aldehyde dehydrogenase and expression of cancer stem cell markers selects for breast cancer cells with enhanced malignant and metastatic ability* Journal of cellular and molecular medicine, 2009. **13**(8b):

p. 2236-2252.

8. Hiraga, T., S. Ito, and H. Nakamura, *Cancer Stem-like Cell Marker CD44 Promotes Bone Metastases by Enhancing Tumorigenicity, Cell Motility, and Hyaluronan Production*. *Cancer research*, 2013. **73**(13): p. 4112-4122.
9. Zöller, M., *CD44: can a cancer-initiating cell profit from an abundantly expressed molecule?* *Nature Reviews Cancer*, 2011. **11**(4): p. 254-267.
10. Visvader, J.E. and G.J. Lindeman, *Cancer stem cells in solid tumours: accumulating evidence and unresolved questions*. *Nature Reviews Cancer*, 2008. **8**(10): p. 755-768.
11. Ponta, H., L. Sherman, and P.A. Herrlich, *CD44: from adhesion molecules to signalling regulators*. *Nature reviews Molecular cell biology*, 2003. **4**(1): p. 33-45.
12. Savani, R.C., et al., *Differential involvement of the hyaluronan (HA) receptors CD44 and receptor for HA-mediated motility in endothelial cell function and angiogenesis*. *Journal of Biological Chemistry*, 2001. **276**(39): p. 36770-36778.
13. Masuko, K., et al., *Anti-tumor effect against human cancer xenografts by a fully human monoclonal antibody to a variant 8-epitope of CD44R1 expressed on cancer stem cells*. *PloS one*, 2012. **7**(1): p. e29728.
14. Majeti, R., *Monoclonal antibody therapy directed against human acute myeloid leukemia stem cells*. *Oncogene*, 2011. **30**(9): p. 1009-1019.
15. Tremmel, M., et al., *A CD44v6 peptide reveals a role of CD44 in VEGFR-2 signaling and angiogenesis*. *Blood*, 2009. **114**(25): p. 5236-5244.

16. Hibino, S., et al., *Laminin α 5 Chain Metastasis-and Angiogenesis-Inhibiting Peptide Blocks Fibroblast Growth Factor 2 Activity by Binding to the Heparan Sulfate Chains of CD44*. *Cancer research*, 2005. **65**(22): p. 10494-10501.
17. Arai, F., et al., *Tie2/angiopoietin-1 signaling regulates hematopoietic stem cell quiescence in the bone marrow niche*. *Cell*, 2004. **118**(2): p. 149-161.
18. He, X.C., J. Zhang, and L. Li, *Cellular and molecular regulation of hematopoietic and intestinal stem cell behavior*. *Annals of the New York Academy of Sciences*, 2005. **1049**(1): p. 28-38.
19. Reya, T., et al., *Stem cells, cancer, and cancer stem cells*. *nature*, 2001. **414**(6859): p. 105-111.
20. Haycock, J.W., *3D cell culture: a review of current approaches and techniques*, in *3D Cell Culture*. 2011, Springer. p. 1-15.
21. Pampaloni, F., E.G. Reynaud, and E.H.K. Stelzer, *The third dimension bridges the gap between cell culture and live tissue*. *Nature reviews Molecular cell biology*, 2007. **8**(10): p. 839-845.
22. Petersen, O.W., et al., *Interaction with basement membrane serves to rapidly distinguish growth and differentiation pattern of normal and malignant human breast epithelial cells*. *Proceedings of the National Academy of Sciences*, 1992. **89**(19): p. 9064-9068.
23. Debnath, J. and J.S. Brugge, *Modelling glandular epithelial cancers in three-dimensional cultures*. *Nature Reviews Cancer*, 2005. **5**(9): p. 675-688.
24. Dawson, E., et al., *Biomaterials for stem cell differentiation*. *Advanced drug delivery reviews*, 2008. **60**(2): p. 215-228.

25. Masters, K.S., et al., *Designing scaffolds for valvular interstitial cells: cell adhesion and function on naturally derived materials*. Journal of Biomedical Materials Research Part A, 2004. **71**(1): p. 172-180.
26. Raof, N.A., et al., *Bioengineering embryonic stem cell microenvironments for exploring inhibitory effects on metastatic breast cancer cells*. Biomaterials, 2011. **32**(17): p. 4130-4139.
27. Smith, B.H., et al., *Three-dimensional culture of mouse renal carcinoma cells in agarose macrobeads selects for a subpopulation of cells with cancer stem cell or cancer progenitor properties*. Cancer research, 2011. **71**(3): p. 716-724.
28. Chen, L., et al., *The enhancement of cancer stem cell properties of MCF-7 cells in 3D collagen scaffolds for modeling of cancer and anti-cancer drugs*. Biomaterials, 2012. **33**(5): p. 1437-1444.
29. Kievit, F.M., et al., *Chitosan–alginate 3D scaffolds as a mimic of the glioma tumor microenvironment*. Biomaterials, 2010. **31**(22): p. 5903-5910.
30. Fischbach, C., et al., *Engineering tumors with 3D scaffolds*. Nature methods, 2007. **4**(10): p. 855-860.
31. Szot, C.S., et al., *3D *in vitro* bioengineered tumors based on collagen I hydrogels*. Biomaterials, 2011. **32**(31): p. 7905-7912.
32. Cushing, M.C. and K.S. Anseth, *Hydrogel cell cultures*. Science, 2007. **316**(5828): p. 1133-1134.
33. Buxton, A.N., et al., *Design and characterization of poly (ethylene glycol) photopolymerizable semi-interpenetrating networks for chondrogenesis of human mesenchymal stem cells*. Tissue engineering, 2007. **13**(10): p. 2549-2560.

34. Papadopoulos, A., et al., *Injectable and photopolymerizable tissue-engineered auricular cartilage using poly (ethylene glycol) dimethacrylate copolymer hydrogels*. Tissue Engineering Part A, 2010. **17**(1-2): p. 161-169.
35. Doroski, D.M., M.E. Levenston, and J.S. Temenoff, *Cyclic tensile culture promotes fibroblastic differentiation of marrow stromal cells encapsulated in poly (ethylene glycol)-based hydrogels*. Tissue Engineering Part A, 2010. **16**(11): p. 3457-3466.
36. Elisseeff, J., et al., *Photoencapsulation of chondrocytes in poly (ethylene oxide)-based semi-interpenetrating networks*. Journal of Biomedical Materials Research, 2000. **51**(2): p. 164-171.
37. Paszek, M.J., et al., *Tensional homeostasis and the malignant phenotype*. Cancer cell, 2005. **8**(3): p. 241-254.
38. Verbridge, S.S., E.M. Chandler, and C. Fischbach, *Tissue-engineered three-dimensional tumor models to study tumor angiogenesis*. Tissue Engineering Part A, 2010. **16**(7): p. 2147-2152.
39. Bissell, M.J. and D. Radisky, *Putting tumours in context*. Nature Reviews Cancer, 2001. **1**(1): p. 46-54.
40. Biddle, A. and I.C. Mackenzie, *Cancer stem cells and EMT in carcinoma*. Cancer and Metastasis Reviews, 2012. **31**(1-2): p. 285-293.
41. McNamara, L.E., et al., *Nanotopographical control of stem cell differentiation*. Journal of tissue engineering, 2010. **1**(1): p. 120623.
42. Suresh, S., *Biomechanics and biophysics of cancer cells*. Acta Materialia, 2007. **55**(12): p. 3989-4014.

43. Makale, M., *Cellular mechanobiology and cancer metastasis*. Birth Defects Research Part C: Embryo Today: Reviews, 2007. **81**(4): p. 329-343.
44. Reilly, G.C. and A.J. Engler, *Intrinsic extracellular matrix properties regulate stem cell differentiation*. Journal of biomechanics, 2010. **43**(1): p. 55-62.
45. Park, J., et al., *Control of stem cell fate and function by engineering physical microenvironments*. Integrative Biology, 2012. **4**(9): p. 1008-1018.
46. Curtis, A. and C. Wilkinson, *Nanotechniques and approaches in biotechnology*. TRENDS in Biotechnology, 2001. **19**(3): p. 97-101.
47. Curtis, A. and M. Riehle, *Tissue engineering: the biophysical background*. Physics in medicine and biology, 2001. **46**(4): p. R47.
48. Singhvi, R., et al., *Engineering cell shape and function*. Science, 1994. **264**(5159): p. 696-698.
49. Engler, A.J., et al., *Extracellular matrix elasticity directs stem cell differentiation*. Journal of Musculoskeletal and Neuronal Interactions, 2007. **7**(4): p. 335.
50. Chen, C.S., et al., *Geometric control of cell life and death*. Science, 1997. **276**(5317): p. 1425-1428.
51. Schrader, J., et al., *Matrix stiffness modulates proliferation, chemotherapeutic response, and dormancy in hepatocellular carcinoma cells*. Hepatology, 2011. **53**(4): p. 1192-1205.
52. Zaman, M.H., et al., *Migration of tumor cells in 3D matrices is governed by matrix stiffness along with cell-matrix adhesion and proteolysis*. Proceedings of the National Academy of Sciences, 2006. **103**(29): p. 10889-10894.

53. Discher, D.E., P. Janmey, and Y.-l. Wang, *Tissue cells feel and respond to the stiffness of their substrate*. Science, 2005. **310**(5751): p. 1139-1143.
54. Chen, R.R., et al., *Integrated approach to designing growth factor delivery systems*. The FASEB Journal, 2007. **21**(14): p. 3896-3903.
55. Leight, J.L., et al., *Manipulation of 3D Cluster Size and Geometry by Release from 2D Micropatterns*. Cell Mol Bioeng. **5**(3): p. 299-306.
56. Fukuda, J. and K. Nakazawa, *Orderly arrangement of hepatocyte spheroids on a microfabricated chip*. Tissue engineering, 2005. **11**(7-8): p. 1254-1262.
57. Mohr, J.C., J.J. de Pablo, and S.P. Palecek, *3-D microwell culture of human embryonic stem cells*. Biomaterials, 2006. **27**(36): p. 6032-6042.
58. Tan, J.L., et al., *Simple approach to micropattern cells on common culture substrates by tuning substrate wettability*. Tissue engineering, 2004. **10**(5-6): p. 865-872.
59. Huebsch, N., et al., *Harnessing traction-mediated manipulation of the cell/matrix interface to control stem-cell fate*. Nature materials, 2010. **9**(6): p. 518-526.
60. Liu, S.Q., et al., *Biomimetic hydrogels for chondrogenic differentiation of human mesenchymal stem cells to neocartilage*. Biomaterials, 2010. **31**(28): p. 7298-7307.
61. Sun, Y., C.S. Chen, and J. Fu, *Forcing stem cells to behave: a biophysical perspective of the cellular microenvironment*. Annual review of biophysics, 2012. **41**: p. 519-542.
62. Engbring, J.A. and H.K. Kleinman, *The basement membrane matrix in malignancy*. The Journal of pathology, 2003. **200**(4): p. 465-470.

63. Kleinman, H.K., et al., *Role of basement membrane in tumor growth and metastasis*. Surgical oncology clinics of North America, 2001. **10**(2): p. 329-38.
64. Kalluri, R., *Basement membranes: structure, assembly and role in tumour angiogenesis*. Nature Reviews Cancer, 2003. **3**(6): p. 422-433.
65. Ikeda, K., et al., *Loss of expression of type IV collagen $\alpha 5$ and $\alpha 6$ chains in colorectal cancer associated with the hypermethylation of their promoter region*. The American journal of pathology, 2006. **168**(3): p. 856-865.
66. Yu, F., et al., *Kruppel-like factor 4 (KLF4) is required for maintenance of breast cancer stem cells and for cell migration and invasion*. Oncogene, 2011. **30**(18): p. 2161-2172.
67. Krohn, A., et al., *CXCR4 receptor positive spheroid forming cells are responsible for tumor invasion in vitro*. Cancer letters, 2009. **280**(1): p. 65-71.
68. Gupta, P.B., et al., *Identification of selective inhibitors of cancer stem cells by high-throughput screening*. Cell, 2009. **138**(4): p. 645-659.
69. Liu, J.C., et al., *Identification of tumorsphere-and tumor-initiating cells in HER2/Neu-induced mammary tumors*. Cancer research, 2007. **67**(18): p. 8671-8681.
70. Fillmore, C.M. and C. Kuperwasser, *Human breast cancer cell lines contain stem-like cells that self-renew, give rise to phenotypically diverse progeny and survive chemotherapy*. Breast Cancer Res, 2008. **10**(2): p. R25.
71. Tao, K., et al., *Imagable 4T1 model for the study of late stage breast cancer*. BMC cancer, 2008. **8**(1): p. 228.

72. He, X. and E. Jabbari, *Material properties and cytocompatibility of injectable MMP degradable poly (lactide ethylene oxide fumarate) hydrogel as a carrier for marrow stromal cells*. *Biomacromolecules*, 2007. **8**(3): p. 780-792.
73. He, X., X. Yang, and E. Jabbari, *Combined effect of osteopontin and BMP-2 derived peptides grafted to an adhesive hydrogel on osteogenic and vasculogenic differentiation of marrow stromal cells*. *Langmuir*, 2012. **28**(12): p. 5387-5397.
74. Woodward, W.A., et al., *On mammary stem cells*. *Journal of Cell Science*, 2005. **118**(16): p. 3585-3594.
75. Fernandez-Gonzalez, R., et al., *In situ analysis of cell populations: long-term label-retaining cells*, in *Protocols for Adult Stem Cells*. 2010, Springer. p. 1-28.
76. Weiswald, L.-B., et al., *In situ protein expression in tumour spheres: development of an immunostaining protocol for confocal microscopy*. *BMC cancer*, 2010. **10**(1): p. 106.
77. Schefe, J.H., et al., *Quantitative real-time RT-PCR data analysis: current concepts and the novel "gene expression's C T difference" formula*. *Journal of molecular medicine*, 2006. **84**(11): p. 901-910.
78. Schmittgen, T.D. and K.J. Livak, *Analyzing real-time PCR data by the comparative CT method*. *Nature protocols*, 2008. **3**(6): p. 1101-1108.
79. Hibino, S., et al., *Identification of an active site on the laminin alpha5 chain globular domain that binds to CD44 and inhibits malignancy*. *Cancer Res*, 2004. **64**(14): p. 4810-6.
80. Hurt, E.M., et al., *Identification of vitronectin as an extrinsic inducer of cancer stem cell differentiation and tumor formation*. *Stem Cells*, 2010. **28**(3): p. 390-8.

81. Woods, A., et al., *A synthetic peptide from the COOH-terminal heparin-binding domain of fibronectin promotes focal adhesion formation*. Mol Biol Cell, 1993. **4**(6): p. 605-13.
82. He, X., J. Ma, and E. Jabbari, *Effect of grafting RGD and BMP-2 protein-derived peptides to a hydrogel substrate on osteogenic differentiation of marrow stromal cells*. Langmuir, 2008. **24**(21): p. 12508-16.
83. Lynn, A.D., T.R. Kyriakides, and S.J. Bryant, *Characterization of the in vitro macrophage response and in vivo host response to poly(ethylene glycol)-based hydrogels*. J Biomed Mater Res A, 2010. **93**(3): p. 941-53.
84. Hirschhaeuser, F., et al., *Multicellular tumor spheroids: an underestimated tool is catching up again*. J Biotechnol. **148**(1): p. 3-15.
85. Nemir, S. and J.L. West, *Synthetic materials in the study of cell response to substrate rigidity*. Ann Biomed Eng. **38**(1): p. 2-20.
86. Tilghman, R.W., et al., *Matrix rigidity regulates cancer cell growth and cellular phenotype*. PLoS One. **5**(9): p. e12905.
87. Britton, K.M., et al., *Breast cancer, side population cells and ABCG2 expression*. Cancer Lett. **323**(1): p. 97-105.
88. Grange, C., et al., *Sca-1 identifies the tumor-initiating cells in mammary tumors of BALB-neuT transgenic mice*. Neoplasia, 2008. **10**(12): p. 1433-43.
89. Welm, B., et al., *Isolation and characterization of functional mammary gland stem cells*. Cell Proliferation, 2003. **36**(s1): p. 17-32.
90. Badve, S. and H. Nakshatri, *Breast-cancer stem cells—beyond semantics*. The lancet oncology, 2012. **13**(1): p. e43-e48.

91. Kai, K., et al., *Breast cancer stem cells*. Breast Cancer, 2010. **17**(2): p. 80-85.
92. Bhat-Nakshatri, P., et al., *SLUG/SNAI2 and tumor necrosis factor generate breast cells with CD44+/CD24- phenotype*. BMC Cancer, 2010. **10**: p. 411.
93. Cho, R.W. and M.F. Clarke, *Recent advances in cancer stem cells*. Curr Opin Genet Dev, 2008. **18**(1): p. 48-53.
94. Yeung, T.M., et al., *Cancer stem cells from colorectal cancer-derived cell lines*. Proc Natl Acad Sci U S A. **107**(8): p. 3722-7.
95. Takaishi, S., et al., *Identification of gastric cancer stem cells using the cell surface marker CD44*. Stem Cells, 2009. **27**(5): p. 1006-20.
96. Dalerba, P., R.W. Cho, and M.F. Clarke, *Cancer stem cells: models and concepts*. Annu Rev Med, 2007. **58**: p. 267-84.
97. Flanagan, L.A., et al., *Neurite branching on deformable substrates*. Neuroreport, 2002. **13**(18): p. 2411.
98. Engler, A.J., et al., *Matrix elasticity directs stem cell lineage specification*. Cell, 2006. **126**(4): p. 677-689.
99. Engler, A.J., et al., *Embryonic cardiomyocytes beat best on a matrix with heart-like elasticity: scar-like rigidity inhibits beating*. Journal of cell science, 2008. **121**(22): p. 3794-3802.
100. Samani, A., J. Zubovits, and D. Plewes, *Elastic moduli of normal and pathological human breast tissues: an inversion-technique-based investigation of 169 samples*. Physics in medicine and biology, 2007. **52**(6): p. 1565.

101. Provenzano, P.P., et al., *Matrix density-induced mechanoregulation of breast cell phenotype, signaling and gene expression through a FAK-ERK linkage*. *Oncogene*, 2009. **28**(49): p. 4326-4343.
102. Levental, K.R., et al., *Matrix crosslinking forces tumor progression by enhancing integrin signaling*. *Cell*, 2009. **139**(5): p. 891-906.
103. Parekh, S.H., et al., *Modulus-driven differentiation of marrow stromal cells in 3D scaffolds that is independent of myosin-based cytoskeletal tension*. *Biomaterials*, 2011. **32**(9): p. 2256-2264.
104. Shaw, M.T. and W.J. MacKnight, *Introduction to polymer viscoelasticity*. 2005: John Wiley & Sons.
105. Heddleston, J.M., et al., *Hypoxia inducible factors in cancer stem cells*. *British journal of cancer*, 2010. **102**(5): p. 789-795.
106. Hsu, Y.-C. and E. Fuchs, *A family business: stem cell progeny join the niche to regulate homeostasis*. *Nature reviews Molecular cell biology*, 2012. **13**(2): p. 103-114.
107. Korkaya, H., S. Liu, and M.S. Wicha, *Breast cancer stem cells, cytokine networks, and the tumor microenvironment*. *The Journal of clinical investigation*, 2011. **121**(10): p. 3804.
108. Lee, B.-H., B. Li, and S.A. Guelcher, *Gel microstructure regulates proliferation and differentiation of MC3T3-E1 cells encapsulated in alginate beads*. *Acta biomaterialia*, 2012. **8**(5): p. 1693-1702.
109. Leal-Egaña, A., et al., *Determination of pore size distribution at the cell-hydrogel interface*. *Journal of nanobiotechnology*, 2011. **9**(24): p. 1-7.

110. Peppas, N.A. and B.D. Barr-Howell, *Characterization of the crosslinked structure of hydrogels*. Hydrogels in medicine and pharmacy, 1986. **1**: p. 27-56.
111. Soeda, A., et al., *Hypoxia promotes expansion of the CD133-positive glioma stem cells through activation of HIF-1 α* . Oncogene, 2009. **28**(45): p. 3949-3959.
112. Peng, T., et al., *Long-term sphere culture cannot maintain a high ratio of cancer stem cells: a mathematical model and experiment*. PloS one, 2011. **6**(11): p. e25518.
113. Vincent, T.L., et al., *Basic fibroblast growth factor mediates transduction of mechanical signals when articular cartilage is loaded*. Arthritis & Rheumatism, 2004. **50**(2): p. 526-533.
114. Adam, R.M., et al., *Signaling through PI3K/Akt mediates stretch and PDGF-BB-dependent DNA synthesis in bladder smooth muscle cells*. The Journal of urology, 2003. **169**(6): p. 2388-2393.
115. Biddle, A. and I.C. Mackenzie, *Cancer stem cells and EMT in carcinoma*. Cancer Metastasis Rev, 2012.
116. Rhim, A.D., et al., *EMT and dissemination precede pancreatic tumor formation*. Cell, 2012. **148**(1-2): p. 349-61.
117. Zeisberg, M. and E.G. Neilson, *Biomarkers for epithelial-mesenchymal transitions*. The Journal of clinical investigation, 2009. **119**(6): p. 1429.
118. Floor, S., et al., *Cancer cells in epithelial-to-mesenchymal transition and tumor-propagating-cancer stem cells: distinct, overlapping or same populations*. Oncogene, 2011. **30**(46): p. 4609-4621.

119. Del Vecchio, C.A., et al., *Epidermal growth factor receptor variant III contributes to cancer stem cell phenotypes in invasive breast carcinoma*. *Cancer Res*, 2012. **72**(10): p. 2657-71.
120. Tschumperlin, D.J., et al., *Mechanotransduction through growth-factor shedding into the extracellular space*. *Nature*, 2004. **429**(6987): p. 83-86.
121. Katoh, M., *Networking of WNT, FGF, Notch, BMP, and Hedgehog signaling pathways during carcinogenesis*. *Stem cell reviews*, 2007. **3**(1): p. 30-38.
122. Théry, M., *Micropatterning as a tool to decipher cell morphogenesis and functions*. *Journal of cell science*, 2010. **123**(24): p. 4201-4213.
123. Yang, X., et al., *Three-Dimensional-Engineered Matrix to Study Cancer Stem Cells and Tumorsphere Formation: Effect of Matrix Modulus*. *Tissue Eng Part A*, 2012.
124. Cox, R.D. and C.D. Church, *Mouse models and the interpretation of human GWAS in type 2 diabetes and obesity*. *Dis Model Mech*, 2011. **4**: p. 155-164.
125. Wels, J., et al., *Migratory neighbors and distant invaders: tumor-associated niche cells*. *Genes Dev*, 2008. **22**(5): p. 559-574.
126. Moeinzadeh, S., et al., *Gelation characteristics and osteogenic differentiation of stromal cells in inert hydrolytically degradable micellar polyethylene glycol hydrogels*. *Biomacromolecules*, 2012. **13**: p. 2073-2086.
127. Abhold, E.L., et al., *EGFR kinase promotes acquisition of stem cell-like properties: a potential therapeutic target in head and neck squamous cell carcinoma stem cells*. *PLoS One*, 2012. **7**(2): p. e32459.

128. Gravdal, K., et al., *A switch from E-cadherin to N-cadherin expression indicates epithelial to mesenchymal transition and is of strong and independent importance for the progress of prostate cancer*. Clin Cancer Res, 2007. **13**(23): p. 7003-11.
129. Nieto, M.A., *The ins and outs of the epithelial to mesenchymal transition in health and disease*. Annu Rev Cell Dev Biol, 2011. **27**: p. 347-76.
130. van Roy, F. and G. Berx, *The cell-cell adhesion molecule E-cadherin*. Cell Mol Life Sci, 2008. **65**(23): p. 3756-88.
131. Rathinam, R. and S.K. Alahari, *Important role of integrins in the cancer biology*. Cancer Metastasis Rev, 2010. **29**(1): p. 223-37.
132. Korsching, E., et al., *The origin of vimentin expression in invasive breast cancer: epithelial-mesenchymal transition, myoepithelial histogenesis or histogenesis from progenitor cells with bilinear differentiation potential?* J Pathol, 2005. **206**(4): p. 451-7.
133. Calvo, A., et al., *Identification of VEGF-regulated genes associated with increased lung metastatic potential: functional involvement of tenascin-C in tumor growth and lung metastasis*. Oncogene, 2008. **27**(40): p. 5373-84.
134. Ercan, C., P.J. van Diest, and M. Vooijs, *Mammary development and breast cancer: the role of stem cells*. Curr Mol Med, 2011. **11**(4): p. 270-85.
135. Butcher, D.T., T. Alliston, and V.M. Weaver, *A tense situation: forcing tumour progression*. Nat Rev Cancer, 2009. **9**(2): p. 108-22.
136. Jalkanen, S. and M. Jalkanen, *Lymphocyte CD44 binds the COOH-terminal heparin-binding domain of fibronectin*. J Cell Biol, 1992. **116**(3): p. 817-25.

137. Teriete, P., et al., *Structure of the regulatory hyaluronan binding domain in the inflammatory leukocyte homing receptor CD44*. Mol Cell, 2004. **13**(4): p. 483-96.
138. Weber, G.F., S. Ashkar, and H. Cantor, *Interaction between CD44 and osteopontin as a potential basis for metastasis formation*. Proc Assoc Am Physicians, 1997. **109**(1): p. 1-9.
139. Faassen, A.E., et al., *A cell surface chondroitin sulfate proteoglycan, immunologically related to CD44, is involved in type I collagen-mediated melanoma cell motility and invasion*. J Cell Biol, 1992. **116**(2): p. 521-31.
140. Piotrowicz, R.S., et al., *A6 peptide activates CD44 adhesive activity, induces FAK and MEK phosphorylation, and inhibits the migration and metastasis of CD44-expressing cells*. Mol Cancer Ther, 2011. **10**(11): p. 2072-82.
141. Giancotti, F.G. and G. Tarone, *Positional control of cell fate through joint integrin/receptor protein kinase signaling*. Annu Rev Cell Dev Biol, 2003. **19**: p. 173-206.
142. Monferran, S., et al., *Alphavbeta3 and alphavbeta5 integrins control glioma cell response to ionising radiation through ILK and RhoB*. Int J Cancer, 2008. **123**(2): p. 357-64.
143. Rizzo, S., G. Attard, and D.L. Hudson, *Prostate epithelial stem cells*. Cell Prolif, 2005. **38**(6): p. 363-74.
144. Galbraith, C.G., K.M. Yamada, and M.P. Sheetz, *The relationship between force and focal complex development*. J Cell Biol, 2002. **159**(4): p. 695-705.
145. Nelson, C.M., et al., *Emergent patterns of growth controlled by multicellular form and mechanics*. Proc Natl Acad Sci U S A, 2005. **102**(33): p. 11594-9.

146. Giannone, G. and M.P. Sheetz, *Substrate rigidity and force define form through tyrosine phosphatase and kinase pathways*. Trends Cell Biol, 2006. **16**(4): p. 213-23.
147. Yu, C.H., et al., *Early integrin binding to Arg-Gly-Asp peptide activates actin polymerization and contractile movement that stimulates outward translocation*. Proc Natl Acad Sci U S A, 2011. **108**(51): p. 20585-90.
148. Akiyama, S.K., K. Nagata, and K.M. Yamada, *Cell surface receptors for extracellular matrix components*. Biochim Biophys Acta, 1990. **1031**(1): p. 91-110.
149. Owens, L.V., et al., *Overexpression of the focal adhesion kinase (p125FAK) in invasive human tumors*. Cancer Res, 1995. **55**(13): p. 2752-5.
150. Luo, M. and J.L. Guan, *Focal adhesion kinase: a prominent determinant in breast cancer initiation, progression and metastasis*. Cancer Lett, 2010. **289**(2): p. 127-39.
151. Xu, L.H., et al., *The focal adhesion kinase suppresses transformation-associated, anchorage-independent apoptosis in human breast cancer cells. Involvement of death receptor-related signaling pathways*. J Biol Chem, 2000. **275**(39): p. 30597-604.
152. Kang, Y. and J. Massague, *Epithelial-mesenchymal transitions: twist in development and metastasis*. Cell, 2004. **118**(3): p. 277-9.
153. Saha, S., et al., *Breast tumour initiating cell fate is regulated by microenvironmental cues from an extracellular matrix*. Integr Biol (Camb), 2012. **4**(8): p. 897-904.